If an idea presents itself to us, we must not reject it simply because it does not agree with the logical deductions of a reigning theory.

—*Claude Bernard,* An Introduction to the Study of Experimental Medicine, *1813*

The aspect of the present position of consensus that I find most remarkable and admirable, is the altruism and generosity with which former opponents of the chemiosmotic hypothesis have not only come to accept it, but have actively promoted it to the status of a theory.

—*Peter Mitchell, Nobel Address, 1978*

19

Oxidative Phosphorylation and Photophosphorylation

OXIDATIVE PHOSPHORYLATION

PHOTOSYNTHESIS: HARVESTING LIGHT ENERGY

Oxidative phosphorylation is the culmination of energy-yielding metabolism in aerobic organisms. All oxidative steps in the degradation of carbohydrates, fats, and amino acids converge at this final stage of cellular respiration, in which the energy of oxidation drives the synthesis of ATP. Photophosphorylation is the means by which photosynthetic organisms capture the energy of sunlight—the ultimate source of energy in the biosphere—and harness it to make ATP. Together, oxidative phosphorylation and photophosphorylation account for most of the ATP synthesized by most organisms most of the time.

In eukaryotes, oxidative phosphorylation occurs in mitochondria, photophosphorylation in chloroplasts. Oxidative phosphorylation involves the *reduction* of O_2 to H_2O with electrons donated by NADH and $FADH_2$; it occurs equally well in light or darkness. Photophosphorylation involves the *oxidation* of H_2O to O_2, with $NADP^+$ as ultimate electron acceptor; it is absolutely dependent on the energy of light. Despite their differences, these two highly efficient energy-converting processes have fundamentally similar mechanisms.

Our current understanding of ATP synthesis in mitochondria and chloroplasts is based on the hypothesis, introduced by Peter Mitchell in 1961, that transmembrane differences in proton concentration are the reservoir for the energy extracted from biological oxidation reactions. This **chemiosmotic theory** has been accepted as one of the great unifying principles of twentieth century biology. It provides insight into the processes of oxidative phosphorylation and photophosphorylation, and into such apparently disparate energy transductions as active transport across membranes and the motion of bacterial flagella.

Oxidative phosphorylation and photophosphorylation are mechanistically similar in three respects. (1) Both processes involve the flow of electrons through a chain of membrane-bound carriers. (2) The free energy made available by this "downhill" (exergonic) electron flow is coupled to the "uphill" transport of protons

across a proton-impermeable membrane, conserving the free energy of fuel oxidation as a transmembrane electrochemical potential (p. 390). (3) The transmembrane flow of protons down their concentration gradient through specific protein channels provides the free energy for synthesis of ATP, catalyzed by a membrane protein complex (ATP synthase) that couples proton flow to phosphorylation of ADP.

The chapter begins with oxidative phosphorylation. We first describe the components of the electron-transfer chain, their organization into large functional complexes in the inner mitochondrial membrane, the path of electron flow through them, and the proton movements that accompany this flow. We then consider the remarkable enzyme complex that, by "rotational catalysis," captures the energy of proton flow in ATP, and the regulatory mechanisms that coordinate oxidative phosphorylation with the many catabolic pathways by which fuels are oxidized. We also describe the roles that mitochondria play in thermogenesis, steroid synthesis, and apoptosis. With this understanding of mitochondrial oxidative phosphorylation, we turn to photophosphorylation, looking first at the absorption of light by photosynthetic pigments, then at the light-driven flow of electrons from H_2O to $NADP^+$ and the molecular basis for coupling electron and proton flow. We also consider the similarities of structure and mechanism between the ATP synthases of chloroplasts and mitochondria, and the evolutionary basis for this conservation of mechanism.

OXIDATIVE PHOSPHORYLATION

19.1 Electron-Transfer Reactions in Mitochondria

The discovery in 1948 by Eugene Kennedy and Albert Lehninger that mitochondria are the site of oxidative phosphorylation in eukaryotes marked the beginning of the modern phase of studies in biological energy transductions. Mitochondria, like gram-negative bacteria, have two membranes **(Fig. 19–1)**. The outer mitochondrial membrane is readily permeable to small molecules (M_r <5,000) and ions, which move freely through transmembrane channels formed by a family of integral membrane proteins called porins. The inner membrane is impermeable to most small molecules and ions, including protons (H^+); the only species that cross this membrane do so through specific transporters. The inner membrane bears the components of the respiratory chain and the ATP synthase.

Albert L. Lehninger, 1917–1986

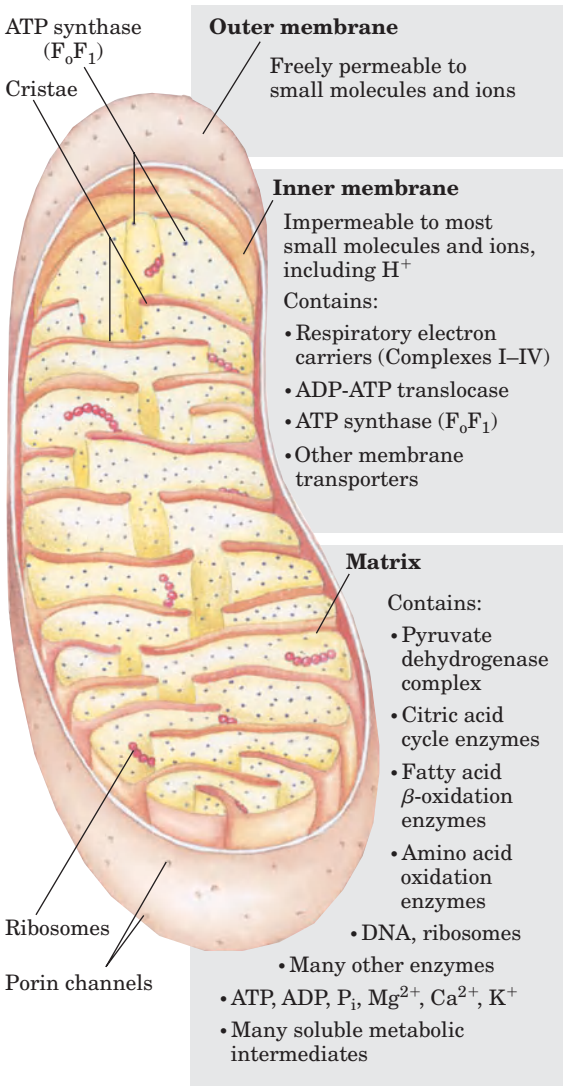

FIGURE 19–1 Biochemical anatomy of a mitochondrion. The convolutions (cristae) of the inner membrane provide a very large surface area. The inner membrane of a single liver mitochondrion may have more than 10,000 sets of electron-transfer systems (respiratory chains) and ATP synthase molecules, distributed over the membrane surface. The mitochondria of heart muscle, which have more profuse cristae and thus a much larger area of inner membrane, contain more than three times as many sets of electron-transfer systems as liver mitochondria. The mitochondrial pool of coenzymes and intermediates is functionally separate from the cytosolic pool. The mitochondria of invertebrates, plants, and microbial eukaryotes are similar to those shown here, but with much variation in size, shape, and degree of convolution of the inner membrane.

The mitochondrial matrix, enclosed by the inner membrane, contains the pyruvate dehydrogenase complex and the enzymes of the citric acid cycle, the fatty acid β-oxidation pathway, and the pathways of amino acid oxidation—all the pathways of fuel oxidation except glycolysis, which takes place in the cytosol. The selectively permeable inner membrane segregates the intermediates and enzymes of cytosolic metabolic pathways

from those of metabolic processes occurring in the matrix. However, specific transporters carry pyruvate, fatty acids, and amino acids or their α-keto derivatives into the matrix for access to the machinery of the citric acid cycle. ADP and P_i are specifically transported into the matrix as newly synthesized ATP is transported out.

Electrons Are Funneled to Universal Electron Acceptors

Oxidative phosphorylation begins with the entry of electrons into the respiratory chain. Most of these electrons arise from the action of dehydrogenases that collect electrons from catabolic pathways and funnel them into universal electron acceptors—nicotinamide nucleotides (NAD^+ or $NADP^+$) or flavin nucleotides (FMN or FAD).

Nicotinamide nucleotide–linked dehydrogenases catalyze reversible reactions of the following general types:

$$\text{Reduced substrate} + NAD^+ \rightleftharpoons \text{oxidized substrate} + NADH + H^+$$

$$\text{Reduced substrate} + NADP^+ \rightleftharpoons \text{oxidized substrate} + NADPH + H^+$$

Most dehydrogenases that act in catabolism are specific for NAD^+ as electron acceptor (Table 19–1). Some are in the cytosol, others are in mitochondria, and still others have mitochondrial and cytosolic isozymes.

NAD-linked dehydrogenases remove two hydrogen atoms from their substrates. One of these is transferred as a hydride ion ($:H^-$) to NAD^+; the other is released as H^+ in the medium (see Fig. 13–24). NADH and NADPH are water-soluble electron carriers that associate *reversibly* with dehydrogenases. NADH carries electrons from catabolic reactions to their point of entry into the respiratory chain, the NADH dehydrogenase complex described below. NADPH generally supplies electrons to anabolic reactions. Cells maintain separate pools of NADPH and NADH, with different redox potentials. This is accomplished by holding the ratio of [reduced form]/[oxidized form] relatively high for NADPH and relatively low for NADH. Neither NADH nor NADPH can cross the inner mitochondrial membrane, but the electrons they carry can be shuttled across indirectly, as we shall see.

Flavoproteins contain a very tightly, sometimes covalently, bound flavin nucleotide, either FMN or FAD (see Fig. 13–27). The oxidized flavin nucleotide can accept either one electron (yielding the semiquinone form) or two (yielding $FADH_2$ or $FMNH_2$). Electron transfer occurs because the flavoprotein has a higher reduction potential than the compound oxidized. The standard reduction potential of a flavin nucleotide, unlike that of NAD or NADP, depends on the protein with which it is associated. Local interactions with functional groups in the protein distort the electron orbitals in the flavin ring, changing the relative stabilities of oxidized and reduced forms. The relevant standard reduction potential is therefore that of the particular flavoprotein, not that of isolated FAD or FMN. The flavin nucleotide should be considered part of the flavoprotein's active site rather than a reactant or product in the electron-transfer reaction. Because flavoproteins can participate in either one- or two-electron transfers, they can serve as intermediates between reactions in which two electrons are donated (as in dehydrogenations) and those in which only one electron is accepted (as in the reduction of a quinone to a hydroquinone, described below).

TABLE 19–1 Some Important Reactions Catalyzed by NAD(P)H-Linked Dehydrogenases

Reaction*	Location†
NAD-linked	
α-Ketoglutarate + CoA + $NAD^+ \rightleftharpoons$ succinyl-CoA + CO_2 + NADH + H^+	M
L-Malate + $NAD^+ \rightleftharpoons$ oxaloacetate + NADH + H^+	M and C
Pyruvate + CoA + $NAD^+ \rightleftharpoons$ acetyl-CoA + CO_2 + NADH + H^+	M
Glyceraldehyde 3-phosphate + P_i + $NAD^+ \rightleftharpoons$ 1,3-bisphosphoglycerate + NADH + H^+	C
Lactate + $NAD^+ \rightleftharpoons$ pyruvate + NADH + H^+	C
β-Hydroxyacyl-CoA + $NAD^+ \rightleftharpoons$ β-ketoacyl-CoA + NADH + H^+	M
NADP-linked	
Glucose 6-phosphate + $NADP^+ \rightleftharpoons$ 6-phosphogluconate + NADPH + H^+	C
NAD- or NADP-linked	
L-Glutamate + H_2O + $NAD(P)^+ \rightleftharpoons$ α-ketoglutarate + NH_4^+ + NAD(P)H	M
Isocitrate + $NAD(P)^+ \rightleftharpoons$ α-ketoglutarate + CO_2 + NAD(P)H + H^+	M and C

*These reactions and their enzymes are discussed in Chapters 14 through 18.

†M designates mitochondria; C, cytosol.

Electrons Pass through a Series of Membrane-Bound Carriers

The mitochondrial respiratory chain consists of a series of sequentially acting electron carriers, most of which are integral proteins with prosthetic groups capable of accepting and donating either one or two electrons. Three types of electron transfers occur in oxidative phosphorylation: (1) direct transfer of electrons, as in the reduction of Fe^{3+} to Fe^{2+}; (2) transfer as a hydrogen atom ($H^+ + e^-$); and (3) transfer as a hydride ion ($:H^-$), which bears two electrons. The term **reducing equivalent** is used to designate a single electron equivalent transferred in an oxidation-reduction reaction.

In addition to NAD and flavoproteins, three other types of electron-carrying molecules function in the respiratory chain: a hydrophobic quinone (ubiquinone) and two different types of iron-containing proteins (cytochromes and iron-sulfur proteins). **Ubiquinone** (also called **coenzyme Q**, or simply **Q**) is a lipid-soluble benzoquinone with a long isoprenoid side chain **(Fig. 19–2)**. The closely related compounds plastoquinone (of plant chloroplasts) and menaquinone (of bacteria) play roles analogous to that of ubiquinone, carrying electrons in membrane-associated electron-transfer chains. Ubiquinone can accept one electron to become the semiquinone radical ($^{\bullet}QH$) or two electrons to form ubiquinol (QH_2) (Fig. 19–2) and, like flavoprotein carriers, it can act at the junction between a two-electron donor and a one-electron acceptor. Because ubiquinone is both small and hydrophobic, it is freely diffusible within the lipid bilayer of the inner mitochondrial membrane and can shuttle reducing equivalents between other, less mobile electron carriers in the membrane. And because it carries both electrons and protons, it plays a central role in coupling electron flow to proton movement.

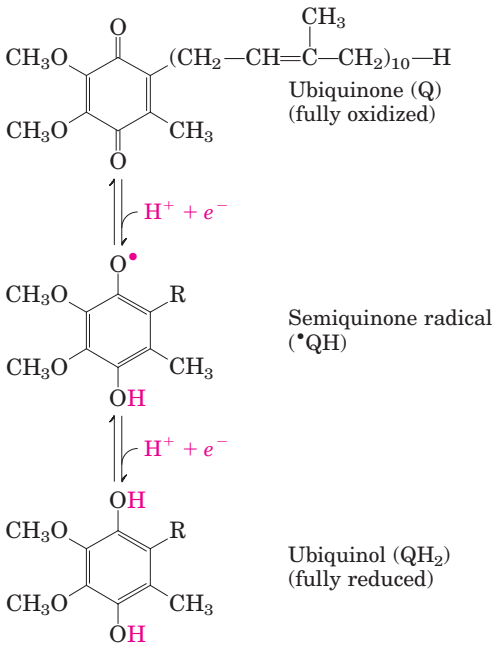

FIGURE 19–2 Ubiquinone (Q, or coenzyme Q). Complete reduction of ubiquinone requires two electrons and two protons, and occurs in two steps through the semiquinone radical intermediate.

The **cytochromes** are proteins with characteristic strong absorption of visible light, due to their iron-containing heme prosthetic groups **(Fig. 19–3)**. Mitochondria contain three classes of cytochromes, designated *a*,

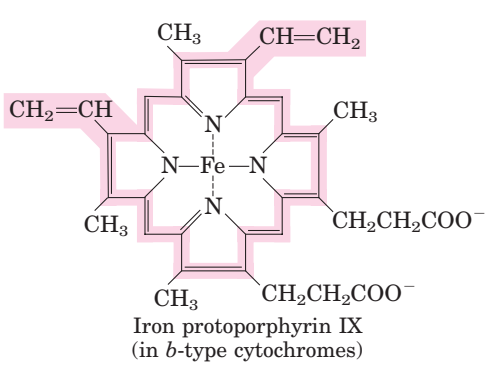

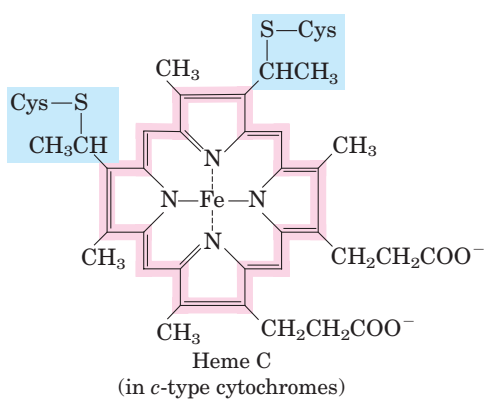

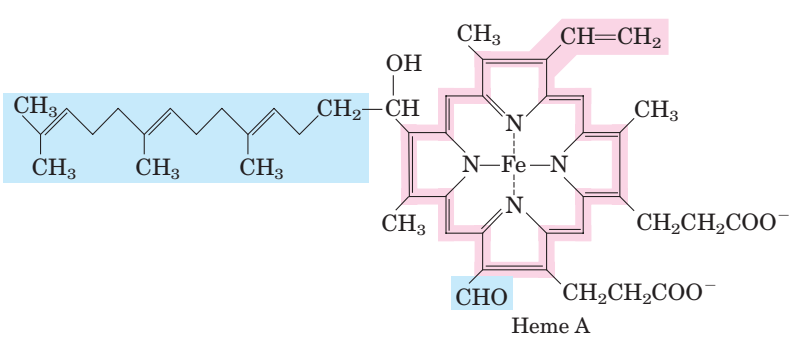

FIGURE 19–3 Prosthetic groups of cytochromes. Each group consists of four five-membered, nitrogen-containing rings in a cyclic structure called a porphyrin. The four nitrogen atoms are coordinated with a central Fe ion, either Fe^{2+} or Fe^{3+}. Iron protoporphyrin IX is found in *b*-type cytochromes and in hemoglobin and myoglobin (see Fig. 4–16). Heme *c* is covalently bound to the protein of cytochrome *c* through thioether bonds to two Cys residues. Heme *a*, found in *a*-type cytochromes, has a long isoprenoid tail attached to one of the five-membered rings. The conjugated double-bond system (shaded pink) of the porphyrin ring accounts for the absorption of visible light by these hemes.

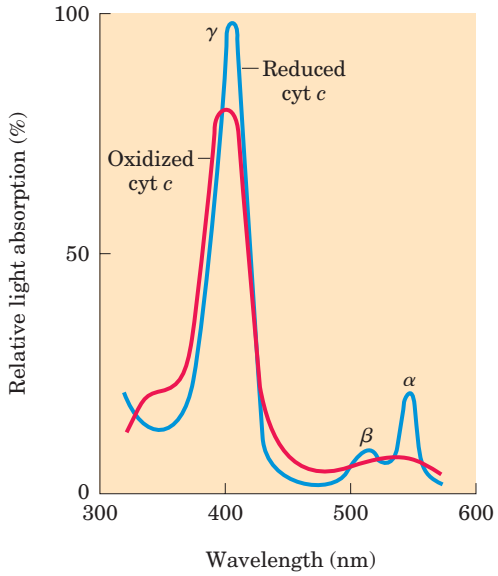

FIGURE 19–4 Absorption spectra of cytochrome *c* (cyt *c*) in its oxidized (red) and reduced (blue) forms. Also labeled are the characteristic α, β, and γ bands of the reduced form.

b, and *c*, which are distinguished by differences in their light-absorption spectra. Each type of cytochrome in its reduced (Fe^{2+}) state has three absorption bands in the visible range **(Fig. 19–4)**. The longest-wavelength band is near 600 nm in type *a* cytochromes, near 560 nm in type *b*, and near 550 nm in type *c*. To distinguish among closely related cytochromes of one type, the exact absorption maximum is sometimes used in the names, as in cytochrome b_{562}.

The heme cofactors of *a* and *b* cytochromes are tightly, but not covalently, bound to their associated proteins; the hemes of *c*-type cytochromes are covalently attached through Cys residues (Fig. 19–3). As with the flavoproteins, the standard reduction potential of the heme iron atom of a cytochrome depends on its interaction with protein side chains and is therefore different for each cytochrome. The cytochromes of type *a* and *b* and some of type *c* are integral proteins of the inner mitochondrial membrane. One striking exception is the cytochrome *c* of mitochondria, a soluble protein that associates through electrostatic interactions with the outer surface of the inner membrane.

In **iron-sulfur proteins**, the iron is present not in heme but in association with inorganic sulfur atoms or with the sulfur atoms of Cys residues in the protein, or both. These iron-sulfur (Fe-S) centers range from simple structures with a single Fe atom coordinated to four Cys—SH groups to more complex Fe-S centers with two or four Fe atoms **(Fig. 19–5)**. **Rieske iron-sulfur proteins** (named after their discoverer, John S. Rieske) are a variation on this theme, in which one Fe atom is coordinated to two His residues rather than two Cys residues. All iron-sulfur proteins participate in one-electron transfers in which one iron atom of the iron-sulfur cluster is oxidized or reduced. At least eight Fe-S proteins function in mitochondrial electron transfer. The reduction potential of Fe-S proteins varies from −0.65 V to +0.45 V, depending on the microenvironment of the iron within the protein.

In the overall reaction catalyzed by the mitochondrial respiratory chain, electrons move from NADH, succinate, or some other primary electron donor through flavoproteins, ubiquinone, iron-sulfur proteins, and cytochromes, and finally to O_2. A look at the methods used to determine the sequence in which the carriers act is instructive, as the same general approaches have been used to study other electron-transfer chains, such as those of chloroplasts.

First, the standard reduction potentials of the individual electron carriers have been determined experimentally (Table 19–2). We would expect the carriers to function in order of increasing reduction potential, because electrons tend to flow spontaneously from carriers of lower $E'°$ to carriers of higher $E'°$. The order of carriers deduced by this method is NADH → Q → cytochrome *b* → cytochrome c_1 → cytochrome *c* → cytochrome *a* → cytochrome a_3 → O_2. Note, however, that the order of standard reduction potentials is not necessarily the same as the order of *actual* reduction potentials under cellular conditions, which depend on the concentration of reduced and oxidized forms (see

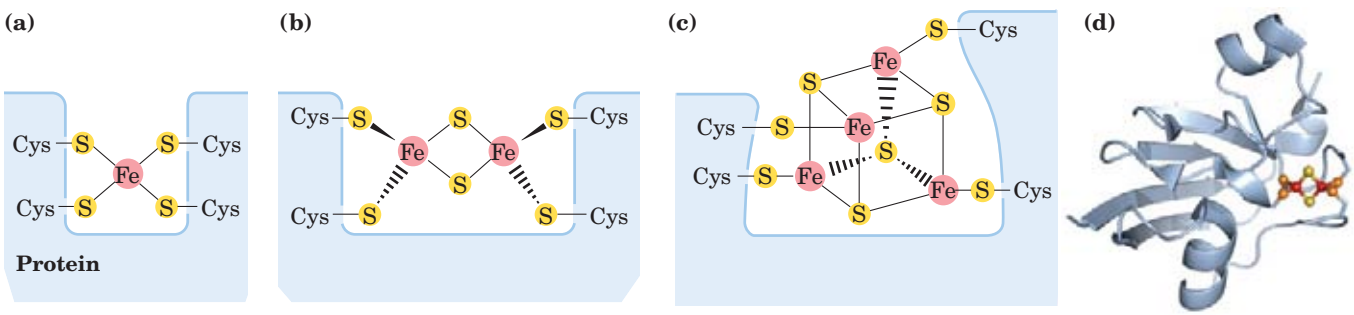

FIGURE 19–5 Iron-sulfur centers. The Fe-S centers of iron-sulfur proteins may be as simple as **(a)**, with a single Fe ion surrounded by the S atoms of four Cys residues. Other centers include both inorganic and Cys S atoms, as in **(b)** 2Fe-2S or **(c)** 4Fe-4S centers. **(d)** The ferredoxin of the cyanobacterium *Anabaena* 7120 has one 2Fe-2S center (PDB ID 1FRD); Fe is red, inorganic S is yellow, and the S of Cys is orange. (Note that in these designations only the inorganic S atoms are counted. For example, in the 2Fe-2S center **(b)**, each Fe ion is actually surrounded by four S atoms.) The exact standard reduction potential of the iron in these centers depends on the type of center and its interaction with the associated protein.

TABLE 19–2 Standard Reduction Potentials of Respiratory Chain and Related Electron Carriers

Redox reaction (half-reaction)	E'° (V)
$2H^+ + 2e^- \longrightarrow H_2$	−0.414
$NAD^+ + H^+ + 2e^- \longrightarrow NADH$	−0.320
$NADP^+ + H^+ + 2e^- \longrightarrow NADPH$	−0.324
NADH dehydrogenase (FMN) $+ 2H^+ + 2e^- \longrightarrow$ NADH dehydrogenase ($FMNH_2$)	−0.30
Ubiquinone $+ 2H^+ + 2e^- \longrightarrow$ ubiquinol	0.045
Cytochrome b (Fe^{3+}) $+ e^- \longrightarrow$ cytochrome b (Fe^{2+})	0.077
Cytochrome c_t (Fe^{3+}) $+ e^- \longrightarrow$ cytochrome c_t (Fe^{2+})	0.22
Cytochrome c (Fe^{3+}) $+ e^- \longrightarrow$ cytochrome c (Fe^{2+})	0.254
Cytochrome a (Fe^{3+}) $+ e^- \longrightarrow$ cytochrome a (Fe^{2+})	0.29
Cytochrome a_3 (Fe^{3+}) $+ e^- \longrightarrow$ cytochrome a_3 (Fe^{2+})	0.35
$\frac{1}{2}O_2 + 2H^+ + 2e^- \longrightarrow H_2O$	0.8166

Eqn 13–5, p. 515). A second method for determining the sequence of electron carriers involves reducing the entire chain of carriers experimentally by providing an electron source but no electron acceptor (no O_2). When O_2 is suddenly introduced into the system, the rate at which each electron carrier becomes oxidized (measured spectroscopically) reveals the order in which the carriers function. The carrier nearest O_2 (at the end of the chain) gives up its electrons first, the second carrier from the end is oxidized next, and so on. Such experiments have confirmed the sequence deduced from standard reduction potentials.

In a final confirmation, agents that inhibit the flow of electrons through the chain have been used in combination with measurements of the degree of oxidation of each carrier. In the presence of O_2 and an electron donor, carriers that function before the inhibited step become fully reduced, and those that function after this step are completely oxidized **(Fig. 19–6)**. By using several inhibitors that block different steps in the chain, investigators have determined the entire sequence; it is the same as deduced in the first two approaches.

Electron Carriers Function in Multienzyme Complexes

The electron carriers of the respiratory chain are organized into membrane-embedded supramolecular complexes that can be physically separated. Gentle treatment of the inner mitochondrial membrane with detergents allows the resolution of four unique electron-carrier complexes, each capable of catalyzing electron transfer through a portion of the chain (Table 19–3; **Fig. 19–7**). Complexes I and II catalyze electron transfer to ubiquinone from two different electron donors: NADH (Complex I) and succinate (Complex II). Complex III carries electrons from reduced ubiquinone to cytochrome c, and Complex IV completes the sequence by transferring electrons from cytochrome c to O_2.

We now look in more detail at the structure and function of each complex of the mitochondrial respiratory chain.

Complex I: NADH to Ubiquinone **Figure 19–8** illustrates the relationship between Complexes I and II and ubiquinone. **Complex I**, also called **NADH:ubiquinone**

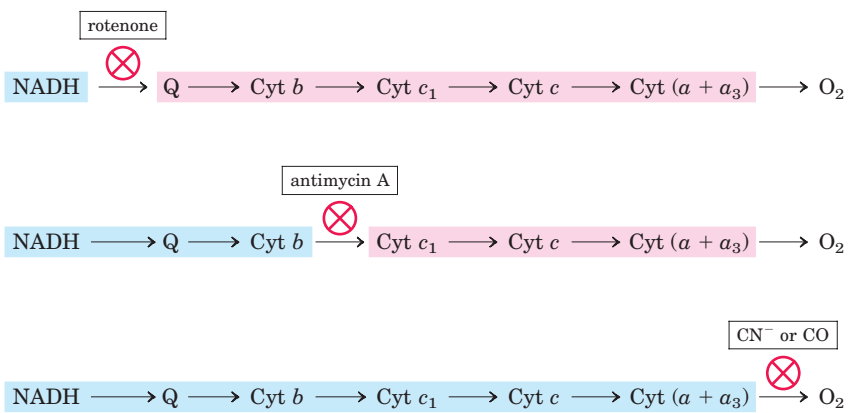

FIGURE 19–6 Method for determining the sequence of electron carriers. This method measures the effects of inhibitors of electron transfer on the oxidation state of each carrier. In the presence of an electron donor and O_2, each inhibitor causes a characteristic pattern of oxidized/reduced carriers: those before the block become reduced (blue), and those after the block become oxidized (pink).

TABLE 19–3 The Protein Components of the Mitochondrial Electron-Transfer Chain

	Enzyme complex/protein	Mass (kDa)	Number of subunits*	Prosthetic group(s)
I	NADH dehydrogenase	850	43 (14)	FMN, Fe-S
II	Succinate dehydrogenase	140	4	FAD, Fe-S
III	Ubiquinone:cytochrome *c* oxidoreductase	250	11	Hemes, Fe-S
	Cytochrome *c*†	13	1	Heme
IV	Cytochrome oxidase	160	13 (3–4)	Hemes; Cu_A, Cu_B

*Numbers of subunits in the bacterial equivalents in parentheses.

†Cytochrome *c* is not part of an enzyme complex; it moves between Complexes III and IV as a freely soluble protein.

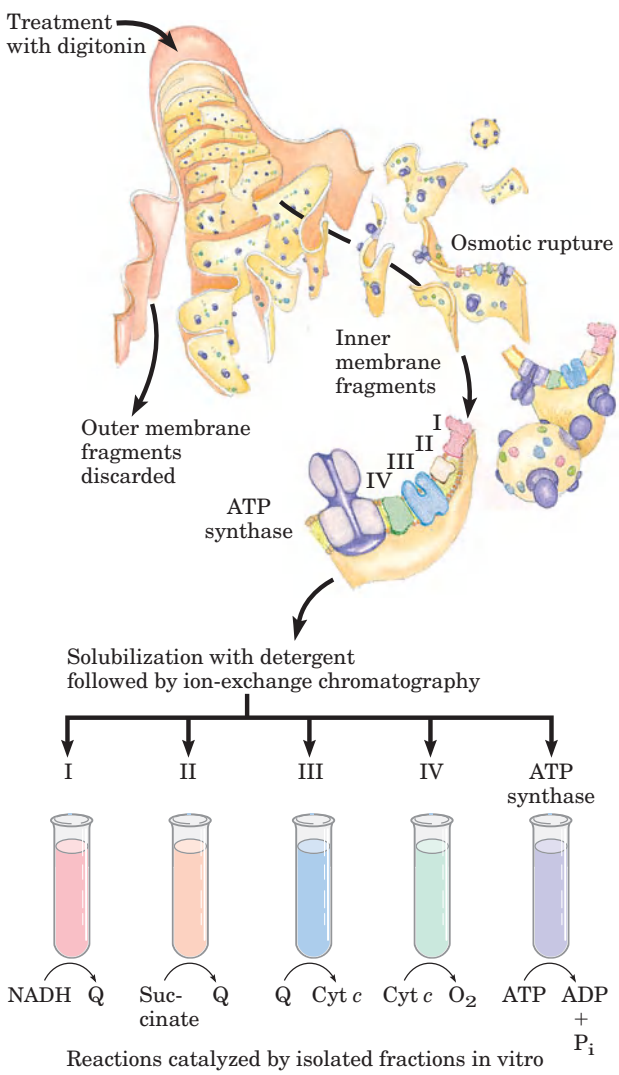

FIGURE 19–7 Separation of functional complexes of the respiratory chain. The outer mitochondrial membrane is first removed by treatment with the detergent digitonin. Fragments of inner membrane are then obtained by osmotic rupture of the mitochondria, and the fragments are gently dissolved in a second detergent. The resulting mixture of inner membrane proteins is resolved by ion-exchange chromatography into different complexes (I through IV) of the respiratory chain, each with its unique protein composition (see Table 19–3), and the enzyme ATP synthase (sometimes called Complex V). The isolated Complexes I through IV catalyze transfers between donors (NADH and succinate), intermediate carriers (Q and cytochrome *c*), and O_2, as shown. In vitro, isolated ATP synthase has only ATP-hydrolyzing (ATPase), not ATP-synthesizing, activity.

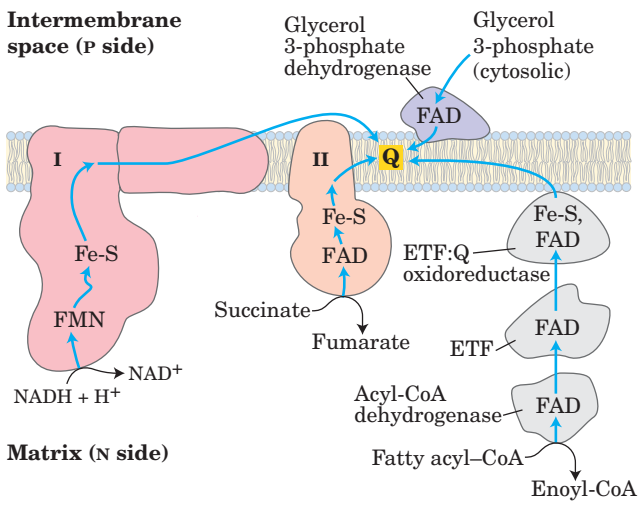

FIGURE 19–8 Path of electrons from NADH, succinate, fatty acyl–CoA, and glycerol 3-phosphate to ubiquinone. Electrons from NADH pass through a flavoprotein to a series of iron-sulfur proteins (in Complex I) and then to Q. Electrons from succinate pass through a flavoprotein and several Fe-S centers (in Complex II) on the way to Q. Glycerol 3-phosphate donates electrons to a flavoprotein (glycerol 3-phosphate dehydrogenase) on the outer face of the inner mitochondrial membrane, from which they pass to Q. Acyl-CoA dehydrogenase (the first enzyme of β oxidation) transfers electrons to electron-transferring flavoprotein (ETF), from which they pass to Q via ETF:ubiquinone oxidoreductase.

oxidoreductase or **NADH dehydrogenase**, is a large enzyme composed of 42 different polypeptide chains, including an FMN-containing flavoprotein and at least six iron-sulfur centers. High-resolution electron microscopy shows Complex I to be L-shaped, with one arm of the L in the membrane and the other extending into the matrix. As shown in **Figure 19–9**, Complex I catalyzes two simultaneous and obligately coupled processes: (1) the exergonic transfer to ubiquinone of a hydride ion from NADH and a proton from the matrix, expressed by

$$NADH + H^+ + Q \longrightarrow NAD^+ + QH_2 \qquad (19–1)$$

and (2) the endergonic transfer of four protons from the matrix to the intermembrane space. Complex I is therefore a proton pump driven by the energy of electron transfer, and the reaction it catalyzes is **vectorial**: it moves protons in a specific direction from one location (the matrix, which becomes negatively charged with the

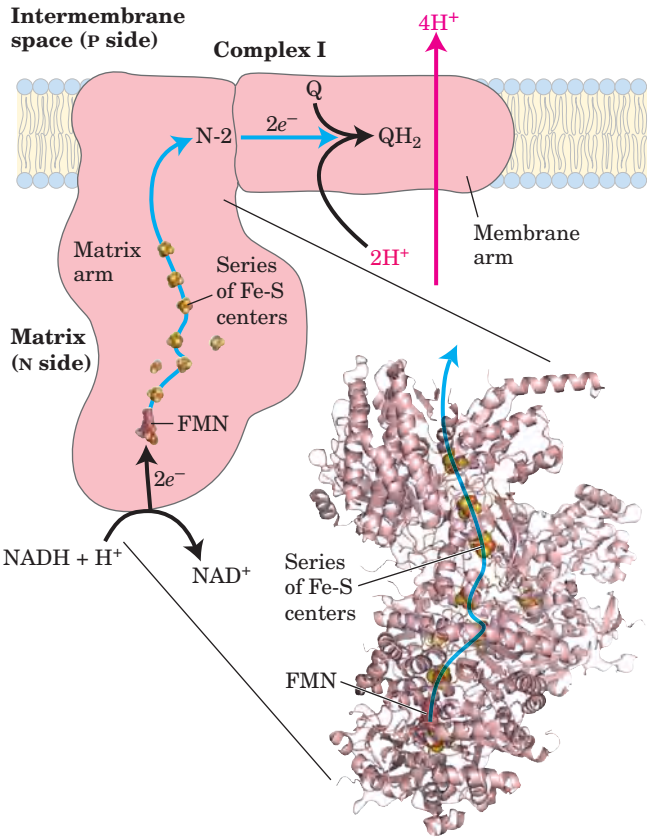

FIGURE 19–9 **NADH:ubiquinone oxidoreductase (Complex I).** Complex I catalyzes the transfer of a hydride ion from NADH to FMN, from which two electrons pass through a series of Fe-S centers to the iron-sulfur protein N-2 in the matrix arm of the complex. The domain that extends into the matrix has been crystallized and its structure solved (PDB ID 2FUG); the structure of the membrane domain of Complex I is not yet known. Electron transfer from N-2 to ubiquinone on the membrane arm forms QH_2, which diffuses into the lipid bilayer. This electron transfer also drives the expulsion from the matrix of four protons per pair of electrons. The detailed mechanism that couples electron and proton transfer in Complex I is not yet known, but probably involves a Q cycle similar to that in Complex III in which QH_2 participates twice per electron pair (see Fig. 19–12). Proton flux produces an electrochemical potential across the inner mitochondrial membrane (N side negative, P side positive), which conserves some of the energy released by the electron-transfer reactions. This electrochemical potential drives ATP synthesis.

departure of protons) to another (the intermembrane space, which becomes positively charged). To emphasize the vectorial nature of the process, the overall reaction is often written with subscripts that indicate the location of the protons: P for the positive side of the inner membrane (the intermembrane space), N for the negative side (the matrix):

$$NADH + 5H^+_N + Q \longrightarrow NAD^+ + QH_2 + 4H^+_P \quad (19–2)$$

Amytal (a barbiturate drug), rotenone (a plant product commonly used as an insecticide), and piericidin A (an antibiotic) inhibit electron flow from the Fe-S centers of Complex I to ubiquinone (Table 19–4) and therefore block the overall process of oxidative phosphorylation.

Ubiquinol (QH_2, the fully reduced form; Fig. 19–2) diffuses in the inner mitochondrial membrane from Complex I to Complex III, where it is oxidized to Q in a process that also involves the outward movement of H^+.

TABLE 19–4 **Agents That Interfere with Oxidative Phosphorylation or Photophosphorylation**

Type of interference	Compound*	Target/mode of action
Inhibition of electron transfer	Cyanide, Carbon monoxide	Inhibit cytochrome oxidase
	Antimycin A	Blocks electron transfer from cytochrome *b* to cytochrome c_1
	Myxothiazol, Rotenone, Amytal, Piericidin A	Prevent electron transfer from Fe-S center to ubiquinone
	DCMU	Competes with Q_B for binding site in PSII
Inhibition of ATP synthase	Aurovertin	Inhibits F_1
	Oligomycin, Venturicidin	Inhibit F_o and CF_o
	DCCD	Blocks proton flow through F_o and CF_o
Uncoupling of phosphorylation from electron transfer	FCCP, DNP	Hydrophobic proton carriers
	Valinomycin	K^+ ionophore
	Thermogenin	In brown adipose tissue, forms proton-conducting pores in inner mitochondrial membrane
Inhibition of ATP-ADP exchange	Atractyloside	Inhibits adenine nucleotide translocase

*DCMU is 3-(3,4-dichlorophenyl)-1,1-dimethylurea; DCCD, dicyclohexylcarbodiimide; FCCP, cyanide-*p*-trifluoromethoxyphenylhydrazone; DNP, 2,4-dinitrophenol.

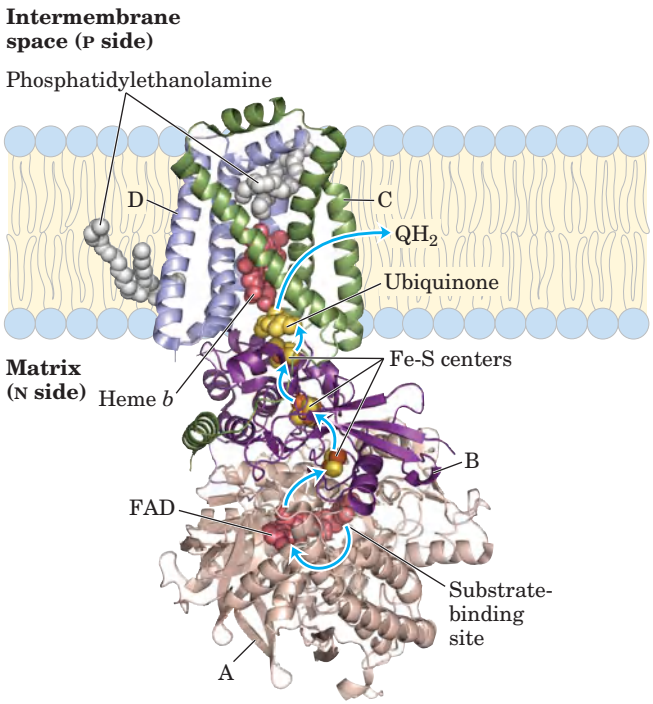

FIGURE 19–10 Structure of Complex II (succinate dehydrogenase). (PDB ID 1ZOY) This complex (shown here is the porcine heart enzyme) has two transmembrane subunits, C and D; the cytoplasmic extensions contain subunits A and B. Just behind the FAD in subunit A is the binding site for succinate. Subunit B has three sets of Fe-S centers; ubiquinone is bound to subunit B; and heme *b* is sandwiched between subunits C and D. Two phosphatidylethanolamine molecules are so tightly bound to subunit D that they show up in the crystal structure. Electrons move (blue arrows) from succinate to FAD, then through the three Fe-S centers to ubiquinone. The heme *b* is not on the main path of electron transfer but protects against the formation of reactive oxygen species (ROS) by electrons that go astray.

Complex II: Succinate to Ubiquinone We encountered **Complex II** in Chapter 16 as **succinate dehydrogenase**, the only membrane-bound enzyme in the citric acid cycle (p. 628). Although smaller and simpler than Complex I, it contains five prosthetic groups of two types and four different protein subunits **(Fig. 19–10)**. Subunits C and D are integral membrane proteins, each with three transmembrane helices. They contain a heme group, heme *b*, and a binding site for ubiquinone, the final electron acceptor in the reaction catalyzed by Complex II. Subunits A and B extend into the matrix; they contain three 2Fe-2S centers, bound FAD, and a binding site for the substrate, succinate. The path of electron transfer from the succinate-binding site to FAD, then through the Fe-S centers to the Q-binding site, is more than 40 Å long, but none of the individual electron-transfer distances exceeds about 11 Å—a reasonable distance for rapid electron transfer (Fig. 19–10).

The heme *b* of Complex II is apparently not in the direct path of electron transfer; it may serve instead to reduce the frequency with which electrons "leak" out of the system, moving from succinate to molecular oxygen to produce the **reactive oxygen species (ROS)** hydrogen peroxide (H_2O_2) and the **superoxide radical** ($^{\bullet}O_2^-$), as described below. Humans with point mutations in Complex II subunits near heme *b* or the quinone-binding site suffer from hereditary paraganglioma. This inherited condition is characterized by benign tumors of the head and neck, commonly in the carotid body, an organ that senses O_2 levels in the blood. These mutations result in greater production of ROS and perhaps greater tissue damage during succinate oxidation. ■

Other substrates for mitochondrial dehydrogenases pass electrons into the respiratory chain at the level of ubiquinone, but not through Complex II. The first step in the β oxidation of fatty acyl–CoA, catalyzed by the flavoprotein **acyl-CoA dehydrogenase** (see Fig. 17–8), involves transfer of electrons from the substrate to the FAD of the dehydrogenase, then to electron-transferring flavoprotein (ETF), which in turn passes its electrons to **ETF:ubiquinone oxidoreductase** (Fig. 19–8). This enzyme transfers electrons into the respiratory chain by reducing ubiquinone. Glycerol 3-phosphate, formed either from glycerol released by triacylglycerol breakdown or by the reduction of dihydroxyacetone phosphate from glycolysis, is oxidized by **glycerol 3-phosphate dehydrogenase** (see Fig. 17–4). This enzyme is a flavoprotein located on the outer face of the inner mitochondrial membrane, and like succinate dehydrogenase and acyl-CoA dehydrogenase it channels electrons into the respiratory chain by reducing ubiquinone (Fig. 19–8). The important role of glycerol 3-phosphate dehydrogenase in shuttling reducing equivalents from cytosolic NADH into the mitochondrial matrix is described in Section 19.2 (see Fig. 19–30). The effect of each of these electron-transferring enzymes is to contribute to the pool of reduced ubiquinone. QH_2 from all these reactions is reoxidized by Complex III.

Complex III: Ubiquinone to Cytochrome *c* The next respiratory complex, **Complex III**, also called **cytochrome bc_1 complex** or **ubiquinone:cytochrome *c* oxidoreductase**, couples the transfer of electrons from ubiquinol (QH_2) to cytochrome *c* with the vectorial transport of protons from the matrix to the intermembrane space. The determinations of the complete structure of this huge complex **(Fig. 19–11)** and of Complex IV (below) by x-ray crystallography, achieved between 1995 and 1998, were landmarks in the study of mitochondrial electron transfer, providing the structural framework to integrate the many biochemical observations on the functions of the respiratory complexes.

The functional unit of Complex III is a dimer, with the two monomeric units of cytochrome *b* surrounding a "cavern" in the middle of the membrane, in which ubiquinone is free to move from the matrix side of the membrane (site Q_N on one monomer) to the intermembrane space (site Q_P of the other monomer) as it shuttles electrons and protons across the inner mitochondrial membrane (Fig. 19–11b).

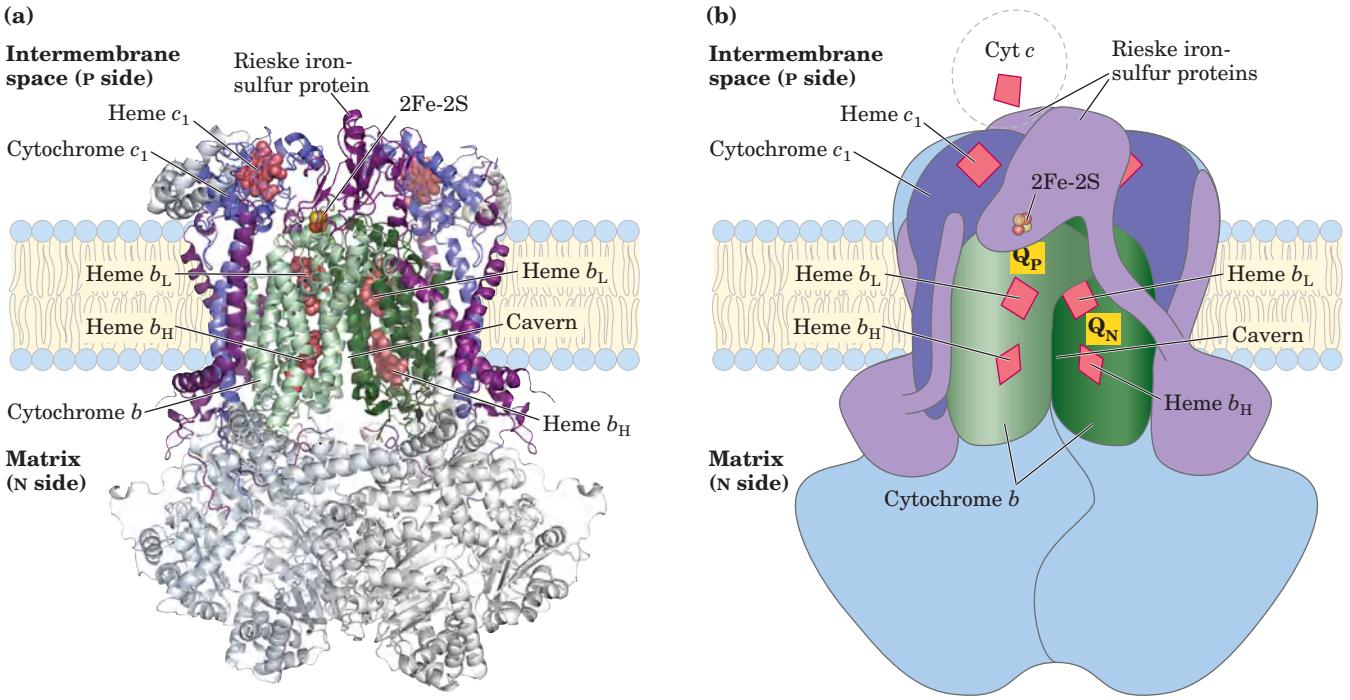

FIGURE 19–11 Cytochrome bc_1 complex (Complex III). The complex is a dimer of identical monomers, each with 11 different subunits. **(a)** The functional core of each monomer is three subunits: cytochrome b (green) with its two hemes (b_H and b_L); the Rieske iron-sulfur protein (purple) with its 2Fe-2S centers; and cytochrome c_1 (blue) with its heme (PDB ID 1BGY). **(b)** This cartoon view of the complex shows how cytochrome c_1 and the Rieske iron-sulfur protein project from the P surface and can interact with cytochrome c (not part of the functional complex) in the intermembrane space. The complex has two distinct binding sites for ubiquinone, Q_N and Q_P, which correspond to the sites of inhibition by two drugs that block oxidative phosphorylation. Antimycin A, which blocks electron flow from heme b_H to Q, binds at Q_N, close to heme b_H on the N (matrix) side of the membrane. Myxothiazol, which prevents electron flow from QH_2 to the Rieske iron-sulfur protein, binds at Q_P, near the 2Fe-2S center and heme b_L on the P side. The dimeric structure is essential to the function of Complex III. The interface between monomers forms two caverns, each containing a Q_P site from one monomer and a Q_N site from the other. The ubiquinone intermediates move within these sheltered caverns.

Complex III crystallizes in two distinct conformations (not shown). In one, the Rieske Fe-S center is close to its electron acceptor, the heme of cytochrome c_1, but relatively distant from cytochrome b and the QH_2-binding site at which the Rieske Fe-S center receives electrons. In the other, the Fe-S center has moved away from cytochrome c_1 and toward cytochrome b. The Rieske protein is thought to oscillate between these two conformations as it is first reduced, then oxidized.

Based on the structure of Complex III and detailed biochemical studies of the redox reactions, a reasonable model, the **Q cycle**, has been proposed for the passage of electrons and protons through the complex. The net equation for the redox reactions of the Q cycle **(Fig. 19–12)** is

$$QH_2 + 2 \text{ cyt } c_1 \text{ (oxidized)} + 2H^+_N \longrightarrow Q + 2 \text{ cyt } c_1 \text{ (reduced)} + 4H^+_P \quad (19–3)$$

The Q cycle accommodates the switch between the two-electron carrier ubiquinone and the one-electron carriers—cytochromes b_{562}, b_{566}, c_1, and c—and explains the measured stoichiometry of four protons translocated per pair of electrons passing through Complex III to cytochrome c. Although the path of electrons through this segment of the respiratory chain is complicated, the net effect of the transfer is simple: QH_2 is oxidized to Q and two molecules of cytochrome c are reduced.

Cytochrome c is a soluble protein of the intermembrane space. After its single heme accepts an electron from Complex III, cytochrome c moves to Complex IV to donate the electron to a binuclear copper center.

Complex IV: Cytochrome c to O_2 In the final step of the respiratory chain, **Complex IV**, also called **cytochrome oxidase**, carries electrons from cytochrome c to molecular oxygen, reducing it to H_2O. Complex IV is a large enzyme (13 subunits; M_r 204,000) of the inner mitochondrial membrane. Bacteria contain a form that is much simpler, with only three or four subunits, but still capable of catalyzing both electron transfer and proton pumping. Comparison of the mitochondrial and bacterial complexes suggests that three subunits are critical to the function **(Fig. 19–13)**.

Mitochondrial subunit II contains two Cu ions complexed with the —SH groups of two Cys residues in a binuclear center (Cu_A; Fig. 19–13b) that resembles the 2Fe-2S centers of iron-sulfur proteins. Subunit I contains two heme groups, designated a and a_3, and another copper ion (Cu_B). Heme a_3 and Cu_B form a second

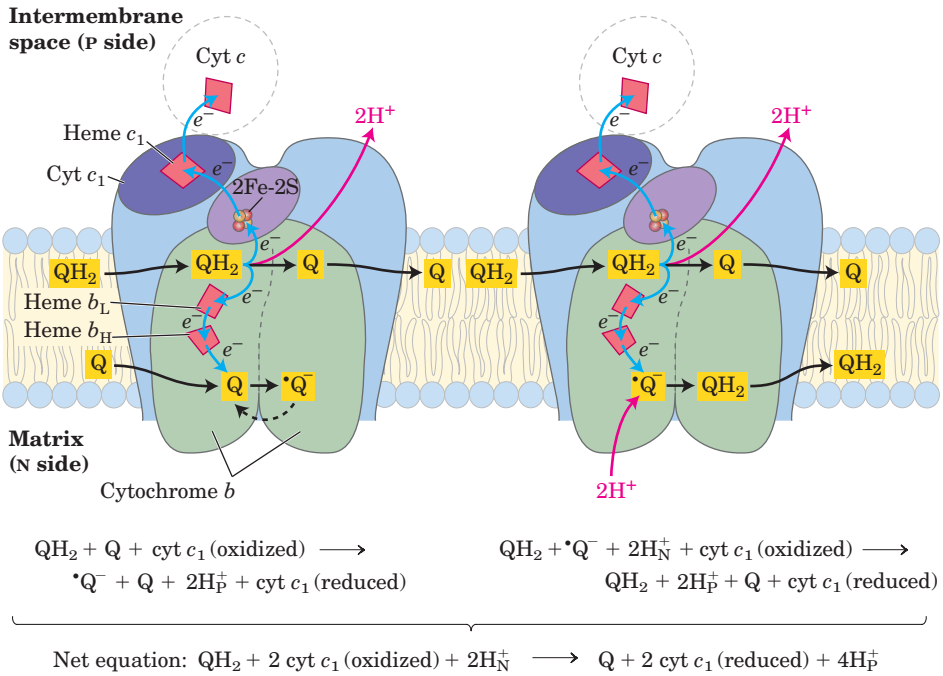

FIGURE 19–12 The Q cycle, shown in two stages. The path of electrons through Complex III is shown by blue arrows. In the first stage (left), Q on the N side is reduced to the semiquinone radical, which in the second stage (right) is converted to QH_2. Meanwhile, on the P side of the membrane, two molecules of QH_2 are oxidized to Q, releasing two protons per Q molecule (four protons in all) into the intermembrane space. Each QH_2 donates one electron (via the Rieske Fe-S center) to cytochrome c_1, and one electron (via cytochrome *b*) to a molecule of Q near the N side, reducing it in two steps to QH_2. This reduction also uses two protons per Q, which are taken up from the matrix.

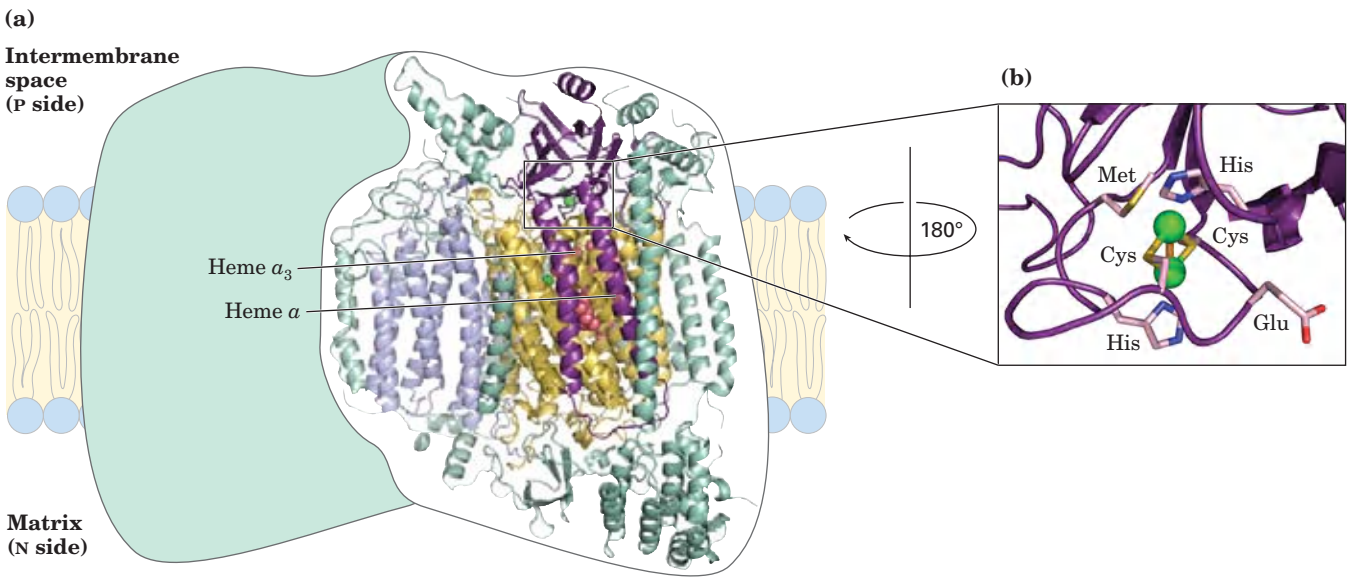

FIGURE 19–13 Structure of cytochrome oxidase (Complex IV). This complex from bovine mitochondria has 13 subunits, but only four core proteins are shown here (PDB ID 1OCC). **(a)** Complex IV, with four subunits in each of two identical units of a dimer. Subunit I (yellow) has two heme groups, *a* and a_3, near a single copper ion, Cu_B (green sphere). Heme a_3 and Cu_B form a binuclear Fe-Cu center. Subunit II (purple) contains two Cu ions complexed with the —SH groups of two Cys residues in a binuclear center, Cu_A, that resembles the 2Fe-2S centers of iron-sulfur proteins. This binuclear center and the cytochrome *c*–binding site are located in a domain of subunit II that protrudes from the P side of the inner membrane (into the intermembrane space). Subunit III (light blue) is essential for rapid proton movement through subunit II. The role of subunit IV (green) is not yet known. **(b)** The binuclear center of Cu_A. The Cu ions share electrons equally. When the center is reduced, the ions have the formal charges $Cu^{1+}Cu^{1+}$; when oxidized, $Cu^{1.5+}Cu^{1.5+}$. Six amino acids residues are ligands around the Cu ions: two His, two Cys, Glu, and Met.

binuclear center that accepts electrons from heme *a* and transfers them to O_2 bound to heme a_3.

Electron transfer through Complex IV is from cytochrome *c* to the Cu_A center, to heme *a*, to the heme a_3–Cu_B center, and finally to O_2 **(Fig. 19–14)**. For every four electrons passing through this complex, the enzyme consumes four "substrate" H^+ from the matrix (N side) in converting O_2 to $2H_2O$. It also uses the energy of this redox reaction to pump one proton outward into the intermembrane space (P side) for each electron that passes through, adding to the electrochemical potential produced by redox-driven proton transport through Complexes I and III. The overall reaction catalyzed by Complex IV is

$$4\ \text{Cyt}\ c\ (\text{reduced}) + 8H^+_N + O_2 \longrightarrow 4\ \text{cyt}\ c\ (\text{oxidized}) + 4H^+_P + 2H_2O \quad (19\text{–}4)$$

This four-electron reduction of O_2 involves redox centers that carry only one electron at a time, and it must occur without the release of incompletely reduced intermediates such as hydrogen peroxide or hydroxyl free radicals—very reactive species that would damage cellular components. The intermediates remain tightly bound to the complex until completely converted to water.

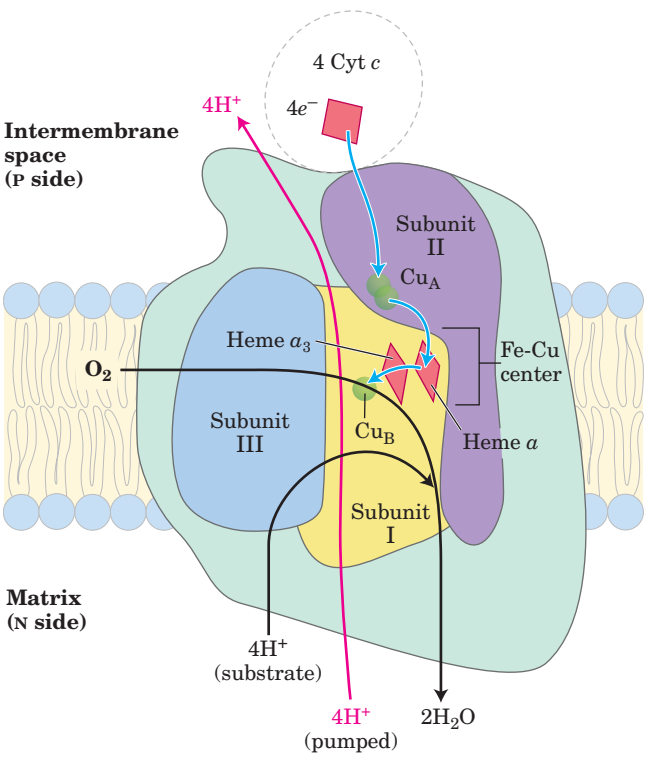

FIGURE 19–14 Path of electrons through Complex IV. The three proteins critical to electron flow are subunits I, II, and III. The larger green structure includes the other 10 proteins in the complex. Electron transfer through Complex IV begins with cytochrome *c* (top). Two molecules of reduced cytochrome *c* each donate an electron to the binuclear center Cu_A. From here electrons pass through heme *a* to the Fe-Cu center (cytochrome a_3 and Cu_B). Oxygen now binds to heme a_3 and is reduced to its peroxy derivative (O_2^{2-}; not shown here) by two electrons from the Fe-Cu center. Delivery of two more electrons from cytochrome *c* (top, making four electrons in all) converts the O_2^{2-} to two molecules of water, with consumption of four "substrate" protons from the matrix. At the same time, four protons are pumped from the matrix by an as yet unknown mechanism.

Mitochondrial Complexes May Associate in Respirasomes

There is growing experimental evidence that in the intact mitochondrion, the respiratory complexes tightly associate with each other in the inner membrane to form **respirasomes**, functional combinations of two or more electron-transfer complexes. For example, when complex III is gently extracted from mitochondrial membranes, it is found to be associated with Complex I and remains associated during gentle electrophoresis. Supercomplexes of Complex III and IV can also be isolated, and when viewed with the electron microscope are of the right size and shape to accommodate the crystal structures of both complexes **(Fig. 19–15)**. The kinetics of electron flow through the series of respiratory complexes would be very different in the two extreme cases of tight versus no association: (1) if complexes were tightly associated, electron transfers would essentially occur through a solid state; and (2) if the complexes functioned separately, electrons would be carried between them by ubiquinone and cytochrome *c*. The kinetic evidence supports electron transfer through a solid state, and thus the respirasome model.

Cardiolipin, the lipid that is especially abundant in the inner mitochondrial membrane (see Figs 10–9 and 11–2), may be critical to the integrity of respirasomes; its removal with detergents, or its absence in certain yeast mutants, results in defective mitochondrial electron transfer and a loss of affinity between the respiratory complexes.

The Energy of Electron Transfer Is Efficiently Conserved in a Proton Gradient

The transfer of two electrons from NADH through the respiratory chain to molecular oxygen can be written as

$$\text{NADH} + H^+ + \tfrac{1}{2}O_2 \longrightarrow \text{NAD}^+ + H_2O \quad (19\text{–}5)$$

This net reaction is highly exergonic. For the redox pair NAD^+/NADH, E'° is −0.320 V, and for the pair O_2/H_2O, E'° is 0.816 V. The $\Delta E'^\circ$ for this reaction is therefore 1.14 V, and the standard free-energy change (see Eqn 13–7, p. 515) is

$$\begin{aligned}\Delta G'^\circ &= -n\mathcal{F}\Delta E'^\circ \quad (19\text{–}6)\\ &= -2(96.5\ \text{kJ/V}\cdot\text{mol})(1.14\ \text{V})\\ &= -220\ \text{kJ/mol (of NADH)}\end{aligned}$$

This *standard* free-energy change is based on the assumption of equal concentrations (1 M) of NADH and

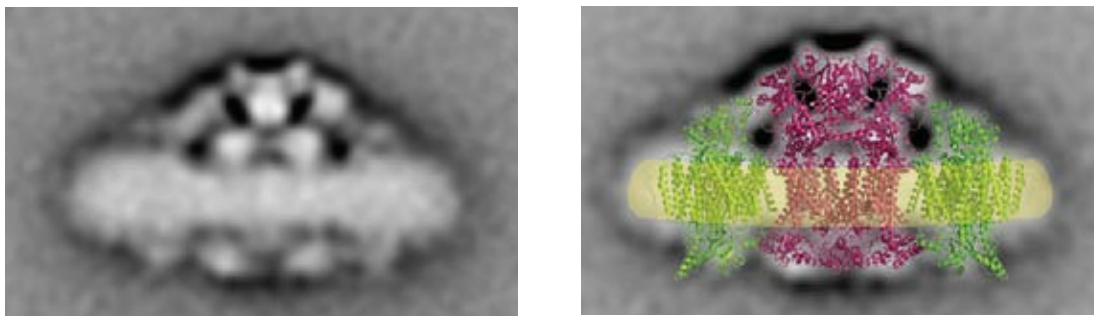

(a) **(b)**

FIGURE 19–15 A putative respirasome composed of Complexes III and IV. (a) Purified supercomplexes containing Complexes III and IV, from yeast, visualized by electron microscopy after staining with uranyl acetate. The electron densities of hundreds of images were averaged to yield this composite view. **(b)** The x-ray structures of one molecule of Complex III (red; from yeast) and two of Complex IV (green; from bovine heart) could be fitted to the electron-density map to suggest one possible mode of interaction of these complexes in a respirasome. This view is in the plane of the bilayer (yellow).

NAD^+. In actively respiring mitochondria, the actions of many dehydrogenases keep the actual [NADH]/[NAD^+] ratio well above unity, and the real free-energy change for the reaction shown in Equation 19–5 is therefore substantially greater (more negative) than −220 kJ/mol. A similar calculation for the oxidation of succinate shows that electron transfer from succinate ($E'°$ for fumarate/succinate = 0.031 V) to O_2 has a smaller, but still negative, standard free-energy change of about −150 kJ/mol.

Much of this energy is used to pump protons out of the matrix. For each pair of electrons transferred to O_2, four protons are pumped out by Complex I, four by Complex III, and two by Complex IV **(Fig. 19–16)**. The *vectorial* equation for the process is therefore

$$NADH + 11H_N^+ + \tfrac{1}{2}O_2 \longrightarrow NAD^+ + 10H_P^+ + H_2O \quad (19–7)$$

The electrochemical energy inherent in this difference in proton concentration and separation of charge

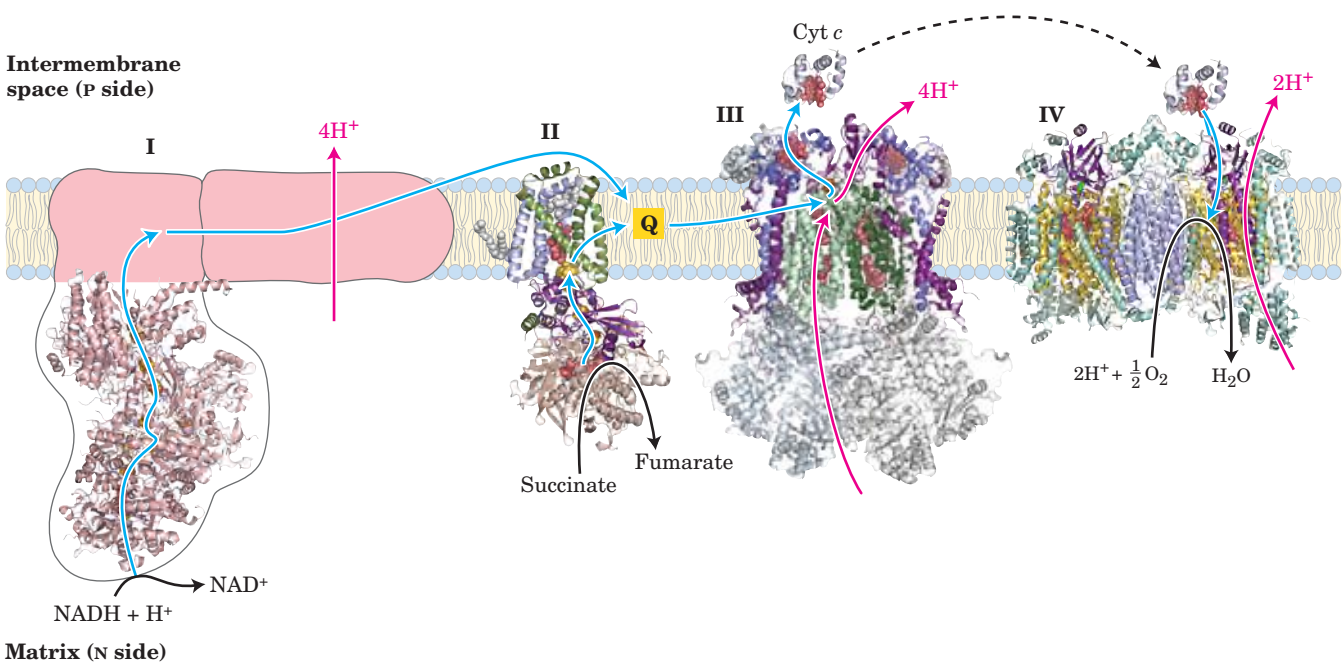

FIGURE 19–16 Summary of the flow of electrons and protons through the four complexes of the respiratory chain. Electrons reach Q through Complexes I and II. The reduced Q (QH_2) serves as a mobile carrier of electrons and protons. It passes electrons to Complex III, which passes them to another mobile connecting link, cytochrome *c*. Complex IV then transfers electrons from reduced cytochrome *c* to O_2. Electron flow through Complexes I, III, and IV is accompanied by proton flow from the matrix to the intermembrane space. Recall that electrons from β oxidation of fatty acids can also enter the respiratory chain through Q (see Fig. 19–8). The structures shown here are from several sources: Complex I, *Thermus thermophilus* (PDB ID 2FUG); Complex II, porcine heart (PDB ID 1ZOY); Complex III, bovine heart (PDB ID 1BGY); cytochrome *c*, equine heart (PDB ID 1HRC); Complex IV, bovine heart (PDB ID 1OCC).

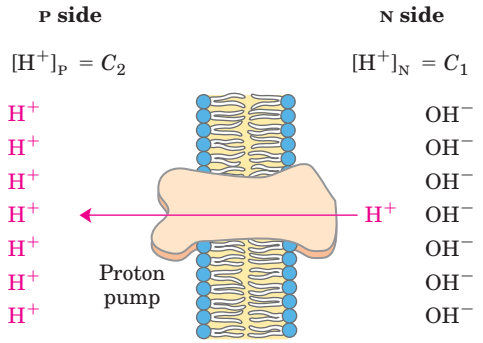

FIGURE 19–17 Proton-motive force. The inner mitochondrial membrane separates two compartments of different $[H^+]$, resulting in differences in chemical concentration (ΔpH) and charge distribution ($\Delta\psi$) across the membrane. The net effect is the proton-motive force (ΔG), which can be calculated as shown here. This is explained more fully in the text.

represents a temporary conservation of much of the energy of electron transfer. The energy stored in such a gradient, termed the **proton-motive force**, has two components: (1) the *chemical potential energy* due to the difference in concentration of a chemical species (H^+) in the two regions separated by the membrane, and (2) the *electrical potential energy* that results from the separation of charge when a proton moves across the membrane without a counterion **(Fig. 19–17)**.

As we showed in Chapter 11, the free-energy change for the creation of an electrochemical gradient by an ion pump is

$$\Delta G = RT \ln\left(\frac{C_2}{C_1}\right) + Z\mathcal{F}\Delta\psi \qquad (19\text{–}8)$$

where C_2 and C_1 are the concentrations of an ion in two regions, and $C_2 > C_1$; Z is the absolute value of its electrical charge (1 for a proton); and $\Delta\psi$ is the transmembrane difference in electrical potential, measured in volts.

For protons at 25 °C,

$$\ln\left(\frac{C_2}{C_1}\right) = 2.3(\log [H^+]_P - \log [H^+]_N)$$

$$= 2.3(pH_N - pH_P) = 2.3\ \Delta pH$$

and Equation 19–8 reduces to

$$\Delta G = 2.3RT\ \Delta pH + \mathcal{F}\Delta\psi \qquad (19\text{–}9)$$
$$= (5.70\ \text{kJ/mol})\Delta pH + (96.5\ \text{kJ/V}\cdot\text{mol})\Delta\psi$$

In actively respiring mitochondria, the measured $\Delta\psi$ is 0.15 to 0.20 V and the pH of the matrix is about 0.75 units more alkaline than that of the intermembrane space.

WORKED EXAMPLE 19–1 Energetics of Electron Transfer

Calculate the amount of energy conserved in the proton gradient across the inner mitochondrial membrane per pair of electrons transferred through the respiratory chain from NADH to oxygen. Assume $\Delta\psi$ is 0.15 V and the pH difference is 0.75 units.

Solution: Equation 19–9 gives the free-energy change when *one* mole of protons moves across the inner membrane. Substituting the measured values for ΔpH (0.75 units) and $\Delta\psi$ (0.15 V) in this equation gives ΔG = 19 kJ/mol (of protons). Because the transfer of two electrons from NADH to O_2 is accompanied by the outward pumping of 10 protons (Eqn 19–7), roughly 200 kJ (of the 220 kJ released by oxidation of 1 mol of NADH) is conserved in the proton gradient.

When protons flow spontaneously *down* their electrochemical gradient, energy is made available to do work. In mitochondria, chloroplasts, and aerobic bacteria, the electrochemical energy in the proton gradient drives the synthesis of ATP from ADP and P_i. We return to the energetics and stoichiometry of ATP synthesis driven by the electrochemical potential of the proton gradient in Section 19.2.

Reactive Oxygen Species Are Generated during Oxidative Phosphorylation

Several steps in the path of oxygen reduction in mitochondria have the potential to produce highly reactive free radicals that can damage cells. The passage of electrons from QH_2 to Complex III, and passage of electrons from Complex I to QH_2, involve the radical $^{\bullet}Q^-$ as an intermediate. The $^{\bullet}Q^-$ can, with a low probability, pass an electron to O_2 in the reaction

$$O_2 + e^- \longrightarrow {}^{\bullet}O_2^-$$

The superoxide free radical thus generated is highly reactive; its formation also leads to production of the even more reactive hydroxyl free radical, $^{\bullet}OH$ **(Fig. 19–18)**.

These reactive oxygen species can wreak havoc, reacting with and damaging enzymes, membrane lipids, and nucleic acids. In actively respiring mitochondria, 0.1% to as much as 4% of the O_2 used in respiration forms $^{\bullet}O_2^-$—more than enough to have lethal effects unless the free radical is quickly disposed of. Factors that slow the flow of electrons through the respiratory chain increase the formation of superoxide, perhaps by prolonging the lifetime of $^{\bullet}O_2^-$ generated in the Q cycle.

To prevent oxidative damage by $^{\bullet}O_2^-$, cells have several forms of the enzyme **superoxide dismutase**, which catalyzes the reaction

$$2\ {}^{\bullet}O_2^- + 2H^+ \longrightarrow H_2O_2 + O_2$$

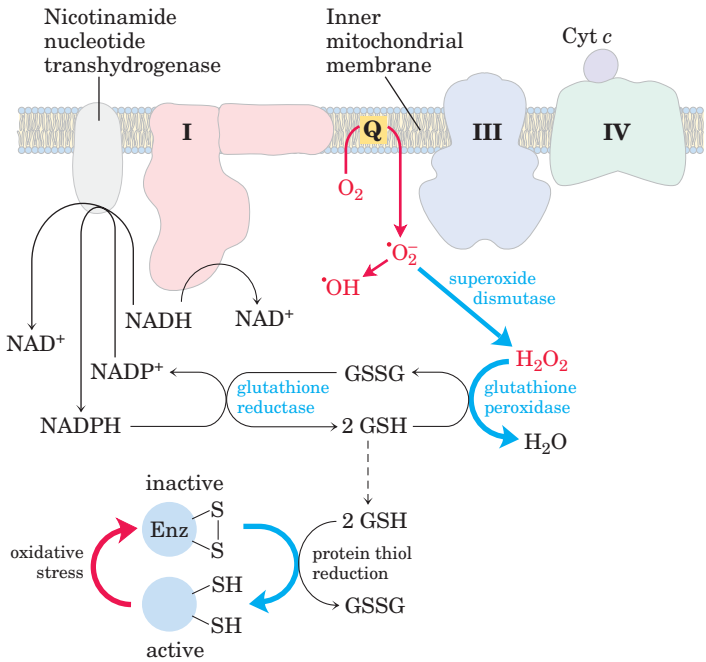

FIGURE 19–18 ROS formation in mitochondria and mitochondrial defenses. When the rate of electron entry into the respiratory chain and the rate of electron transfer through the chain are mismatched, superoxide radical ($\cdot O_2^-$) production increases at Complexes I and III as the partially reduced ubiquinone radical ($\cdot Q^-$) donates an electron to O_2. Superoxide acts on aconitase, a 4Fe-4S protein, to release Fe^{2+}. In the presence of Fe^{2+}, the Fenton reaction leads to formation of the highly reactive hydroxyl free radical ($\cdot OH$). The reactions shown in blue defend the cell against the damaging effects of superoxide. Reduced glutathione (GSH; see Fig. 22–27) donates electrons for the reduction of H_2O_2 and of the oxidized Cys residues (—S—S—) of enzymes and other proteins, and GSH is regenerated from the oxidized form (GSSG) by reduction with NADPH.

The hydrogen peroxide (H_2O_2) thus generated is rendered harmless by the action of **glutathione peroxidase** (Fig. 19–18). Glutathione reductase recycles the oxidized glutathione to its reduced form, using electrons from the NADPH generated by nicotinamide nucleotide transhydrogenase (in the mitochondrion) or by the pentose phosphate pathway (in the cytosol; see Fig. 14–20). Reduced glutathione also serves to keep protein sulfhydryl groups in their reduced state, preventing some of the deleterious effects of oxidative stress (Fig. 19–18). Nicotinamide nucleotide transhydrogenase is critical in this process: it produces the NADPH essential for glutathione reductase activity.

Plant Mitochondria Have Alternative Mechanisms for Oxidizing NADH

Plant mitochondria supply the cell with ATP during periods of low illumination or darkness by mechanisms entirely analogous to those used by nonphotosynthetic organisms. In the light, the principal source of mitochondrial NADH is a reaction in which glycine, produced by a process known as photorespiration, is converted to serine (see Fig. 20–21):

$$2\ \text{Glycine} + \text{NAD}^+ \longrightarrow \text{serine} + CO_2 + NH_3 + \text{NADH} + H^+$$

For reasons discussed in Chapter 20, plants must carry out this reaction even when they do not need NADH for ATP production. To regenerate NAD^+ from unneeded NADH, plant mitochondria transfer electrons from NADH directly to ubiquinone and from ubiquinone directly to O_2, bypassing Complexes III and IV and their proton pumps. In this process the energy in NADH is dissipated as heat, which can sometimes be of value to the plant (Box 19–1). Unlike cytochrome oxidase (Complex IV), the alternative QH_2 oxidase is not inhibited by cyanide. Cyanide-resistant NADH oxidation is therefore the hallmark of this unique plant electron-transfer pathway.

SUMMARY 19.1 Electron-Transfer Reactions in Mitochondria

- Chemiosmotic theory provides the intellectual framework for understanding many biological energy transductions, including oxidative phosphorylation and photophosphorylation. The mechanism of energy coupling is similar in both cases: the energy of electron flow is conserved by the concomitant pumping of protons across the membrane, producing an electrochemical gradient, the proton-motive force.
- In mitochondria, hydride ions removed from substrates by NAD-linked dehydrogenases donate electrons to the respiratory (electron-transfer) chain, which transfers the electrons to molecular O_2, reducing it to H_2O.
- Shuttle systems convey reducing equivalents from cytosolic NADH to mitochondrial NADH. Reducing equivalents from all NAD-linked dehydrogenations are transferred to mitochondrial NADH dehydrogenase (Complex I).
- Reducing equivalents are then passed through a series of Fe-S centers to ubiquinone, which transfers the electrons to cytochrome *b*, the first carrier in Complex III. In this complex, electrons take two separate paths through two *b*-type cytochromes and cytochrome c_1 to an Fe-S center. The Fe-S center passes electrons, one at a time, through cytochrome *c* and into Complex IV, cytochrome oxidase. This copper-containing enzyme, which also contains cytochromes *a* and a_3, accumulates electrons, then passes them to O_2, reducing it to H_2O.
- Some electrons enter this chain of carriers through alternative paths. Succinate is oxidized by succinate dehydrogenase (Complex II), which contains a flavoprotein that passes electrons

through several Fe-S centers to ubiquinone. Electrons derived from the oxidation of fatty acids pass to ubiquinone via the electron-transferring flavoprotein.

- Potentially harmful reactive oxygen species produced in mitochondria are inactivated by a set of protective enzymes, including superoxide dismutase and glutathione peroxidase.
- Plants, fungi, and unicellular eukaryotes have, in addition to the typical cyanide-sensitive path for electron transfer, an alternative, cyanide-resistant NADH oxidation pathway.

BOX 19–1 Hot, Stinking Plants and Alternative Respiratory Pathways

Many flowering plants attract insect pollinators by releasing odorant molecules that mimic an insect's natural food sources or potential egg-laying sites. Plants pollinated by flies or beetles that normally feed on or lay their eggs in dung or carrion sometimes use foul-smelling compounds to attract these insects.

One family of stinking plants is the Araceae, which includes philodendrons, arum lilies, and skunk cabbages. These plants have tiny flowers densely packed on an erect structure, the spadix, surrounded by a modified leaf, the spathe. The spadix releases odors of rotting flesh or dung. Before pollination the spadix also heats up, in some species to as much as 20 to 40 °C above the ambient temperature. Heat production (thermogenesis) helps evaporate odorant molecules for better dispersal, and because rotting flesh and dung are usually warm from the hyperactive metabolism of scavenging microbes, the heat itself might also attract insects. In the case of the eastern skunk cabbage (Fig. 1), which flowers in late winter or early spring when snow still covers the ground, thermogenesis allows the spadix to grow up through the snow.

How does a skunk cabbage heat its spadix? The mitochondria of plants, fungi, and unicellular eukaryotes have electron-transfer systems that are essentially the same as those in animals, but they also have an alternative respiratory pathway. A cyanide-resistant QH_2 oxidase transfers electrons from the ubiquinone pool directly to oxygen, bypassing the two proton-translocating steps of Complexes III and IV (Fig. 2). Energy that might have been conserved as ATP is instead released as heat. Plant mitochondria also

FIGURE 1 Eastern skunk cabbage.

have an alternative NADH dehydrogenase, insensitive to the Complex I inhibitor rotenone (see Table 19–4), that transfers electrons from NADH in the matrix directly to ubiquinone, bypassing Complex I and its associated proton pumping. And plant mitochondria have yet another NADH dehydrogenase, on the external face of the inner membrane, that transfers electrons from NADPH or NADH in the intermembrane space to ubiquinone, again bypassing Complex I. Thus when electrons enter the alternative respiratory pathway through the rotenone-insensitive NADH dehydrogenase, the external NADH dehydrogenase, or succinate dehydrogenase (Complex II), and pass to O_2 via the cyanide-resistant alternative oxidase, energy is not conserved as ATP but is released as heat. A skunk cabbage can use the heat to melt snow, produce a foul stench, or attract beetles or flies.

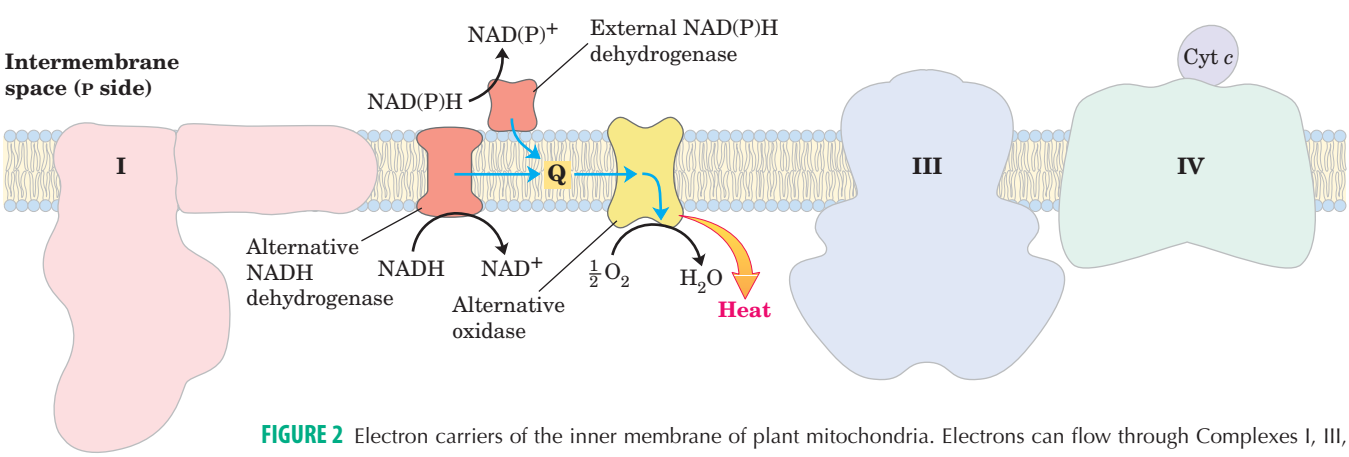

FIGURE 2 Electron carriers of the inner membrane of plant mitochondria. Electrons can flow through Complexes I, III, and IV, as in animal mitochondria, or through plant-specific alternative carriers by the paths shown with blue arrows.

19.2 ATP Synthesis

How is a concentration gradient of protons transformed into ATP? We have seen that electron transfer releases, and the proton-motive force conserves, more than enough free energy (about 200 kJ) per "mole" of electron pairs to drive the formation of a mole of ATP, which requires about 50 kJ (p. 503). Mitochondrial oxidative phosphorylation therefore poses no thermodynamic problem. But what is the chemical mechanism that couples proton flux with phosphorylation?

The **chemiosmotic model**, proposed by Peter Mitchell, is the paradigm for this mechanism. According to the model **(Fig. 19–19)**, the electrochemical energy inherent in the difference in proton concentration and the separation of charge across the inner mitochondrial membrane—the proton-motive force—drives the synthesis of ATP as protons flow passively back into the matrix through a proton pore associated with **ATP synthase**. To emphasize this crucial role of the proton-motive force, the equation for ATP synthesis is sometimes written

$$ADP + P_i + nH^+_P \longrightarrow ATP + H_2O + nH^+_N \quad (19\text{–}10)$$

Mitchell used "chemiosmotic" to describe enzymatic reactions that involve, simultaneously, a chemical reaction and a transport process. The operational definition of "coupling" is shown in **Figure 19–20**. When isolated mitochondria are suspended in a buffer containing ADP, P_i, and an oxidizable substrate such as succinate, three easily measured processes occur: (1) the substrate is oxidized (succinate yields fumarate), (2) O_2 is consumed, and (3) ATP is synthesized. Oxygen consumption and ATP synthesis depend on the presence of an oxidizable substrate (succinate in this case) as well as ADP and P_i.

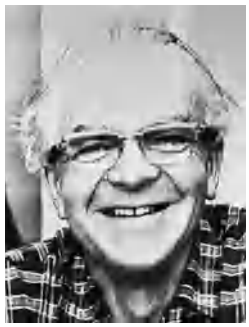

Peter Mitchell, 1920–1992

Because the energy of substrate oxidation drives ATP synthesis in mitochondria, we would expect inhibitors of the passage of electrons to O_2 (such as cyanide, carbon monoxide, and antimycin A) to block ATP synthesis (Fig. 19–20a). More surprising is the finding that the converse is also true: inhibition of ATP synthesis blocks electron transfer in intact mitochondria. This obligatory coupling can be demonstrated in isolated mitochondria by providing O_2 and oxidizable substrates, but not ADP (Fig. 19–20b). Under these conditions, no ATP synthesis can occur and electron transfer to O_2 does not proceed. Coupling of oxidation and phosphorylation can also be demonstrated using oligomycin or venturicidin, toxic antibiotics that bind to the ATP synthase in mitochondria. These compounds are potent inhibitors of both ATP synthesis *and* the transfer of electrons through the chain of carriers to O_2 (Fig. 19–20b). Because oligomycin is known to interact not directly with the electron carriers but with ATP synthase, it follows that electron transfer and ATP synthesis are obligately coupled: neither reaction occurs without the other.

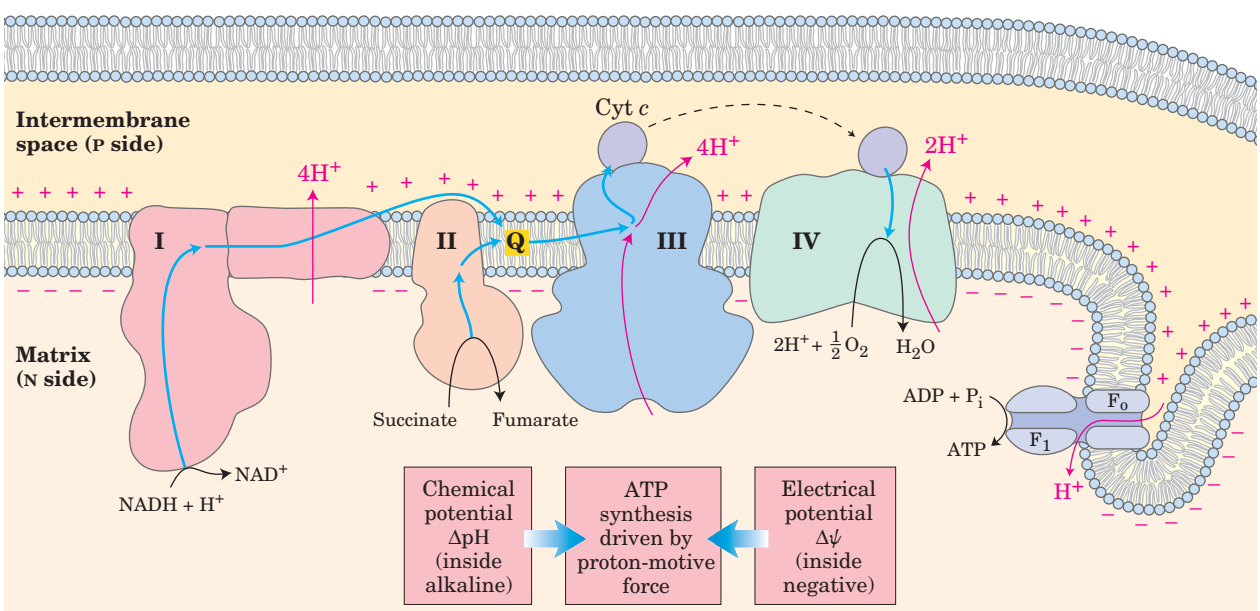

FIGURE 19–19 Chemiosmotic model. In this simple representation of the chemiosmotic theory applied to mitochondria, electrons from NADH and other oxidizable substrates pass through a chain of carriers arranged asymmetrically in the inner membrane. Electron flow is accompanied by proton transfer across the membrane, producing both a chemical gradient (ΔpH) and an electrical gradient ($\Delta\psi$). The inner mitochondrial membrane is impermeable to protons; protons can reenter the matrix only through proton-specific channels (F_o). The proton-motive force that drives protons back into the matrix provides the energy for ATP synthesis, catalyzed by the F_1 complex associated with F_o.

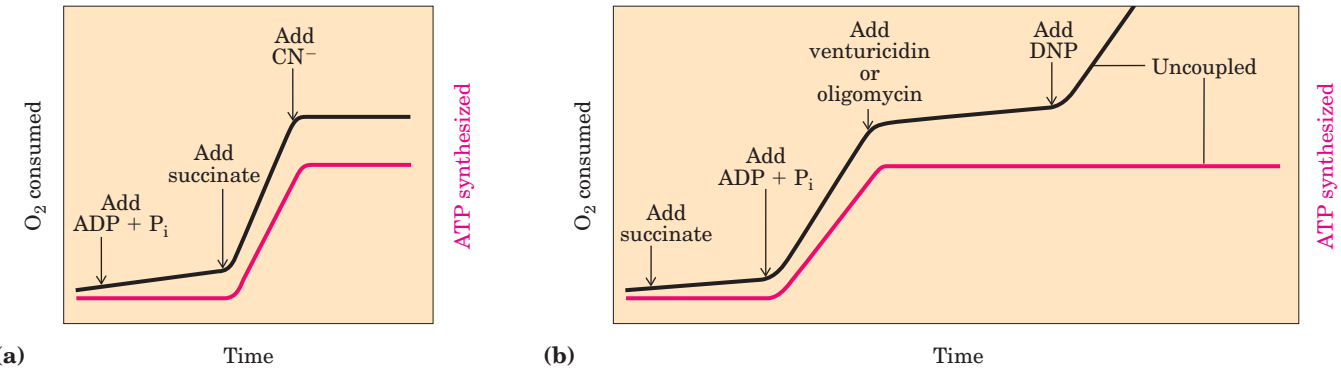

FIGURE 19–20 Coupling of electron transfer and ATP synthesis in mitochondria. In experiments to demonstrate coupling, mitochondria are suspended in a buffered medium and an O_2 electrode monitors O_2 consumption. At intervals, samples are removed and assayed for the presence of ATP. **(a)** Addition of ADP and P_i alone results in little or no increase in either respiration (O_2 consumption; black) or ATP synthesis (red). When succinate is added, respiration begins immediately and ATP is synthesized. Addition of cyanide (CN^-), which blocks electron transfer between cytochrome oxidase (Complex IV) and O_2, inhibits both respiration and ATP synthesis. **(b)** Mitochondria provided with succinate respire and synthesize ATP only when ADP and P_i are added. Subsequent addition of venturicidin or oligomycin, inhibitors of ATP synthase, blocks both ATP synthesis and respiration. Dinitrophenol (DNP) is an uncoupler, allowing respiration to continue without ATP synthesis.

Chemiosmotic theory readily explains the dependence of electron transfer on ATP synthesis in mitochondria. When the flow of protons into the matrix through the proton channel of ATP synthase is blocked (with oligomycin, for example), no path exists for the return of protons to the matrix, and the continued extrusion of protons driven by the activity of the respiratory chain generates a large proton gradient. The proton-motive force builds up until the cost (free energy) of pumping protons out of the matrix against this gradient equals or exceeds the energy released by the transfer of electrons from NADH to O_2. At this point electron flow must stop; the free energy for the overall process of electron flow coupled to proton pumping becomes zero, and the system is at equilibrium.

Certain conditions and reagents, however, can uncouple oxidation from phosphorylation. When intact mitochondria are disrupted by treatment with detergent or by physical shear, the resulting membrane fragments can still catalyze electron transfer from succinate or NADH to O_2, but no ATP synthesis is coupled to this respiration. Certain chemical compounds cause uncoupling without disrupting mitochondrial structure. Chemical uncouplers include 2,4-dinitrophenol (DNP) and carbonylcyanide-*p*-trifluoromethoxyphenylhydrazone (FCCP) (Table 19–4; **Fig. 19–21**), weak acids with hydrophobic properties that permit them to diffuse readily across mitochondrial membranes. After entering the matrix in the protonated form, they can release a proton, thus dissipating the proton gradient. Ionophores such as valinomycin (see Fig. 11–45) allow inorganic ions to pass easily through membranes. Ionophores uncouple electron transfer from oxidative phosphorylation by dissipating the electrical contribution to the electrochemical gradient across the mitochondrial membrane.

A prediction of the chemiosmotic theory is that, because the role of electron transfer in mitochondrial ATP synthesis is simply to pump protons to create the electrochemical potential of the proton-motive force, an artificially created proton gradient should be able to replace electron transfer in driving ATP synthesis. This has been experimentally confirmed **(Fig. 19–22)**. Mitochondria manipulated so as to impose a difference of proton concentration and a separation of charge across the inner membrane synthesize ATP *in the absence of an oxidizable substrate*; the proton-motive force alone suffices to drive ATP synthesis.

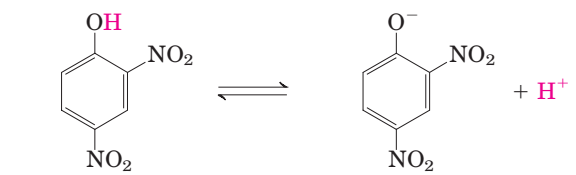

2,4-Dinitrophenol (DNP)

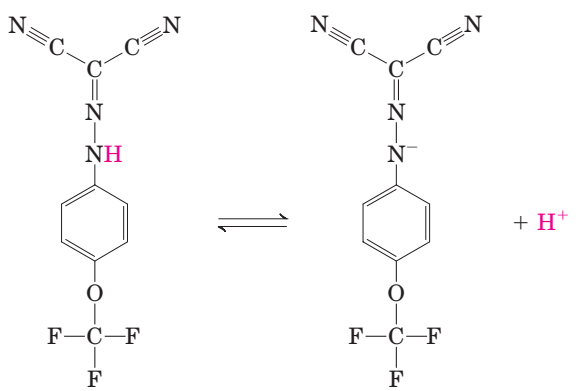

Carbonylcyanide-*p*-trifluoromethoxyphenylhydrazone (FCCP)

FIGURE 19–21 Two chemical uncouplers of oxidative phosphorylation. Both DNP and FCCP have a dissociable proton and are very hydrophobic. They carry protons across the inner mitochondrial membrane, dissipating the proton gradient. Both also uncouple photophosphorylation (see Fig. 19–63).

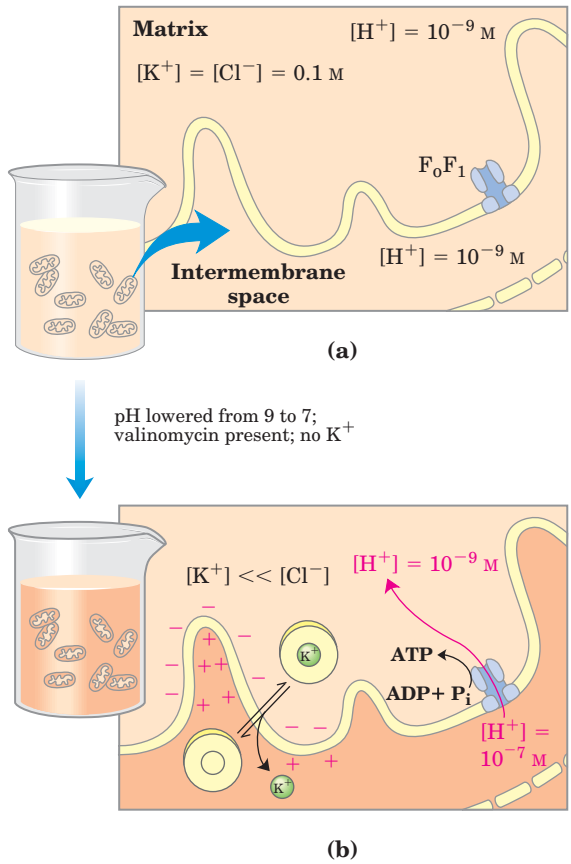

FIGURE 19–22 Evidence for the role of a proton gradient in ATP synthesis. An artificially imposed electrochemical gradient can drive ATP synthesis in the absence of an oxidizable substrate as electron donor. In this two-step experiment, **(a)** isolated mitochondria are first incubated in a pH 9 buffer containing 0.1 M KCl. Slow leakage of buffer and KCl into the mitochondria eventually brings the matrix into equilibrium with the surrounding medium. No oxidizable substrates are present. **(b)** Mitochondria are now separated from the pH 9 buffer and resuspended in pH 7 buffer containing valinomycin but no KCl. The change in buffer creates a difference of two pH units across the inner mitochondrial membrane. The outward flow of K^+, carried (by valinomycin) down its concentration gradient without a counterion, creates a charge imbalance across the membrane (matrix negative). The sum of the chemical potential provided by the pH difference and the electrical potential provided by the separation of charges is a proton-motive force large enough to support ATP synthesis in the absence of an oxidizable substrate.

ATP Synthase Has Two Functional Domains, F_o and F_1

Mitochondrial ATP synthase is an F-type ATPase (see Fig. 11–39) similar in structure and mechanism to the ATP synthases of chloroplasts and bacteria. This large enzyme complex of the inner mitochondrial membrane catalyzes the formation of ATP from ADP and P_i, accompanied by the flow of protons from the P to the N side of the membrane (Eqn 19–10). ATP synthase, also called Complex V, has two distinct components: F_1, a peripheral membrane protein, and F_o (o denoting oligomycin-sensitive), which is integral to the membrane. F_1, the first factor recognized as essential for oxidative phosphorylation, was identified and purified by Efraim Racker and his colleagues in the early 1960s.

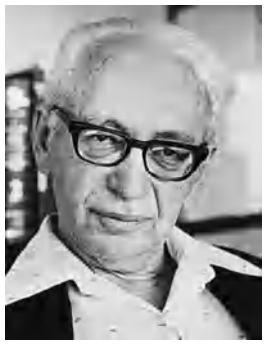

Efraim Racker, 1913–1991

In the laboratory, small membrane vesicles formed from inner mitochondrial membranes carry out ATP synthesis coupled to electron transfer. When F_1 is gently extracted, the "stripped" vesicles still contain intact respiratory chains and the F_o portion of ATP synthase. The vesicles can catalyze electron transfer from NADH to O_2 but cannot produce a proton gradient: F_o has a proton pore through which protons leak as fast as they are pumped by electron transfer, and without a proton gradient the F_1-depleted vesicles cannot make ATP. Isolated F_1 catalyzes ATP hydrolysis (the reversal of synthesis) and was therefore originally called **F_1ATPase**. When purified F_1 is added back to the depleted vesicles, it reassociates with F_o, plugging its proton pore and restoring the membrane's capacity to couple electron transfer and ATP synthesis.

ATP Is Stabilized Relative to ADP on the Surface of F_1

Isotope exchange experiments with purified F_1 reveal a remarkable fact about the enzyme's catalytic mechanism: on the enzyme surface, the reaction ADP + P_i $\rightleftharpoons$ ATP + H_2O is readily reversible—the free-energy change for ATP synthesis is close to zero! When ATP is hydrolyzed by F_1 in the presence of ^{18}O-labeled water, the P_i released contains an ^{18}O atom. Careful measurement of the ^{18}O content of P_i formed in vitro by F_1-catalyzed hydrolysis of ATP reveals that the P_i has not one, but three or four ^{18}O atoms **(Fig. 19–23)**. This indicates that the terminal pyrophosphate bond in ATP is cleaved and re-formed repeatedly before P_i leaves the enzyme surface. With P_i free to tumble in its binding site, each hydrolysis inserts ^{18}O randomly at one of the four positions in the molecule. This exchange reaction occurs in unenergized F_oF_1 complexes (with no proton gradient) and with isolated F_1—the exchange does not require the input of energy.

Kinetic studies of the initial rates of ATP synthesis and hydrolysis confirm the conclusion that $\Delta G'^\circ$ for ATP synthesis on the enzyme is near zero. From the measured rates of hydrolysis ($k_1 = 10\ s^{-1}$) and synthesis ($k_{-1} = 24\ s^{-1}$), the calculated equilibrium constant for the reaction

$$\text{Enz-ATP} \rightleftharpoons \text{Enz–(ADP + } P_i\text{)}$$

is

$$K'_{eq} = \frac{k_{-1}}{k_1} = \frac{24\ s^{-1}}{10\ s^{-1}} = 2.4$$

From this K'_{eq}, the calculated apparent $\Delta G'^\circ$ is close to zero. This is much different from the K'_{eq} of about 10^5

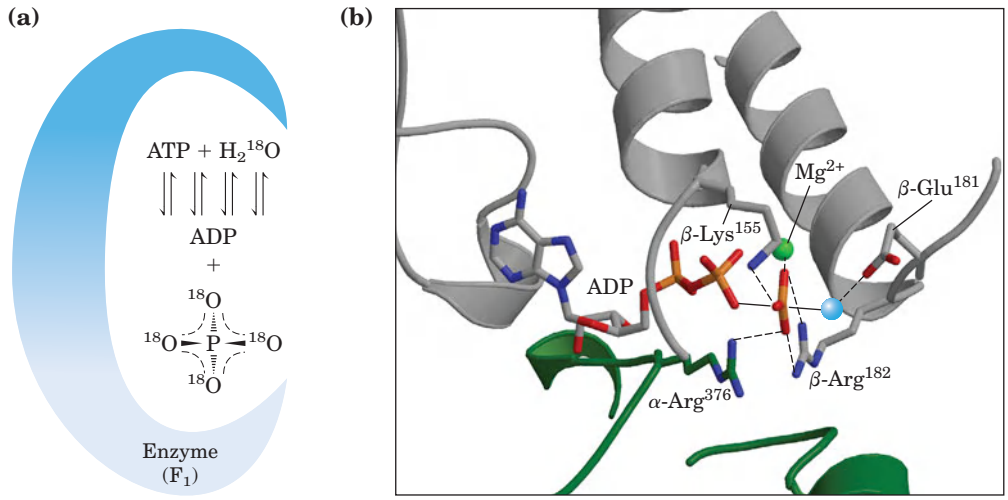

FIGURE 19–23 Catalytic mechanism of F_1. (a) ^{18}O-exchange experiment. F_1 solubilized from mitochondrial membranes is incubated with ATP in the presence of ^{18}O-labeled water. At intervals, a sample of the solution is withdrawn and analyzed for the incorporation of ^{18}O into the P_i produced from ATP hydrolysis. In minutes, the P_i contains three or four ^{18}O atoms, indicating that both ATP hydrolysis and ATP synthesis have occurred several times during the incubation. **(b)** The likely transition state complex for ATP hydrolysis and synthesis by ATP synthase (derived from PDB ID 1BMF). The α subunit is shown in green, β in gray. The positively charged residues β-Arg^{182} and α-Arg^{376} coordinate two oxygens of the pentavalent phosphate intermediate; β-Lys^{155} interacts with a third oxygen, and the Mg^{2+} ion (green sphere) further stabilizes the intermediate. The blue sphere represents the leaving group (H_2O). These interactions result in the ready equilibration of ATP and ADP + P_i in the active site.

($\Delta G'^\circ = -30.5$ kJ/mol) for the hydrolysis of ATP free in solution (not on the enzyme surface).

What accounts for the huge difference? ATP synthase stabilizes ATP relative to ADP + P_i by binding ATP more tightly, releasing enough energy to counterbalance the cost of making ATP. Careful measurements of the binding constants show that F_oF_1 binds ATP with very high affinity ($K_d \leq 10^{-12}$ M) and ADP with much lower affinity ($K_d \approx 10^{-5}$ M). The difference in K_d corresponds to a difference of about 40 kJ/mol in binding energy, and this binding energy drives the equilibrium toward formation of the product ATP.

The Proton Gradient Drives the Release of ATP from the Enzyme Surface

Although ATP synthase equilibrates ATP with ADP + P_i, in the absence of a proton gradient the newly synthesized ATP does not leave the surface of the enzyme. It is the proton gradient that causes the enzyme to release the ATP formed on its surface. The reaction coordinate diagram of the process **(Fig. 19–24)** illustrates the difference between the mechanism of ATP synthase and that of many other enzymes that catalyze endergonic reactions.

For the continued synthesis of ATP, the enzyme must cycle between a form that binds ATP very tightly and a form that releases ATP. Chemical and crystallographic studies of the ATP synthase have revealed the structural basis for this alternation in function.

Each β Subunit of ATP Synthase Can Assume Three Different Conformations

Mitochondrial F_1 has nine subunits of five different types, with the composition $\alpha_3\beta_3\gamma\delta\varepsilon$. Each of the three β subunits has one catalytic site for ATP synthesis. The crystallographic determination of the F_1 structure by John E. Walker and colleagues revealed structural details

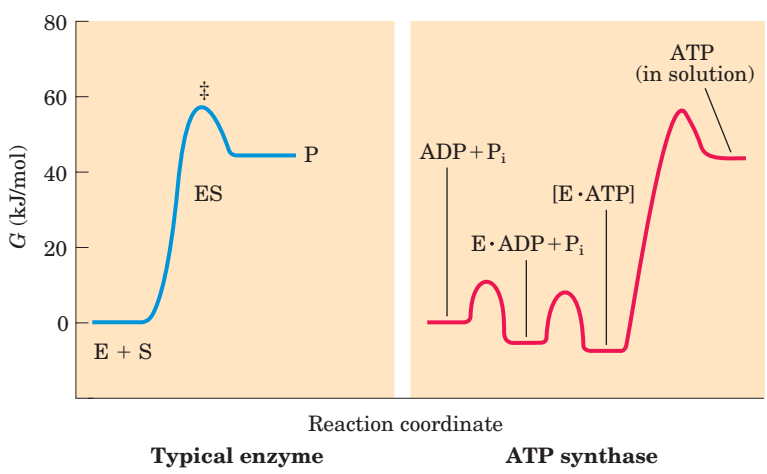

FIGURE 19–24 Reaction coordinate diagrams for ATP synthase and for a more typical enzyme. In a typical enzyme-catalyzed reaction (left), reaching the transition state (‡) between substrate and product is the major energy barrier to overcome. In the reaction catalyzed by ATP synthase (right), release of ATP from the enzyme, not formation of ATP, is the major energy barrier. The free-energy change for the formation of ATP from ADP and P_i in aqueous solution is large and positive, but on the enzyme surface, the very tight binding of ATP provides sufficient binding energy to bring the free energy of the enzyme-bound ATP close to that of ADP + P_i, so the reaction is readily reversible. The equilibrium constant is near 1. The free energy required for the release of ATP is provided by the proton-motive force.

very helpful in explaining the catalytic mechanism of the enzyme. The knoblike portion of F_1 is a flattened sphere, 8 nm high and 10 nm across, consisting of alternating α and β subunits arranged like the sections of an orange **(Fig. 19–25a, b, c)**. The polypeptides that make up the stalk in the F_1 crystal structure are asymmetrically arranged, with one domain of the single γ subunit making up a central shaft that passes through F_1, and another domain of γ associated primarily with one of the three β subunits, designated β-empty (Fig. 19–25c). Although the amino acid sequences of the three β subunits are identical, *their conformations differ*, in part because of the association of the γ subunit with just one of the three. The structures of the δ and ε subunits are not revealed in these crystallographic studies.

The conformational differences among β subunits extend to differences in their ATP/ADP-binding sites. When researchers crystallized the protein in the presence of ADP and App(NH)p, a close structural analog of ATP that cannot be hydrolyzed by the ATPase activity of F_1, the binding site of one of the three β subunits was filled with App(NH)p, the second was filled with ADP, and the third was empty. The corresponding β subunit conformations are designated β-ATP, β-ADP, and β-empty (Fig. 19–25c). This difference in nucleotide binding among the three subunits is critical to the mechanism of the complex.

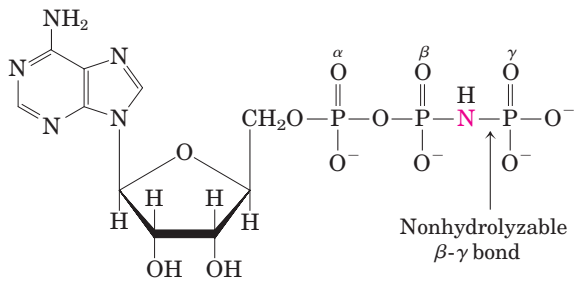

App(NH)p (β,γ-imidoadenosine 5′-triphosphate)

The F_o complex making up the proton pore is composed of three subunits, a, b, and c, in the proportion $ab_2c_{10–12}$. Subunit c is a small (M_r 8,000), very hydrophobic

John E. Walker

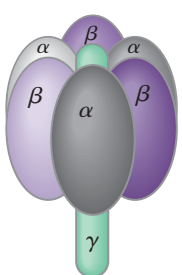

(a)

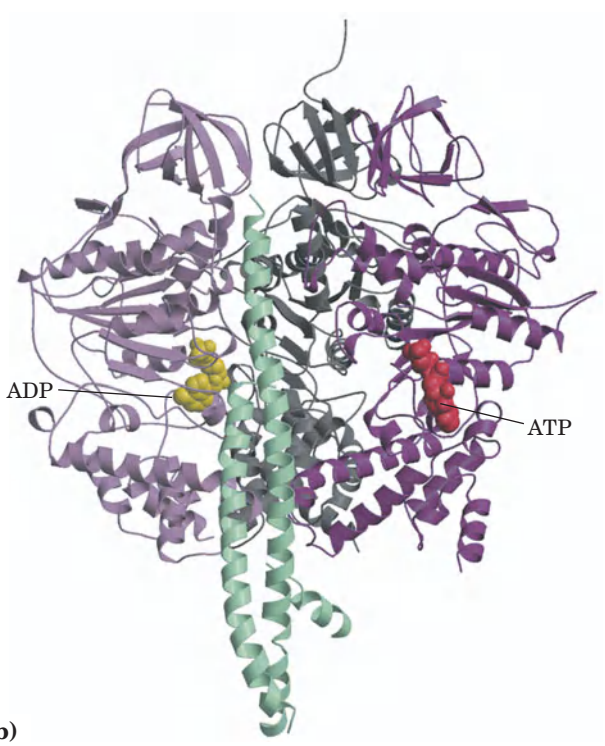

(b)

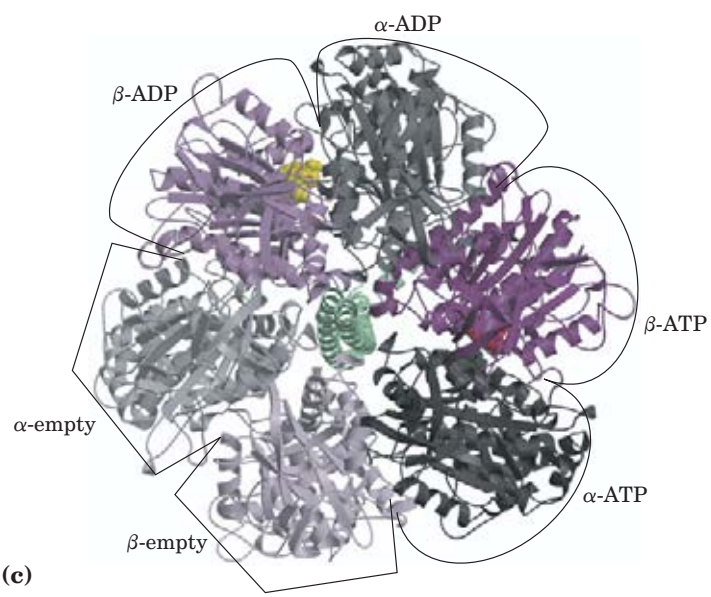

(c)

FIGURE 19–25 Mitochondrial ATP synthase complex. (a) Structure of the F_1 complex, deduced from crystallographic and biochemical studies. In F_1, three α and three β subunits are arranged like the segments of an orange, with alternating α (shades of gray) and β (shades of purple) subunits around a central shaft, the γ subunit (green). **(b)** Crystal structure of bovine F_1 (PDB ID 1BMF), viewed from the side. Two α subunits and one β subunit have been omitted to reveal the central shaft (γ subunit) and the binding sites for ATP and ADP on the β subunits. The δ and ε subunits are not shown here. **(c)** F_1 viewed from above (that is, from the N side of the membrane), showing the three β and three α subunits and the central shaft (γ subunit, green). Each β subunit, near its interface with the neighboring α subunit, has a nucleotide-binding site critical to the catalytic activity. The single γ subunit associates primarily with one of the three $\alpha\beta$ pairs, forcing each of the three β subunits into slightly different conformations, with different nucleotide-binding sites. In the crystalline enzyme, one subunit (β-ADP) has ADP (yellow) in its binding site, the next (β-ATP) has ATP (red), and the third (β-empty) has no bound nucleotide.

(figure continued on next page)

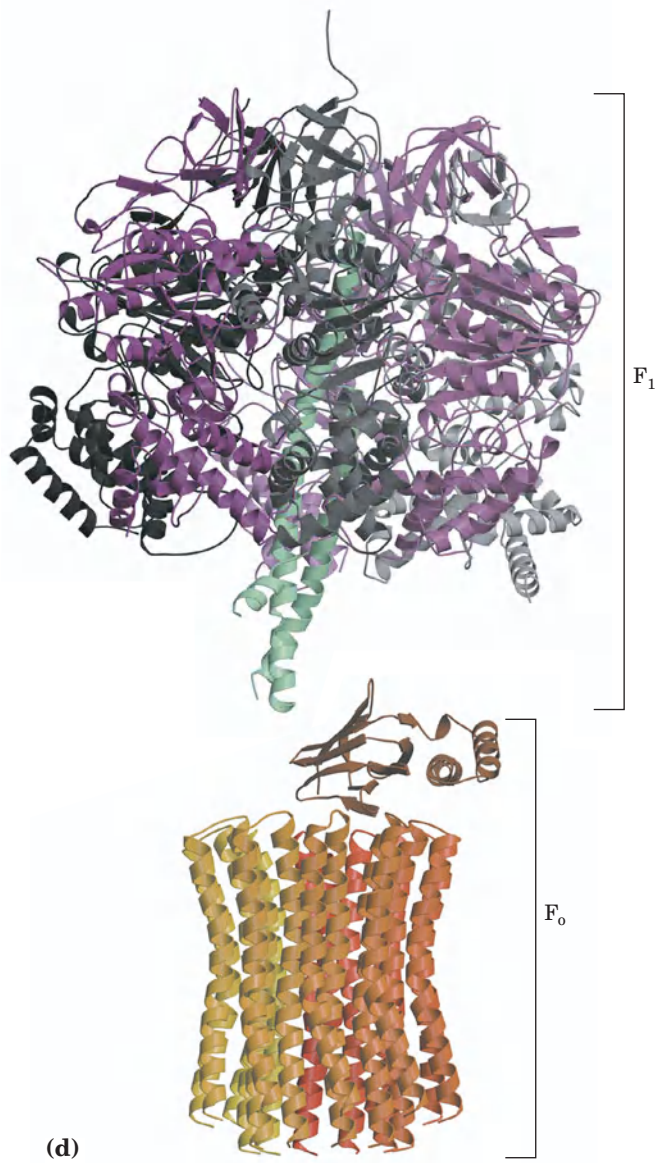

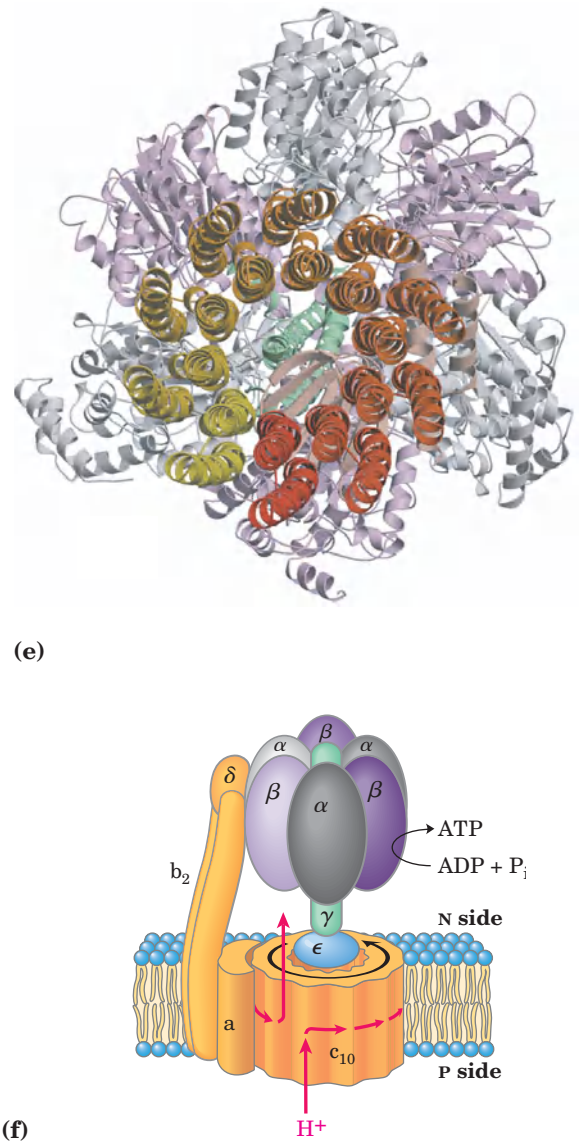

FIGURE 19–25 (continued) **(d)** Side view of the F_oF_1 structure. This is a composite, in which the crystallographic coordinates of bovine mitochondrial F_1 (shades of purple and gray) have been combined with those of yeast mitochondrial F_o (shades of yellow and orange) (PDB ID 1QO1). Subunits a, b, δ, and ε were not part of the crystal structure shown here. **(e)** The F_oF_1 structure, viewed end-on in the direction P side to N side. The major structures visible in this cross section are the two transmembrane helices of each of 10 c subunits arranged in concentric circles. **(f)** Diagram of the F_oF_1 complex, deduced from biochemical and crystallographic studies. The two b subunits (b_2) of F_o associate firmly with the α and β subunits of F_1, holding them fixed relative to the membrane. In F_o, the membrane-embedded cylinder of c subunits (c_{10}) is attached to the shaft made up of F_1 subunits γ and ε. As protons flow through the membrane from the P side to the N side through F_o, the cylinder and shaft rotate, and the β subunits of F_1 change conformation as the γ subunit associates with each in turn.

polypeptide, consisting almost entirely of two transmembrane helices, with a small loop extending from the matrix side of the membrane. The crystal structure of the yeast F_oF_1, solved in 1999, shows the arrangement of the c subunits. The yeast complex has 10 c subunits, each with two transmembrane helices roughly perpendicular to the plane of the membrane and arranged in two concentric circles (Fig. 19–25d, e). The inner circle is made up of the amino-terminal helices of each c subunit; the outer circle, about 55 Å in diameter, is made up of the carboxyl-terminal helices. The ε and γ subunits of F_1 form a leg-and-foot that projects from the bottom (membrane) side of F_1 and stands firmly on the ring of c subunits. The schematic drawing in Figure 19–25f combines the structural information from studies of bovine F_1 and yeast F_oF_1.

Rotational Catalysis Is Key to the Binding-Change Mechanism for ATP Synthesis

On the basis of detailed kinetic and binding studies of the reactions catalyzed by F_oF_1, Paul Boyer proposed a **rotational catalysis** mechanism in which the three active sites of F_1 take turns catalyzing ATP synthesis **(Fig. 19–26)**. A given β subunit starts in the β-ADP conformation, which binds ADP and P_i from the surrounding medium. The subunit now changes conformation, as-


Paul Boyer

suming the β-ATP form that tightly binds and stabilizes ATP, bringing about the ready equilibration of ADP + P_i with ATP on the enzyme surface. Finally, the subunit changes to the β-empty conformation, which has very low affinity for ATP, and the newly synthesized ATP leaves the enzyme surface. Another round of catalysis begins when this subunit again assumes the β-ADP form and binds ADP and P_i.

The conformational changes central to this mechanism are driven by the passage of protons through the F_o portion of ATP synthase. The streaming of protons through the F_o "pore" causes the cylinder of c subunits and the attached γ subunit to rotate about the long axis of γ, which is perpendicular to the plane of the membrane. The γ subunit passes through the center of the $\alpha_3\beta_3$ spheroid, which is held stationary relative to the membrane surface by the b_2 and δ subunits (Fig. 19–25f). With each rotation of 120°, γ comes into contact with a different β subunit, and the contact forces that β subunit into the β-empty conformation.

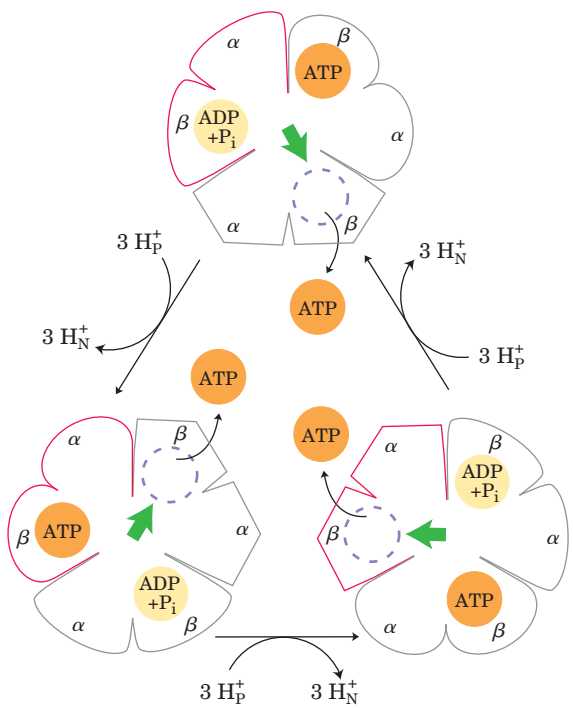

FIGURE 19–26 Binding-change model for ATP synthase. The F_1 complex has three nonequivalent adenine nucleotide–binding sites, one for each pair of α and β subunits. At any given moment, one of these sites is in the β-ATP conformation (which binds ATP tightly), a second is in the β-ADP (loose-binding) conformation, and a third is in the β-empty (very-loose-binding) conformation. The proton-motive force causes rotation of the central shaft—the γ subunit, shown as a green arrowhead—which comes into contact with each αβ subunit pair in succession. This produces a cooperative conformational change in which the β-ATP site is converted to the β-empty conformation, and ATP dissociates; the β-ADP site is converted to the β-ATP conformation, which promotes condensation of bound ADP + P_i to form ATP; and the β-empty site becomes a β-ADP site, which loosely binds ADP + P_i entering from the solvent. This model, based on experimental findings, requires that at least two of the three catalytic sites alternate in activity; ATP cannot be released from one site unless and until ADP and P_i are bound at the other.

The three β subunits interact in such a way that when one assumes the β-empty conformation, its neighbor to one side *must* assume the β-ADP form, and the other neighbor the β-ATP form. Thus one complete rotation of the γ subunit causes each β subunit to cycle through all three of its possible conformations, and for each rotation, three ATP are synthesized and released from the enzyme surface.

One strong prediction of this binding-change model is that the γ subunit should rotate in one direction when F_oF_1 is synthesizing ATP and in the opposite direction when the enzyme is hydrolyzing ATP. This prediction was confirmed in elegant experiments in the laboratories of Masasuke Yoshida and Kazuhiko Kinosita, Jr. The rotation of γ in a single F_1 molecule was observed microscopically by attaching a long, thin, fluorescent actin polymer to γ and watching it move relative to $\alpha_3\beta_3$ immobilized on a microscope slide, as ATP was hydrolyzed. When the entire F_oF_1 complex (not just F_1) was used in a similar experiment, the entire ring of c subunits rotated with γ **(Fig. 19–27)**. The "shaft" rotated in the predicted direction through 360°. The rotation was not smooth, but occurred in three discrete steps of 120°. As calculated from the known rate of ATP hydrolysis by one F_1 molecule and from the frictional drag on the long actin polymer, the efficiency of this mechanism in converting chemical energy into motion is close to 100%. It is, in Boyer's words, "a splendid molecular machine!"

Chemiosmotic Coupling Allows Nonintegral Stoichiometries of O_2 Consumption and ATP Synthesis

Before the general acceptance of the chemiosmotic model for oxidative phosphorylation, the assumption was that the overall reaction equation would take the following form:

$$x\text{ADP} + x\text{P}_i + \tfrac{1}{2}\text{O}_2 + \text{H}^+ + \text{NADH} \longrightarrow x\text{ATP} + \text{H}_2\text{O} + \text{NAD}^+ \quad (19\text{–}11)$$

with the value of x—sometimes called the **P/O ratio** or the **P/2e^- ratio**—always an integer. When intact mitochondria are suspended in solution with an oxidizable substrate such as succinate or NADH and are provided with O_2, ATP synthesis is readily measurable, as is the decrease in O_2. Measurement of P/O, however, is complicated by the fact that intact mitochondria consume ATP in many reactions taking place in the matrix, and they consume O_2 for purposes other than oxidative phosphorylation. Most experiments have yielded P/O (ATP to $\frac{1}{2}O_2$) ratios of between 2 and 3 when NADH was the electron donor, and between 1 and 2 when succinate was the

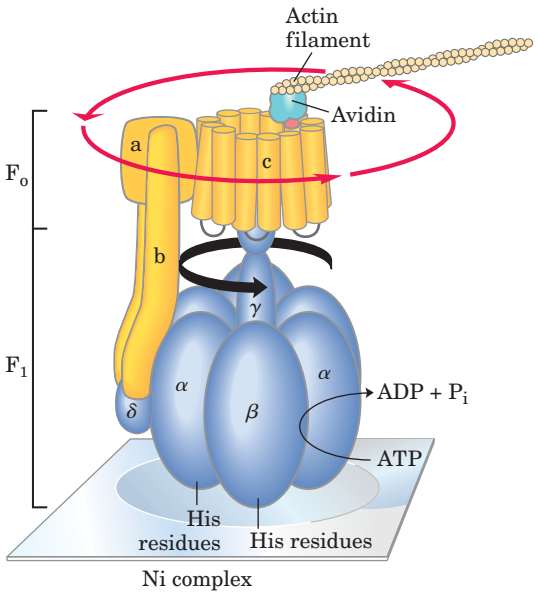

FIGURE 19–27 Experimental demonstration of rotation of F_o and γ. F_1 genetically engineered to contain a run of His residues adheres tightly to a microscope slide coated with a Ni complex; biotin is covalently attached to a c subunit of F_o. The protein avidin, which binds biotin very tightly, is covalently attached to long filaments of actin labeled with a fluorescent probe. Biotin-avidin binding now attaches the actin filaments to the c subunit. When ATP is provided as substrate for the ATPase activity of F_1, the labeled filament is seen to rotate continuously in one direction, proving that the F_o cylinder of c subunits rotates. In another experiment, a fluorescent actin filament was attached directly to the γ subunit. The series of fluorescence micrographs (read left to right) shows the position of the actin filament at intervals of 133 ms. Note that as the filament rotates, it makes a discrete jump about every eleventh frame. Presumably the cylinder and shaft move as one unit.

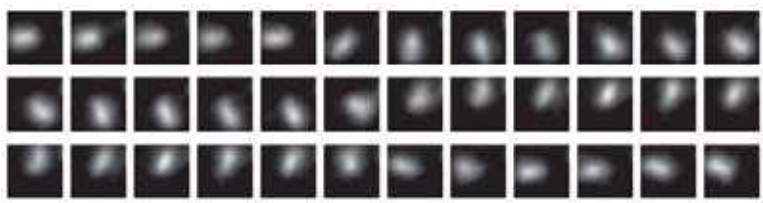

donor. Given the assumption that P/O should have an integral value, most experimenters agreed that the P/O ratios must be 3 for NADH and 2 for succinate, and for years those values appeared in research papers and textbooks.

With introduction of the chemiosmotic paradigm for coupling ATP synthesis to electron transfer, there was no theoretical requirement for P/O to be integral. The relevant questions about stoichiometry became, How many protons are pumped outward by electron transfer from one NADH to O_2, and how many protons must flow inward through the F_oF_1 complex to drive the synthesis of one ATP? The measurement of proton fluxes is technically complicated; the investigator must take into account the buffering capacity of mitochondria, nonproductive leakage of protons across the inner membrane, and use of the proton gradient for functions other than ATP synthesis, such as driving the transport of substrates across the inner mitochondrial membrane (described below). The consensus values for number of protons pumped out per pair of electrons are 10 for NADH and 6 for succinate. The most widely accepted experimental value for number of protons required to drive the synthesis of an ATP molecule is 4, of which 1 is used in transporting P_i, ATP, and ADP across the mitochondrial membrane (see below). If 10 protons are pumped out per NADH and 4 must flow in to produce 1 ATP, the proton-based P/O ratio is 2.5 for NADH as the electron donor and 1.5 (6/4) for succinate. We use the P/O values of 2.5 and 1.5 throughout this book, but the values 3.0 and 2.0 are still common in the biochemical literature. The final word on proton stoichiometry will probably not be written until we know the full details of the F_oF_1 reaction mechanism.

The Proton-Motive Force Energizes Active Transport

Although the primary role of the proton gradient in mitochondria is to furnish energy for the synthesis of ATP, the proton-motive force also drives several transport processes essential to oxidative phosphorylation. The inner mitochondrial membrane is generally impermeable to charged species, but two specific systems transport ADP and P_i into the matrix and ATP out to the cytosol **(Fig. 19–28)**.

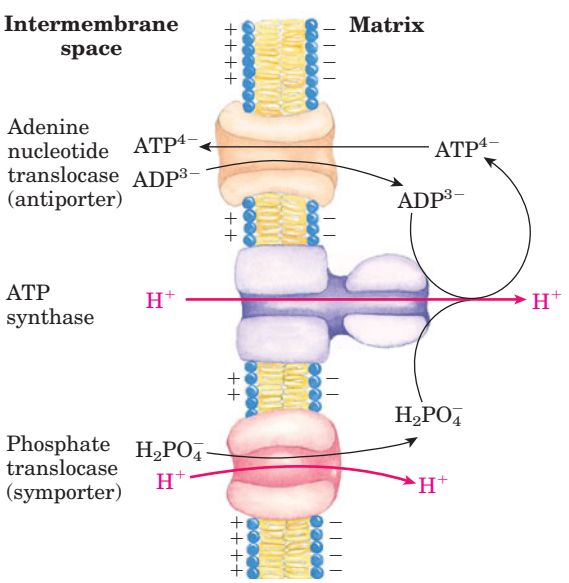

FIGURE 19–28 Adenine nucleotide and phosphate translocases. Transport systems of the inner mitochondrial membrane carry ADP and P_i into the matrix and newly synthesized ATP into the cytosol. The adenine nucleotide translocase is an antiporter; the same protein moves ADP into the matrix and ATP out. The effect of replacing ATP^{4-} with ADP^{3-} in the matrix is the net efflux of one negative charge, which is favored by the charge difference across the inner membrane (outside positive). At pH 7, P_i is present as both HPO_4^{2-} and $H_2PO_4^-$; the phosphate translocase is specific for $H_2PO_4^-$. There is no net flow of charge during symport of $H_2PO_4^-$ and H^+, but the relatively low proton concentration in the matrix favors the inward movement of H^+. Thus the proton-motive force is responsible both for providing the energy for ATP synthesis and for transporting substrates (ADP and P_i) into and product (ATP) out of the mitochondrial matrix. All three of these transport systems can be isolated as a single membrane-bound complex (ATP synthasome).

The **adenine nucleotide translocase**, integral to the inner membrane, binds ADP^{3-} in the intermembrane space and transports it into the matrix in exchange for an ATP^{4-} molecule simultaneously transported outward (see Fig. 13–11 for the ionic forms of ATP and ADP). Because this antiporter moves four negative charges out for every three moved in, its activity is favored by the transmembrane electrochemical gradient, which gives the matrix a net negative charge; the proton-motive force drives ATP-ADP exchange. Adenine nucleotide translocase is specifically inhibited by atractyloside, a toxic glycoside formed by a species of thistle. If the transport of ADP into and ATP out of mitochondria is inhibited, cytosolic ATP cannot be regenerated from ADP, explaining the toxicity of atractyloside.

A second membrane transport system essential to oxidative phosphorylation is the **phosphate translocase**, which promotes symport of one $H_2PO_4^-$ and one H^+ into the matrix. This transport process, too, is favored by the transmembrane proton gradient (Fig. 19–28). Notice that the process requires movement of one proton from the P to the N side of the inner membrane, consuming some of the energy of electron transfer. A complex of the ATP synthase and both translocases, the **ATP synthasome**, can be isolated from mitochondria by gentle dissection with detergents, suggesting that the functions of these three proteins are very tightly integrated.

Shuttle Systems Indirectly Convey Cytosolic NADH into Mitochondria for Oxidation

The NADH dehydrogenase of the inner mitochondrial membrane of animal cells can accept electrons only from NADH in the matrix. Given that the inner membrane is not permeable to NADH, how can the NADH generated by glycolysis in the cytosol be reoxidized to NAD^+ by O_2 via the respiratory chain? Special shuttle systems carry reducing equivalents from cytosolic NADH into mitochondria by an indirect route. The most active NADH shuttle, which functions in liver, kidney, and heart mitochondria, is the **malate-aspartate shuttle (Fig. 19–29)**. The reducing equivalents of cytosolic NADH are first transferred to cytosolic oxaloacetate to yield malate, catalyzed by cytosolic

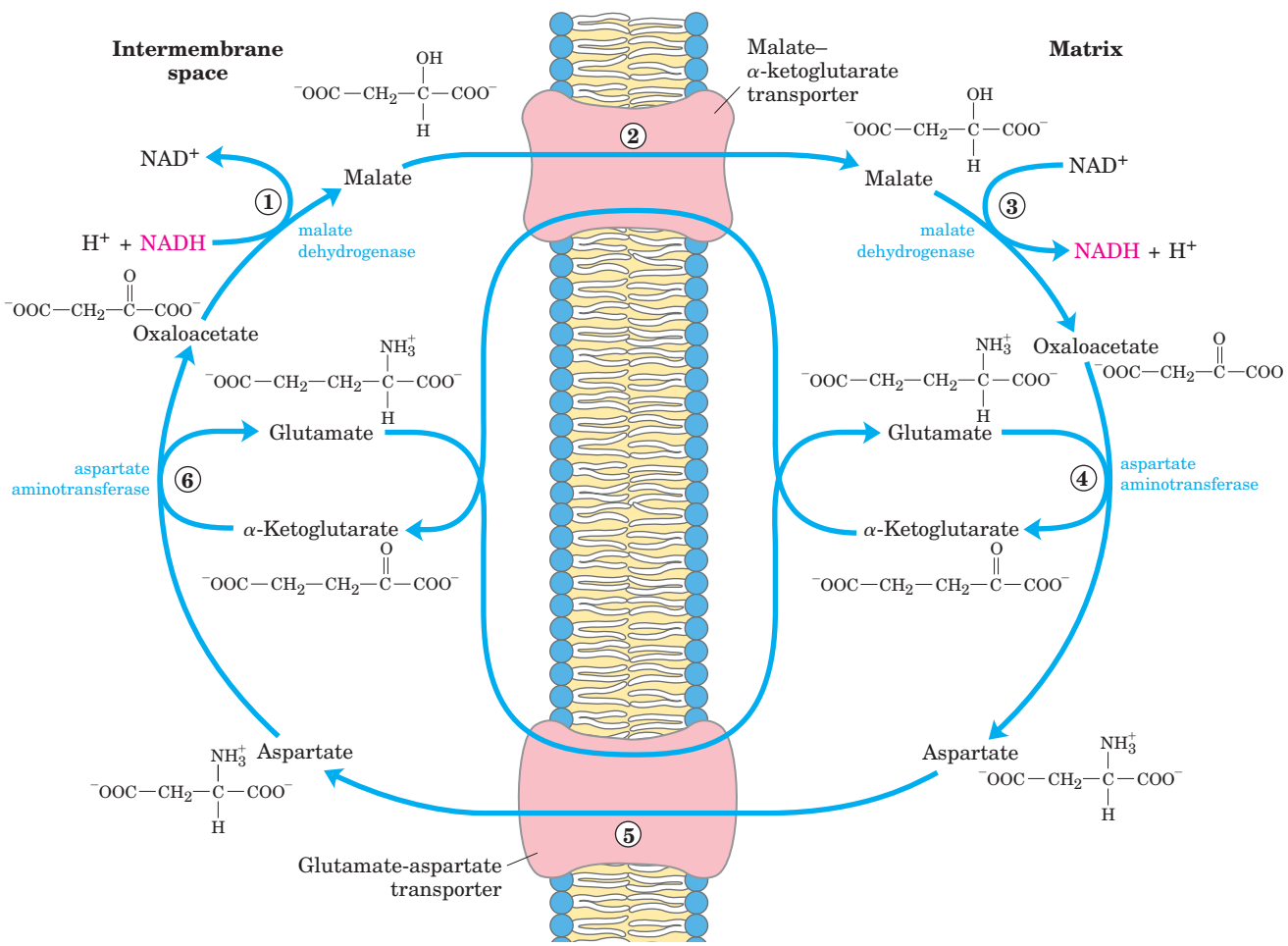

FIGURE 19–29 Malate-aspartate shuttle. This shuttle for transporting reducing equivalents from cytosolic NADH into the mitochondrial matrix is used in liver, kidney, and heart. ① NADH in the cytosol (intermembrane space) passes two reducing equivalents to oxaloacetate, producing malate. ② Malate crosses the inner membrane via the malate–α-ketoglutarate transporter. ③ In the matrix, malate passes two reducing equivalents to NAD^+, and the resulting NADH is oxidized by the respiratory chain; the oxaloacetate formed from malate cannot pass directly into the cytosol. ④ Oxaloacetate is first transaminated to aspartate, and ⑤ aspartate can leave via the glutamate-aspartate transporter. ⑥ Oxaloacetate is regenerated in the cytosol, completing the cycle.

malate dehydrogenase. The malate thus formed passes through the inner membrane via the malate–α-ketoglutarate transporter. Within the matrix the reducing equivalents are passed to NAD^+ by the action of matrix malate dehydrogenase, forming NADH; this NADH can pass electrons directly to the respiratory chain. About 2.5 molecules of ATP are generated as this pair of electrons passes to O_2. Cytosolic oxaloacetate must be regenerated by transamination reactions and the activity of membrane transporters to start another cycle of the shuttle.

Skeletal muscle and brain use a different NADH shuttle, the **glycerol 3-phosphate shuttle (Fig. 19–30)**. It differs from the malate-aspartate shuttle in that it delivers the reducing equivalents from NADH to ubiquinone and thus into Complex III, not Complex I (Fig. 19–8), providing only enough energy to synthesize 1.5 ATP molecules per pair of electrons.

The mitochondria of plants have an *externally* oriented NADH dehydrogenase that can transfer electrons directly from cytosolic NADH into the respiratory chain at the level of ubiquinone. Because this pathway bypasses the NADH dehydrogenase of Complex I and the associated proton movement, the yield of ATP from cytosolic NADH is less than that from NADH generated in the matrix (Box 19–1).

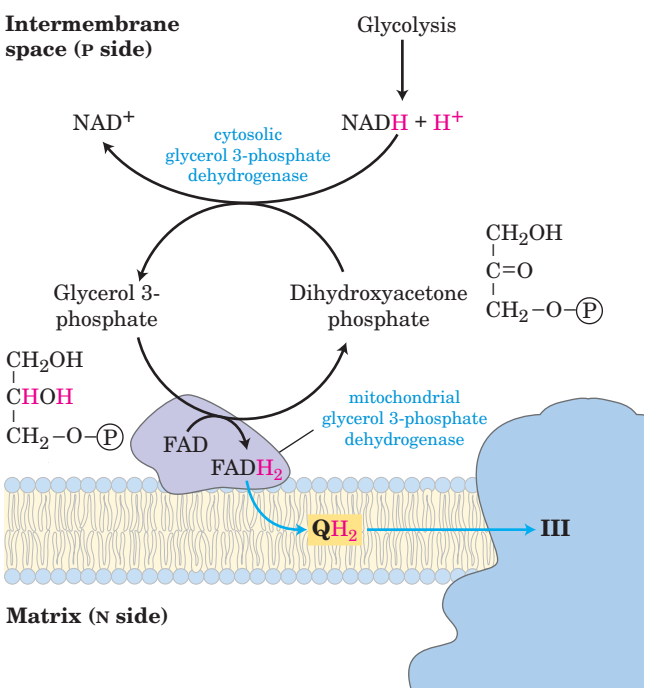

FIGURE 19–30 Glycerol 3-phosphate shuttle. This alternative means of moving reducing equivalents from the cytosol to the mitochondrial matrix operates in skeletal muscle and the brain. In the cytosol, dihydroxyacetone phosphate accepts two reducing equivalents from NADH in a reaction catalyzed by cytosolic glycerol 3-phosphate dehydrogenase. An isozyme of glycerol 3-phosphate dehydrogenase bound to the outer face of the inner membrane then transfers two reducing equivalents from glycerol 3-phosphate in the intermembrane space to ubiquinone. Note that this shuttle does not involve membrane transport systems.

SUMMARY 19.2 ATP Synthesis

- The flow of electrons through Complexes I, III, and IV results in pumping of protons across the inner mitochondrial membrane, making the matrix alkaline relative to the intermembrane space. This proton gradient provides the energy (in the form of the proton-motive force) for ATP synthesis from ADP and P_i by ATP synthase (F_oF_1 complex) in the inner membrane.
- ATP synthase carries out "rotational catalysis," in which the flow of protons through F_o causes each of three nucleotide-binding sites in F_1 to cycle from (ADP + P_i)–bound to ATP-bound to empty conformations.
- ATP formation on the enzyme requires little energy; the role of the proton-motive force is to push ATP from its binding site on the synthase.
- The ratio of ATP synthesized per $\frac{1}{2}O_2$ reduced to H_2O (the P/O ratio) is about 2.5 when electrons enter the respiratory chain at Complex I, and 1.5 when electrons enter at ubiquinone.
- Energy conserved in a proton gradient can drive solute transport uphill across a membrane.
- The inner mitochondrial membrane is impermeable to NADH and NAD^+, but NADH equivalents are moved from the cytosol to the matrix by either of two shuttles. NADH equivalents moved in by the malate-aspartate shuttle enter the respiratory chain at Complex I and yield a P/O ratio of 2.5; those moved in by the glycerol 3-phosphate shuttle enter at ubiquinone and give a P/O ratio of 1.5.

19.3 Regulation of Oxidative Phosphorylation

Oxidative phosphorylation produces most of the ATP made in aerobic cells. Complete oxidation of a molecule of glucose to CO_2 yields 30 or 32 ATP (Table 19–5). By comparison, glycolysis under anaerobic conditions (lactate fermentation) yields only 2 ATP per glucose. Clearly, the evolution of oxidative phosphorylation provided a tremendous increase in the energy efficiency of catabolism. Complete oxidation to CO_2 of the coenzyme A derivative of palmitate (16:0), which also occurs in the mitochondrial matrix, yields 108 ATP per palmitoyl-CoA (see Table 17–1). A similar calculation can be made for the ATP yield from oxidation of each of the amino acids (Chapter 18). Aerobic oxidative pathways that result in electron transfer to O_2 accompanied by oxidative phosphorylation therefore account for the vast majority of the ATP produced in catabolism, so the regulation of ATP production by oxidative phosphorylation to match the cell's fluctuating needs for ATP is absolutely essential.

TABLE 19–5 ATP Yield from Complete Oxidation of Glucose

Process	Direct product	Final ATP
Glycolysis	2 NADH (cytosolic) 2 ATP	3 or 5* 2
Pyruvate oxidation (two per glucose)	2 NADH (mitochondrial matrix)	5
Acetyl-CoA oxidation in citric acid cycle (two per glucose)	6 NADH (mitochondrial matrix) 2 $FADH_2$ 2 ATP or 2 GTP	15 3 2
Total yield per glucose		30 or 32

*The number depends on which shuttle system transfers reducing equivalents into the mitochondrion.

Oxidative Phosphorylation Is Regulated by Cellular Energy Needs

The rate of respiration (O_2 consumption) in mitochondria is tightly regulated; it is generally limited by the availability of ADP as a substrate for phosphorylation. Dependence of the rate of O_2 consumption on the availability of the P_i acceptor ADP (Fig. 19–20b), the **acceptor control** of respiration, can be remarkable. In some animal tissues, the **acceptor control ratio**, the ratio of the maximal rate of ADP-induced O_2 consumption to the basal rate in the absence of ADP, is at least 10.

The intracellular concentration of ADP is one measure of the energy status of cells. Another, related measure is the **mass-action ratio** of the ATP-ADP system, $[ATP]/([ADP][P_i])$. Normally this ratio is very high, so the ATP-ADP system is almost fully phosphorylated. When the rate of some energy-requiring process (protein synthesis, for example) increases, the rate of breakdown of ATP to ADP and P_i increases, lowering the mass-action ratio. With more ADP available for oxidative phosphorylation, the rate of respiration increases, causing regeneration of ATP. This continues until the mass-action ratio returns to its normal high level, at which point respiration slows again. The rate of oxidation of cellular fuels is regulated with such sensitivity and precision that the $[ATP]/([ADP][P_i])$ ratio fluctuates only slightly in most tissues, even during extreme variations in energy demand. In short, ATP is formed only as fast as it is used in energy-requiring cellular activities.

An Inhibitory Protein Prevents ATP Hydrolysis during Hypoxia

We have already encountered ATP synthase as an ATP-driven proton pump (see Fig. 11–39), catalyzing the reverse of ATP synthesis. When a cell is hypoxic (deprived of oxygen), as in a heart attack or stroke, electron transfer to oxygen slows, and so does the pumping of protons. The proton-motive force soon collapses. Under these conditions, the ATP synthase could operate in reverse, hydrolyzing ATP to pump protons outward and causing a disastrous drop in ATP levels. This is prevented by a small

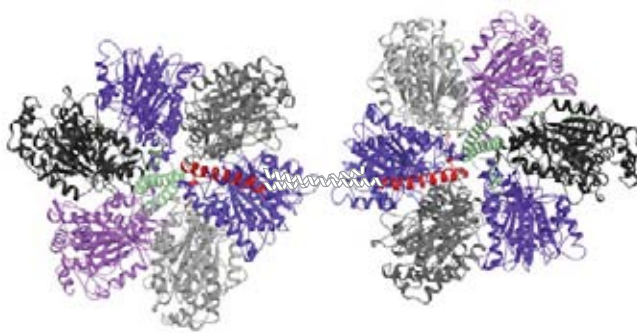

FIGURE 19–31 Structure of bovine F_1-ATPase in a complex with its regulatory protein IF_1. (Derived from PDB ID 1OHH) Two F_1 molecules are viewed here as in Figure 19–25c. The inhibitor IF_1 (red) binds to the $\alpha\beta$ interface of the subunits in the diphosphate (ADP) conformation (α-ADP and β-ADP), freezing the two F_1 complexes and thereby blocking ATP hydrolysis (and synthesis). (Parts of IF_1 that failed to resolve in the crystals of F_1 are shown in white outline as they occur in crystals of isolated IF_1.) This complex is stable only at the low cytosolic pH characteristic of cells that are producing ATP by glycolysis; when aerobic metabolism resumes, the cytosolic pH rises, the inhibitor is destabilized, and ATP synthase becomes active.

(84 amino acids) protein inhibitor, IF_1, which simultaneously binds to two ATP synthase molecules, inhibiting their ATPase activity **(Fig. 19–31)**. IF_1 is inhibitory only in its dimeric form, which is favored at pH lower than 6.5. In a cell starved for oxygen, the main source of ATP becomes glycolysis, and the pyruvic or lactic acid thus formed lowers the pH in the cytosol and the mitochondrial matrix. This favors IF_1 dimerization, leading to inhibition of the ATPase activity of ATP synthase and thereby preventing wasteful hydrolysis of ATP. When aerobic metabolism resumes, production of pyruvic acid slows, the pH of the cytosol rises, the IF_1 dimer is destabilized, and the inhibition of ATP synthase is lifted.

Hypoxia Leads to ROS Production and Several Adaptive Responses

In hypoxic cells there is an imbalance between the input of electrons from fuel oxidation in the mitochondrial matrix and transfer of electrons to molecular oxygen, leading to increased formation of reactive oxygen

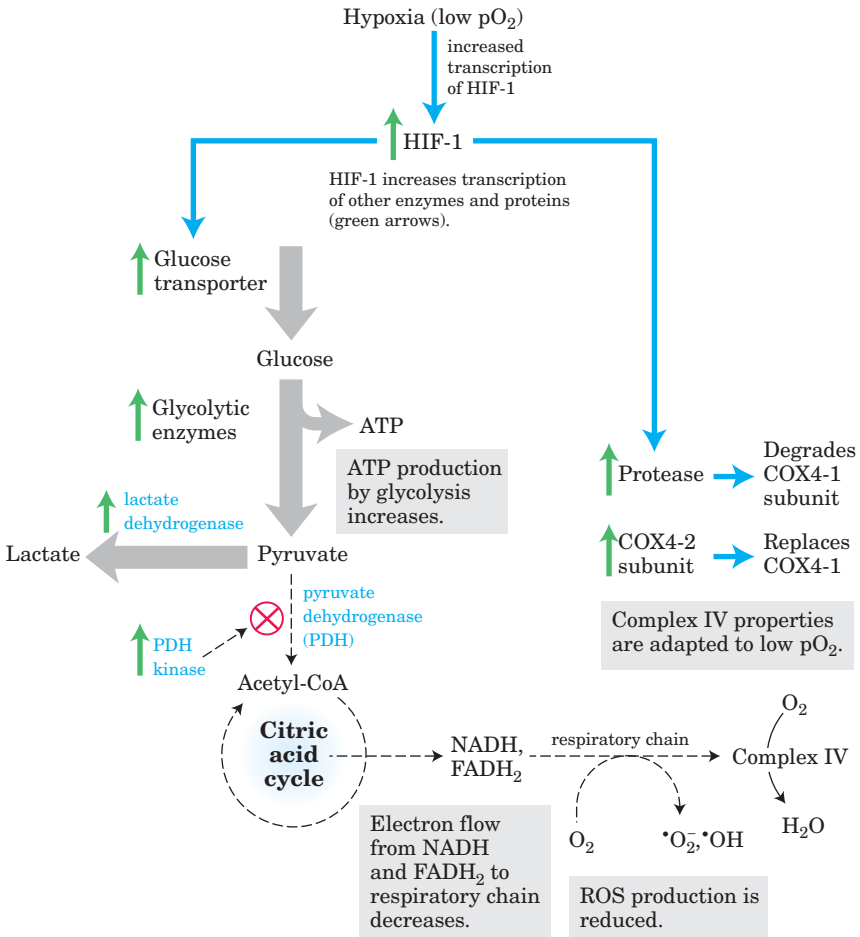

FIGURE 19–32 Hypoxia-inducible factor (HIF-1) regulates gene expression to reduce ROS formation. Under conditions of low oxygen (hypoxia), HIF-1 is synthesized in greater amounts and acts as a transcription factor, increasing the synthesis of glucose transporter, glycolytic enzymes, pyruvate dehydrogenase kinase (PDH kinase), lactate dehydrogenase, a protease that degrades the cytochrome oxidase subunit COX4-1, and cytochrome oxidase subunit COX4-2. These changes counter the formation of ROS by decreasing the supply of NADH and $FADH_2$ and making cytochrome oxidase of Complex IV more effective. Thick gray arrows signify reactions stimulated by HIF-1; thin, broken arrows show reactions slowed by HIF-1.

species. In addition to the glutathione peroxidase system (Fig. 19–18), cells have two other lines of defense against ROS **(Fig. 19–32)**. One is regulation of pyruvate dehydrogenase (PDH), the enzyme that delivers acetyl-CoA to the citric acid cycle (Chapter 16). Under hypoxic conditions, PDH kinase phosphorylates mitochondrial PDH, inactivating it and slowing the delivery of $FADH_2$ and NADH from the citric acid cycle to the respiratory chain. A second means of preventing ROS formation is the replacement of one subunit of Complex IV, known as COX4-1, with another subunit, COX4-2, that is better suited to hypoxic conditions. With COX4-1, the catalytic properties of Complex IV are optimal for respiration at normal oxygen concentrations; with COX4-2, Complex IV is optimized for operation under hypoxic conditions.

The changes in PDH activity and the COX4-2 content of Complex IV are both mediated by HIF-1, the hypoxia-inducible factor. HIF-1 accumulates in hypoxic cells and, acting as a transcription factor, triggers increased synthesis of PDH kinase, COX4-2, and a protease that degrades COX4-1. Recall that HIF-1 also mediates the changes in glucose transport and glycolytic enzymes that produce the Pasteur effect (see Box 14–1).

When these mechanisms for dealing with ROS are insufficient, due to genetic mutation affecting one of the protective proteins or under conditions of very high rates of ROS production, mitochondrial function is compromised. Mitochondrial damage is thought to be involved in aging, heart failure, certain rare cases of diabetes (described below), and several maternally inherited genetic diseases that affect the nervous system. ■

ATP-Producing Pathways Are Coordinately Regulated

The major catabolic pathways have interlocking and concerted regulatory mechanisms that allow them to function together in an economical and self-regulating manner to produce ATP and biosynthetic precursors. The relative concentrations of ATP and ADP control not only the rates of electron transfer and oxidative phosphorylation but also the rates of the citric acid cycle, pyruvate oxidation, and glycolysis **(Fig. 19–33)**.

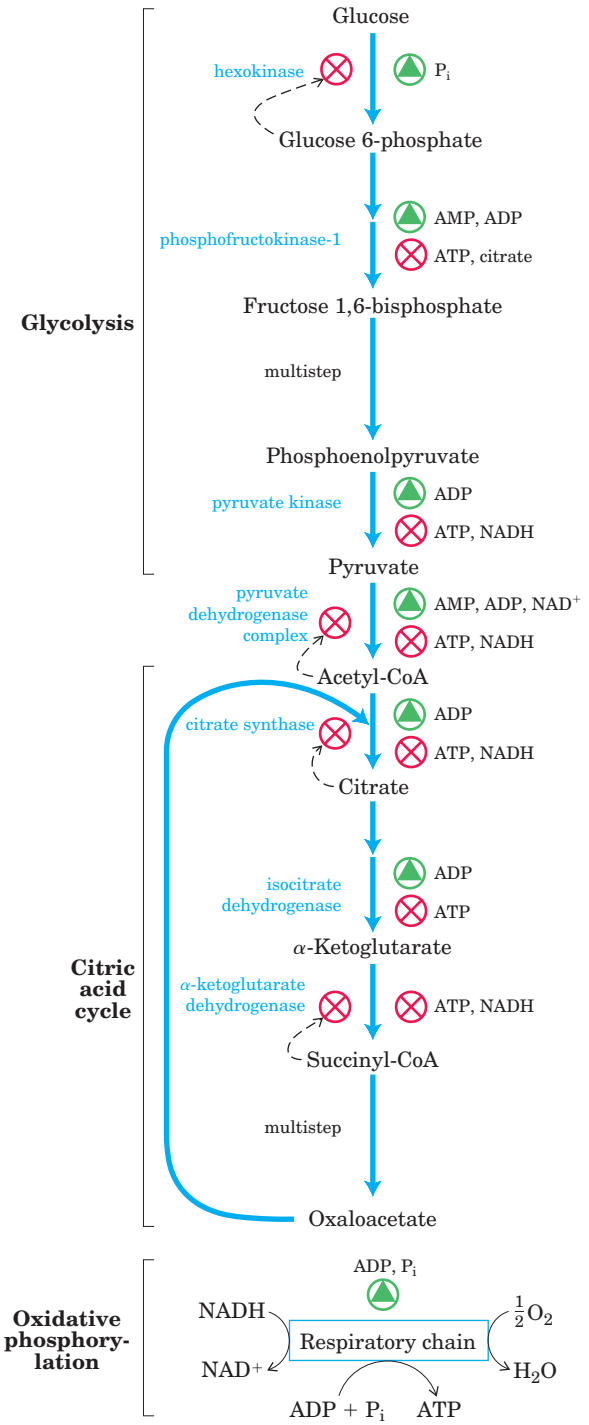

FIGURE 19–33 Regulation of the ATP-producing pathways. This diagram shows the interlocking regulation of glycolysis, pyruvate oxidation, the citric acid cycle, and oxidative phosphorylation by the relative concentrations of ATP, ADP, and AMP, and by NADH. High [ATP] (or low [ADP] and [AMP]) produces low rates of glycolysis, pyruvate oxidation, acetate oxidation via the citric acid cycle, and oxidative phosphorylation. All four pathways are accelerated when the use of ATP and the formation of ADP, AMP, and P_i increase. The interlocking of glycolysis and the citric acid cycle by citrate, which inhibits glycolysis, supplements the action of the adenine nucleotide system. In addition, increased levels of NADH and acetyl-CoA also inhibit the oxidation of pyruvate to acetyl-CoA, and a high [NADH]/[NAD^+] ratio inhibits the dehydrogenase reactions of the citric acid cycle (see Fig. 16–18).

Whenever ATP consumption increases, the rate of electron transfer and oxidative phosphorylation increases. Simultaneously, the rate of pyruvate oxidation via the citric acid cycle increases, increasing the flow of electrons into the respiratory chain. These events can in turn evoke an increase in the rate of glycolysis, increasing the rate of pyruvate formation. When conversion of ADP to ATP lowers the ADP concentration, acceptor control slows electron transfer and thus oxidative phosphorylation. Glycolysis and the citric acid cycle are also slowed, because ATP is an allosteric inhibitor of the glycolytic enzyme phosphofructokinase-1 (see Fig. 15–14) and of pyruvate dehydrogenase (see Fig. 16–18).

Phosphofructokinase-1 is also inhibited by citrate, the first intermediate of the citric acid cycle. When the cycle is "idling," citrate accumulates within mitochondria, then is transported into the cytosol. When the concentrations of both ATP and citrate rise, they produce a concerted allosteric inhibition of phosphofructokinase-1 that is greater than the sum of their individual effects, slowing glycolysis.

SUMMARY 19.3 Regulation of Oxidative Phosphorylation

- Oxidative phosphorylation is regulated by cellular energy demands. The intracellular [ADP] and the mass-action ratio [ATP]/([ADP][P_i]) are measures of a cell's energy status.
- In hypoxic (oxygen-deprived) cells, a protein inhibitor blocks ATP hydrolysis by the reverse activity of ATP synthase, preventing a drastic drop in [ATP].
- The adaptive responses to hypoxia, mediated by HIF-1, slow electron transfer into the respiratory chain and modify Complex IV to act more efficiently under low-oxygen conditions.
- ATP and ADP concentrations set the rate of electron transfer through the respiratory chain via a series of interlocking controls on respiration, glycolysis, and the citric acid cycle.

19.4 Mitochondria in Thermogenesis, Steroid Synthesis, and Apoptosis

Although ATP production is a central role for the mitochondrion, this organelle has other functions that, in specific tissues or under specific circumstances, are also crucial. In adipose tissue, mitochondria generate heat to protect vital organs from low ambient temperature; in the adrenal glands and the gonads, mitochondria are the sites of steroid hormone synthesis; and in most or all tissues they are key participants in apoptosis (programmed cell death).

Uncoupled Mitochondria in Brown Adipose Tissue Produce Heat

We noted above that respiration slows when the cell is adequately supplied with ATP. There is a remarkable and instructive exception to this general rule. Most newborn mammals, including humans, have a type of adipose tissue called **brown adipose tissue** (**BAT**; p. 917) in which fuel oxidation serves, not to produce ATP, but to generate heat to keep the newborn warm. This specialized adipose tissue is brown because of the presence of large numbers of mitochondria and thus high concentrations of cytochromes, with heme groups that are strong absorbers of visible light.

The mitochondria of brown adipocytes are much like those of other mammalian cells, except in having a unique protein in their inner membrane. **Thermogenin**, also called the **uncoupling protein** (the product of the *UCP1* gene), provides a path for protons to return to the matrix without passing through the F_oF_1 complex **(Fig. 19–34)**. As a result of this short-circuiting of protons, the energy of oxidation is not conserved by ATP formation but is dissipated as heat, which contributes to maintaining the body temperature (see Fig. 23–17). Hibernating animals also depend on the activity of uncoupled BAT mitochondria to generate heat during their long dormancy (see Box 17–1). We will return to the role of thermogenin when we discuss the regulation of body mass in Chapter 23 (pp. 931–932).

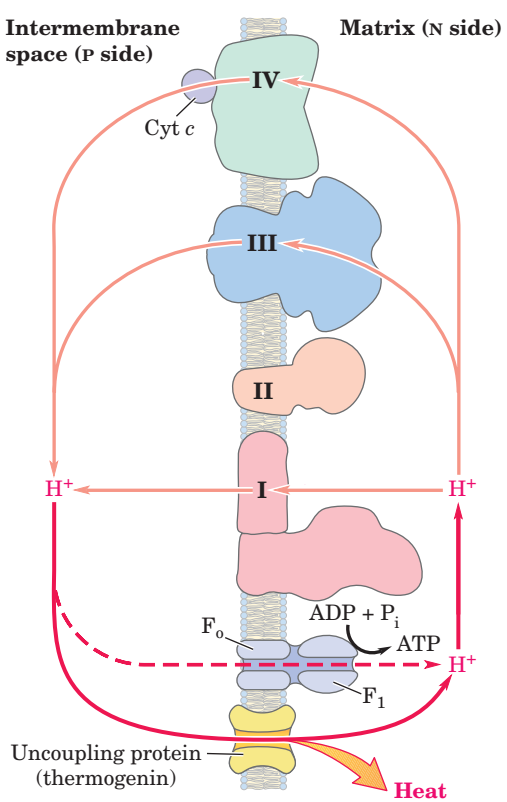

FIGURE 19–34 Heat generation by uncoupled mitochondria. The uncoupling protein (thermogenin) in the mitochondria of brown adipose tissue, by providing an alternative route for protons to reenter the mitochondrial matrix, causes the energy conserved by proton pumping to be dissipated as heat.

Mitochondrial P-450 Oxygenases Catalyze Steroid Hydroxylations

Mitochondria are the site of biosynthetic reactions that produce steroid hormones, including the sex hormones, glucocorticoids, mineralocorticoids, and vitamin D hormone. These compounds are synthesized from cholesterol or a related sterol in a series of hydroxylations catalyzed by enzymes of the **cytochrome P-450** family, all of which have a critical heme group (its absorption at 450 nm gives this family its name). In the hydroxylation reactions, one atom of molecular oxygen is incorporated into the substrate and the second is reduced to H_2O:

$$R\text{—}H + O_2 + NADPH \longrightarrow R\text{—}OH + H_2O + NADP^+$$

There are dozens of P-450 enzymes, all situated in the inner mitochondrial membrane with their catalytic site exposed to the matrix. Steroidogenic cells are packed with mitochondria specialized for steroid synthesis; the mitochondria are generally larger than those in other tissues and have more extensive and highly convoluted inner membranes **(Fig. 19–35)**.

The path of electron flow in the mitochondrial P-450 system is complex, involving a flavoprotein and an iron-sulfur protein that carry electrons from NADPH to the P-450 heme **(Fig. 19–36)**. The detailed structure of a P-450 enzyme confers its substrate specificity, and its heme group, which interacts directly with O_2, anchors the catalytic activity shared by all P-450 enzymes.

Another large family of P-450 enzymes is found in the endoplasmic reticulum of hepatocytes. These enzymes catalyze reactions similar to the mitochondrial P-450 reactions, but their substrates include a wide variety of hydrophobic compounds, many of which are **xenobiotics**—compounds not found in nature but synthesized industrially. The P-450 enzymes of the ER have very broad and overlapping substrate specificities.

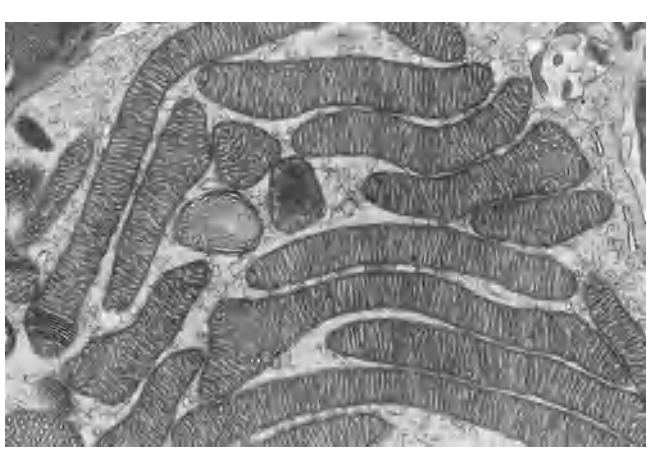

FIGURE 19–35 Mitochondria of adrenal gland, specialized for steroid synthesis. As seen in this electron micrograph of a thin section of adrenal gland, the mitochondria are profuse and have extensive cristae, providing a large surface for the P-450 enzymes of the inner membrane.

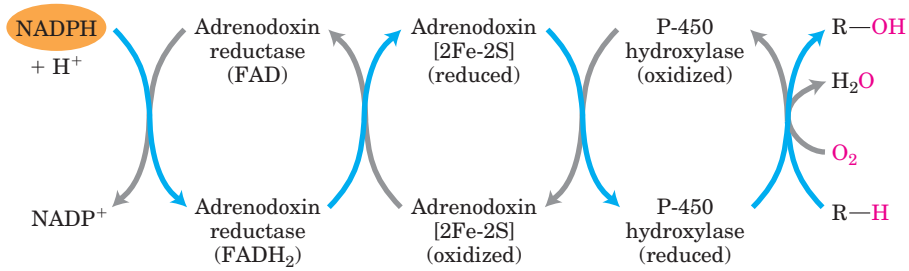

FIGURE 19–36 Path of electron flow in mitochondrial cytochrome P-450 reactions in adrenal gland. Two electrons are transferred from NADPH to the FAD-containing flavoprotein adrenodoxin reductase, which passes the electrons, one at a time, to adrenodoxin, a small, soluble 2Fe-2S protein. Adrenodoxin passes single electrons to the cytochrome P-450 hydroxylase, which interacts directly with O_2 and the substrate (R—H) to form the products, H_2O and R—OH.

Hydroxylation of the hydrophobic compounds makes them more water soluble, and they can then be cleared by the kidneys and excreted in urine. Among the substrates for these P-450 oxygenases are many commonly used prescription drugs. Metabolism by P-450 enzymes limits the drugs' lifetime in the bloodstream and their therapeutic effects. Humans differ in their genetic complement of P-450 enzymes in the ER, and in the extent to which certain P-450 enzymes have been induced, such as by a history of ethanol ingestion. In principle, therefore, an individual's genetics and personal history could figure into determinations of therapeutic drug dose; in practice, this precise tailoring of dosage is not yet economically feasible, but it may become so. ■

Mitochondria Are Central to the Initiation of Apoptosis

Apoptosis, also called **programmed cell death**, is a process in which individual cells die for the good of the organism (for example, in the course of normal embryonic development), and the organism conserves the cells' molecular components (amino acids, nucleotides, and so forth). Apoptosis may be triggered by an external signal, acting at a plasma membrane receptor, or by internal events such as a DNA damage, viral infection, oxidative stress from the accumulation of ROS, or another stress such as a heat shock.

Mitochondria play a critical role in triggering apoptosis. When a stressor gives the signal for cell death, one early consequence is an increase in the permeability of the outer mitochondrial membrane, allowing cytochrome *c* to escape from the intermembrane space into the cytosol **(Fig. 19–37)**. The increased permeability is due to the opening of the **permeability transition pore complex (PTPC)**, a multisubunit protein in the outer membrane; its opening and closing are affected by several proteins that stimulate or suppress apoptosis. When released into the cytosol, cytochrome *c*

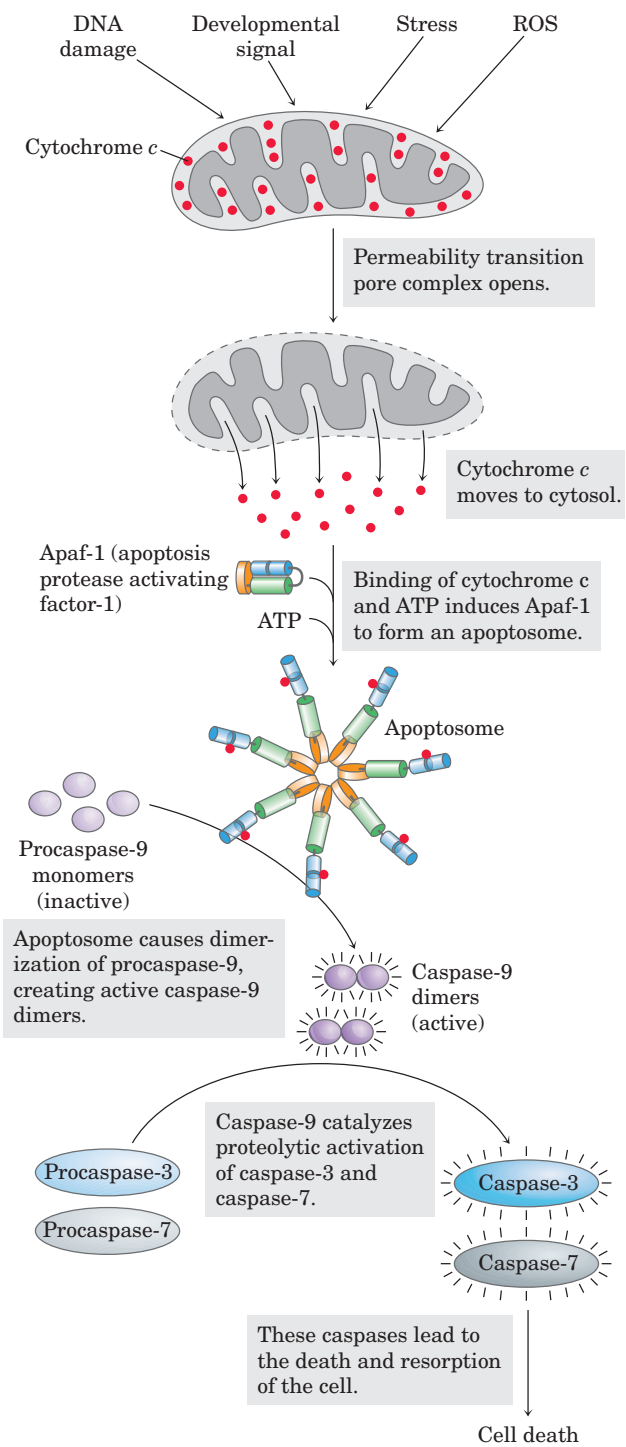

FIGURE 19–37 Role of cytochrome *c* in apoptosis. Cytochrome *c* is a small, soluble, mitochondrial protein, located in the intermembrane space, that carries electrons between Complex III and Complex IV during respiration. In a completely separate role, as outlined here, it acts as a trigger for apoptosis by stimulating the activation of a family of proteases called caspases.

interacts with monomers of the protein **Apaf-1 (apoptosis protease activating factor-1)**, causing the formation of an **apoptosome** composed of seven Apaf-1 and seven cytochrome *c* molecules. The apoptosome provides the platform on which the protease procaspase-9 is activated to caspase-9, a member of a family of highly specific proteases (the **caspases**) involved in apoptosis. They share a critical *C*ys residue at their active site, and all cleave proteins only on the carboxyl-terminal side of *Asp* residues, thus the name "caspases." Activated caspase-9 initiates a cascade of proteolytic activations, with one caspase activating a second, and it in turn activating a third, and so forth (see Fig. 12–51). (This role of cytochrome *c* in apoptosis is a clear case of "moonlighting," in that one protein plays two very different roles in the cell; see Box 16–1.)

SUMMARY 19.4 Mitochondria in Thermogenesis, Steroid Synthesis, and Apoptosis

- In the brown adipose tissue of newborns, electron transfer is uncoupled from ATP synthesis and the energy of fuel oxidation is dissipated as metabolic heat.
- Hydroxylation reaction steps in the synthesis of steroid hormones in steroidogenic tissues (adrenal gland, gonads, liver, and kidney) take place in specialized mitochondria.
- Mitochondrial cytochrome *c*, released into the cytosol, participates in activation of caspase-9, one of the proteases involved in apoptosis.

19.5 Mitochondrial Genes: Their Origin and the Effects of Mutations

Mitochondria contain their own genome, a circular, double-stranded DNA (mtDNA) molecule. Each of the hundreds or thousands of mitochondria in a typical cell has about five copies of this genome. The human mitochondrial chromosome **(Fig. 19–38)** contains 37 genes (16,569 bp), including 13 that encode subunits of proteins of the respiratory chain (Table 19–6); the remaining genes code for rRNA and tRNA molecules essential to the protein-synthesizing machinery of mitochondria. The great majority of mitochondrial proteins—about 900 different types—are encoded by nuclear genes, synthesized on cytoplasmic ribosomes, then imported into and assembled in the mitochondria (Chapter 27).

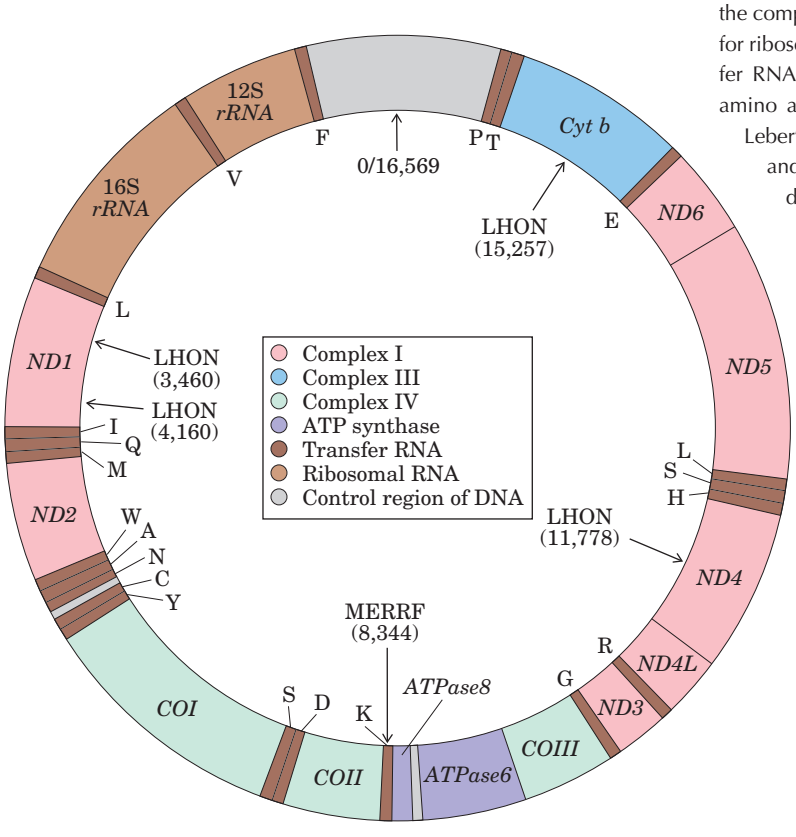

(a)

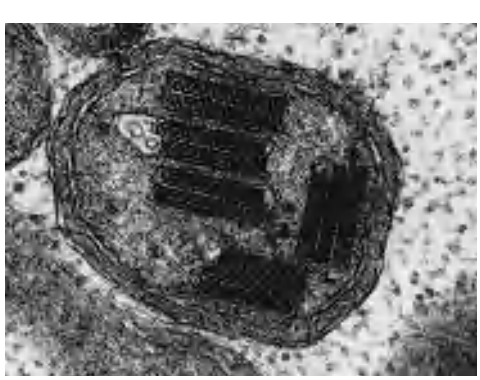

(b)

FIGURE 19–38 Mitochondrial genes and mutations. (a) Map of human mitochondrial DNA, showing the genes that encode proteins of Complex I, the NADH dehydrogenase (*ND1* to *ND6*); the cytochrome *b* of Complex III (*Cyt b*); the subunits of cytochrome oxidase (Complex IV) (*COI* to *COIII*); and two subunits of ATP synthase (*ATPase6* and *ATPase8*). The colors of the genes correspond to those of the complexes shown in Figure 19–7. Also included here are the genes for ribosomal RNAs (*rRNA*) and for some mitochondrion-specific transfer RNAs; tRNA specificity is indicated by the one-letter codes for amino acids. Arrows indicate the positions of mutations that cause Leber's hereditary optic neuropathy (LHON) and myoclonic epilepsy and ragged-red fiber disease (MERRF). Numbers in parentheses indicate the position of the altered nucleotides (nucleotide 1 is at the top of the circle and numbering proceeds counterclockwise). **(b)** Electron micrograph of an abnormal mitochondrion from the muscle of an individual with MERRF, showing the paracrystalline protein inclusions sometimes present in the mutant mitochondria.

TABLE 19–6 Respiratory Proteins Encoded by Mitochondrial Genes in Humans

Complex	Number of subunits	Number of subunits encoded by mitochondrial DNA
I NADH dehydrogenase	43	7
II Succinate dehydrogenase	4	0
III Ubiquinone:cytochrome *c* oxidoreductase	11	1
IV Cytochrome oxidase	13	3
V ATP synthase	8	2

Mitochondria Evolved from Endosymbiotic Bacteria

The existence of mitochondrial DNA, ribosomes, and tRNAs supports the hypothesis of the endosymbiotic origin of mitochondria (see Fig. 1–36), which holds that the first organisms capable of aerobic metabolism, including respiration-linked ATP production, were bacteria. Primitive eukaryotes that lived anaerobically (by fermentation) acquired the ability to carry out oxidative phosphorylation when they established a symbiotic relationship with bacteria living in their cytosol. After much evolution and the movement of many bacterial genes into the nucleus of the "host" eukaryote, the endosymbiotic bacteria eventually became mitochondria.

This hypothesis presumes that early free-living bacteria had the enzymatic machinery for oxidative phosphorylation and predicts that their modern bacterial descendants must have respiratory chains closely similar to those of modern eukaryotes. They do. Aerobic bacteria carry out NAD-linked electron transfer from substrates to O_2, coupled to the phosphorylation of cytosolic ADP. The dehydrogenases are located in the bacterial cytosol and the respiratory chain in the plasma membrane. The electron carriers translocate protons outward across the plasma membrane as electrons are transferred to O_2. Bacteria such as *Escherichia coli* have F_oF_1 complexes in their plasma membranes; the F_1 portion protrudes into the cytosol and catalyzes ATP synthesis from ADP and P_i as protons flow back into the cell through the proton channel of F_o.

The respiration-linked extrusion of protons across the bacterial plasma membrane also provides the driving force for other processes. Certain bacterial transport systems bring about uptake of extracellular nutrients (lactose, for example) against a concentration gradient, in symport with protons (see Fig. 11–42). And the rotary motion of bacterial flagella is provided by "proton turbines," molecular rotary motors driven not by ATP but directly by the transmembrane electrochemical potential generated by respiration-linked proton pumping **(Fig. 19–39)**. It seems likely that the chemiosmotic mechanism evolved early, before the emergence of eukaryotes.

Mutations in Mitochondrial DNA Accumulate throughout the Life of the Organism

The respiratory chain is the major producer of reactive oxygen species in cells, so mitochondrial contents, including the mitochondrial genome, suffer the greatest exposure to, and damage by, ROS. Moreover, the mitochondrial DNA replication system is less effective than the nuclear system at correcting mistakes made during replication and at repairing DNA damage. As a consequence of these two factors, defects in mtDNA accumulate over time. One theory of aging is that this gradual accumulation of defects with increasing age is the primary cause of many of the "symptoms" of aging, which include, for example, progressive weakening of skeletal and heart muscle.

A unique feature of mitochondrial inheritance is the variation among individual cells, and between one individual organism and another, in the effects of a mtDNA mutation. A typical cell has hundreds or thou-

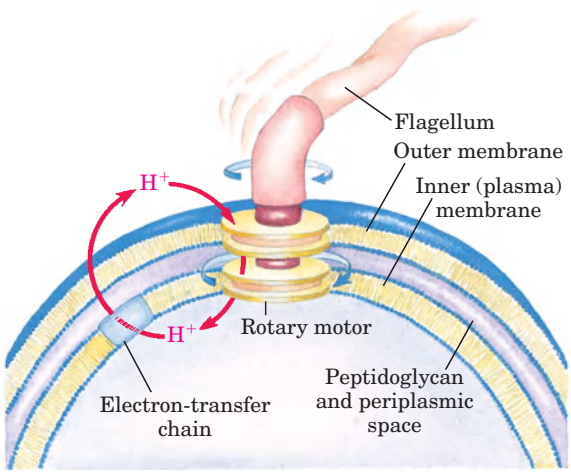

FIGURE 19–39 Rotation of bacterial flagella by proton-motive force. The shaft and rings at the base of the flagellum make up a rotary motor that has been called a "proton turbine." Protons ejected by electron transfer flow back into the cell through the turbine, causing rotation of the shaft of the flagellum. This motion differs fundamentally from the motion of muscle and of eukaryotic flagella and cilia, for which ATP hydrolysis is the energy source.

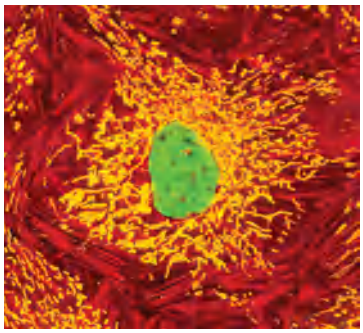

FIGURE 19–40 Single cells contain many mitochondria. A typical animal cell has hundreds or thousands of mitochondria, some fraction of which may contain genomes with mutations that affect mitochondrial function. This ovine (sheep) kidney epithelial cell was cultured in the laboratory, fixed, and then stained with fluorescent probes that show mitochondria as gold, microfilaments of actin red, and nuclei green when observed in the fluorescence microscope.

sands of mitochondria, each with its own genome copy **(Fig. 19–40)**. Suppose that, in a female organism, damage to one mitochondrial genome occurs in a germ cell from which oocytes develop, such that the germ cell contains mainly mitochondria with wild-type genes but one mitochondrion with a mutant gene. During the course of oocyte maturation, as this germ cell and its descendants repeatedly divide, the defective mitochondrion replicates and its progeny, all defective, are randomly distributed to daughter cells. Eventually, the mature egg cells contain different proportions of the defective mitochondria. When an egg cell is fertilized and undergoes the many divisions of embryonic development, the resulting somatic cells differ in their proportion of mutant mitochondria **(Fig. 19–41a)**. (Keep in mind that a developing embryo derives all of its mitochondria from the egg, none from the sperm cell.) This **heteroplasmy** (in contrast to **homoplasmy**, in which every mitochondrial genome in every cell is the same) results in mutant phenotypes of varying degrees of severity. Cells (and tissues) containing mostly wild-type mitochondria have the wild-type phenotype; they are essentially normal. Other heteroplasmic cells will have intermediate phenotypes, some almost normal, others (with a high proportion of mutant mitochondria) abnormal (Fig. 19–41b). If the abnormal phenotype is associated with a disease (see below), individuals with the same mtDNA mutation may have disease symptoms of differing severity—depending on the number and distribution of affected mitochondria.

Some Mutations in Mitochondrial Genomes Cause Disease

A growing number of human diseases have been attributed to mutations in mitochondrial genes that reduce the cell's capacity to produce ATP. Some tissues and cell types—neurons, myocytes of both skeletal and cardiac muscle, and β cells of the pancreas—are less able than others to tolerate lowered ATP production and are therefore more affected by mutations in mitochondrial proteins.

A group of genetic diseases known as the **mitochondrial encephalomyopathies** affect primarily the brain and skeletal muscle. These diseases are invariably

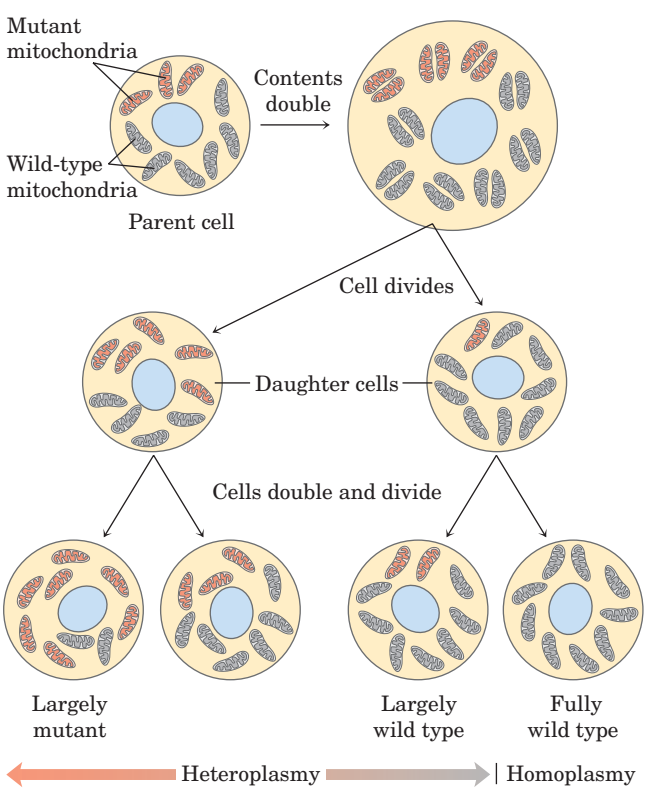

(a)

FIGURE 19–41 Heteroplasmy in mitochondrial genomes. (a) When a mature egg cell is fertilized, all of the mitochondria in the resulting diploid cell (zygote) are maternal; none come from the sperm. If some fraction of the maternal mitochondria have a mutant gene, the random distribution of mitochondria during subsequent cell divisions yields some daughter cells with mostly mutant mitochondria, some with mostly wild-type mitochondria, and some in between; thus the daughter cells show varying degrees of heteroplasmy. **(b)** Different degrees of heteroplasmy produce different cellular phenotypes. This section of human muscle tissue is from an individual with defective cytochrome oxidase. The cells have been stained to make wild-type cells blue and cells with mutant cytochrome oxidase brown. As the micrograph shows, different cells in the same tissue are affected to different degrees by the mitochondrial mutation.

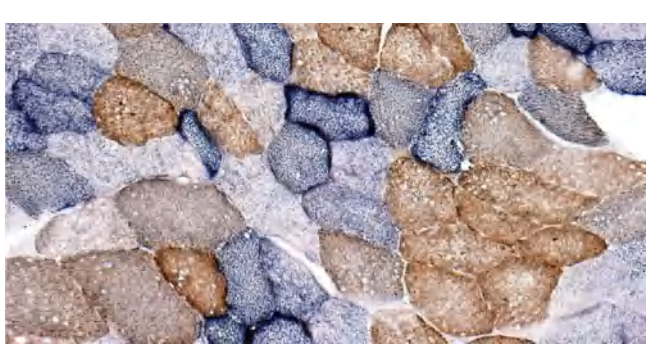

(b)

inherited from the mother, because, as noted above, a developing embryo derives all its mitochondria from the egg. The rare disease **Leber's hereditary optic neuropathy (LHON)** affects the central nervous system, including the optic nerves, causing bilateral loss of vision in early adulthood. A single base change in the mitochondrial gene *ND4* (Fig. 19–38a) changes an Arg residue to a His residue in a polypeptide of Complex I, and the result is mitochondria partially defective in electron transfer from NADH to ubiquinone. Although these mitochondria can produce some ATP by electron transfer from succinate, they apparently cannot supply sufficient ATP to support the very active metabolism of neurons. One result is damage to the optic nerve, leading to blindness. A single base change in the mitochondrial gene for cytochrome *b*, a component of Complex III, also produces LHON, demonstrating that the pathology results from a general reduction of mitochondrial function, not specifically from a defect in electron transfer through Complex I.

A mutation (in *ATP6*) that affects the proton pore in ATP synthase leads to low rates of ATP synthesis while leaving the respiratory chain intact. The oxidative stress due to the continued supply of electrons from NADH increases the production of ROS, and the damage to mitochondria caused by ROS sets up a vicious cycle. Half of individuals with this mutant gene die within days or months of birth.

Myoclonic epilepsy and ragged-red fiber disease (MERRF) is caused by a mutation in the mitochondrial gene that encodes a tRNA specific for lysine ($tRNA^{Lys}$). This disease, characterized by uncontrollable muscular jerking, apparently results from defective production of several of the proteins that require mitochondrial tRNAs for their synthesis. Skeletal muscle fibers of individuals with MERRF have abnormally shaped mitochondria that sometimes contain paracrystalline structures (Fig. 19–38b). Other mutations in mitochondrial genes are believed to be responsible for the progressive muscular weakness that characterizes mitochondrial myopathy and for enlargement and deterioration of the heart muscle in hypertrophic cardiomyopathy. According to one hypothesis on the progressive changes that accompany aging, the accumulation of mutations in mtDNA during a lifetime of exposure to DNA-damaging agents such as $^{\bullet}O_2^-$ results in mitochondria that cannot supply sufficient ATP for normal cellular function. Mitochondrial disease can also result from mutations in any of the 900 nuclear genes that encode mitochondrial proteins. ■

Diabetes Can Result from Defects in the Mitochondria of Pancreatic β Cells

The mechanism that regulates the release of insulin from pancreatic β cells hinges on the ATP concentration in those cells. When blood glucose is high, β cells take up glucose and oxidize it by glycolysis and the citric acid cycle, raising [ATP] above a threshold level **(Fig. 19–42)**. When [ATP] exceeds this threshold, an ATP-gated K^+ channel in the plasma membrane closes, depolarizing the membrane and triggering insulin release (see Fig. 23–28). Pancreatic β cells with defects in oxidative phosphorylation cannot increase [ATP] above this threshold, and the resulting failure of insulin release effectively produces diabetes. For example, defects in the gene for glucokinase, the hexokinase IV isozyme present in β cells, lead to a rare form of diabetes, MODY2 (see Box 15–3); low glucokinase activity prevents the generation of above-threshold [ATP], blocking insulin secretion. Mutations in the mitochondrial $tRNA^{Lys}$ or $tRNA^{Leu}$ genes also compromise mitochondrial ATP production, and type 2 diabetes mellitus is common among individuals with these defects (although these cases make up a very small fraction of all cases of diabetes).

When nicotinamide nucleotide transhydrogenase, which is part of the mitochondrial defense against ROS (see Fig. 19–18), is genetically defective, the accumulation of ROS damages mitochondria, slowing ATP production and blocking insulin release by β cells (Fig. 19–42). Damage caused by ROS, including damage to mtDNA, may also underlie other human diseases; there is some evidence for its involvement in Alzheimer's, Parkinson's, and Huntington's diseases and in heart failure, as well as in aging. ■

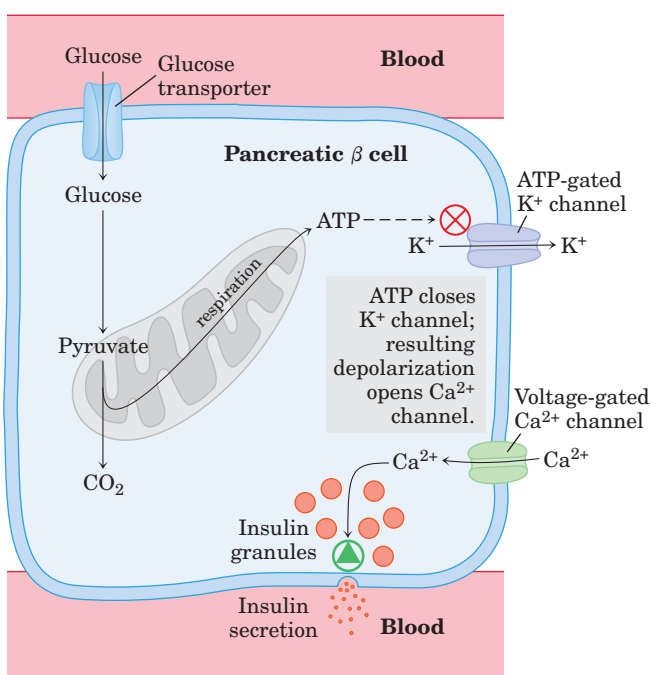

FIGURE 19–42 Defective oxidative phosphorylation in pancreatic β cells blocks insulin secretion. Normally, when blood glucose rises, the production of ATP in β cells increases. ATP, by blocking K^+ channels, depolarizes the plasma membrane and thus opens the voltage-gated Ca^{2+} channels. The resulting influx of Ca^{2+} triggers exocytosis of insulin-containing secretory vesicles, releasing insulin. When oxidative phosphorylation in β cells is defective, [ATP] is never sufficient to trigger this process, and insulin is not released.

SUMMARY 19.5 Mitochondrial Genes: Their Origin and the Effects of Mutations

- A small proportion of human mitochondrial proteins, 13 in all, are encoded by the mitochondrial genome and synthesized in mitochondria. About 900 mitochondrial proteins are encoded in nuclear genes and imported into mitochondria after their synthesis.
- Mitochondria arose from aerobic bacteria that entered into an endosymbiotic relationship with ancestral eukaryotes.
- Mutations in the mitochondrial genome accumulate over the life of the organism. Mutations in the genes that encode components of the respiratory chain, ATP synthase, and the ROS-scavenging system, and even in tRNA genes, can cause a variety of human diseases, which often most severely affect muscle, heart, pancreatic β cells, and brain.

PHOTOSYNTHESIS: HARVESTING LIGHT ENERGY

We now turn to another reaction sequence in which the flow of electrons is coupled to the synthesis of ATP: light-driven phosphorylation. The capture of solar energy by photosynthetic organisms and its conversion to the chemical energy of reduced organic compounds is the ultimate source of nearly all biological energy. Photosynthetic and heterotrophic organisms live in a balanced steady state in the biosphere **(Fig. 19–43)**. Photosynthetic organisms trap solar energy and form ATP and NADPH, which they use as energy sources to make carbohydrates and other organic compounds from CO_2 and H_2O; simultaneously, they release O_2 into the atmosphere. Aerobic heterotrophs (humans, for example, as well as plants during dark periods) use the O_2 so formed to degrade the energy-rich organic products of photosynthesis to CO_2 and H_2O, generating ATP. The CO_2 returns to the atmosphere, to be used again by photosynthetic organisms. Solar energy thus provides the driving force for the continuous cycling of CO_2 and O_2 through the biosphere and provides the reduced substrates—fuels, such as glucose—on which nonphotosynthetic organisms depend.

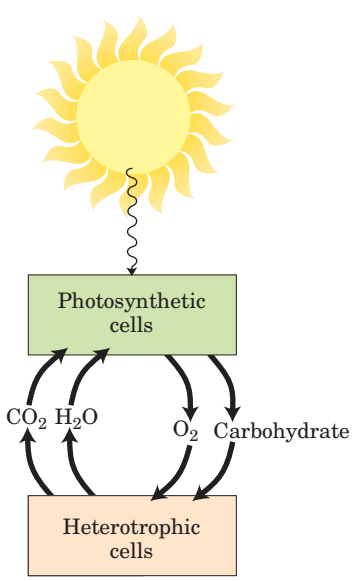

FIGURE 19–43 Solar energy as the ultimate source of all biological energy. Photosynthetic organisms use the energy of sunlight to manufacture glucose and other organic products, which heterotrophic cells use as energy and carbon sources.

Photosynthesis occurs in a variety of bacteria and in unicellular eukaryotes (algae) as well as in vascular plants. Although the process in these organisms differs in detail, the underlying mechanisms are remarkably similar, and much of our understanding of photosynthesis in vascular plants is derived from studies of simpler organisms. The overall equation for photosynthesis in vascular plants describes an oxidation-reduction reaction in which H_2O donates electrons (as hydrogen) for the reduction of CO_2 to carbohydrate (CH_2O):

$$CO_2 + H_2O \xrightarrow{\text{light}} O_2 + (CH_2O)$$

19.6 General Features of Photophosphorylation

Unlike NADH (the major electron donor in oxidative phosphorylation), H_2O is a poor donor of electrons; its standard reduction potential is 0.816 V, compared with −0.320 V for NADH. Photophosphorylation differs from oxidative phosphorylation in requiring the input of energy in the form of light to *create* a good electron donor and a good electron acceptor. In photophosphorylation, electrons flow through a series of membrane-bound carriers including cytochromes, quinones, and iron-sulfur proteins, while protons are pumped across a membrane to create an electrochemical potential. Electron transfer and proton pumping are catalyzed by membrane complexes homologous in structure and function to Complex III of mitochondria. The electrochemical potential they produce is the driving force for ATP synthesis from ADP and P_i, catalyzed by a membrane-bound ATP synthase complex closely similar to that of oxidative phosphorylation.

Photosynthesis in plants encompasses two processes: the **light-dependent reactions**, or **light reactions**, which occur only when plants are illuminated, and the **carbon-assimilation reactions** (or **carbon-fixation reactions**), sometimes misleadingly called the dark reactions, which are driven by products of the light reactions **(Fig. 19–44)**. In the light reactions, chlorophyll and other pigments of photosynthetic cells absorb light energy and conserve it as ATP and NADPH; simultaneously, O_2 is evolved. In the carbon-assimilation reactions, ATP and

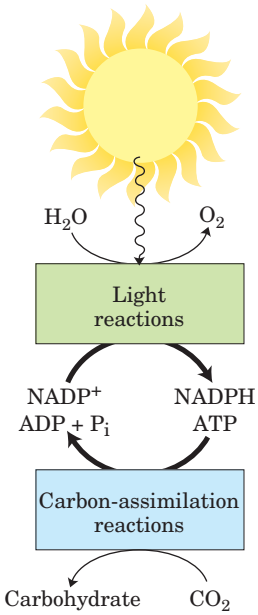

FIGURE 19–44 The light reactions of photosynthesis generate energy-rich NADPH and ATP at the expense of solar energy. NADPH and ATP are used in the carbon-assimilation reactions, which occur in light or darkness, to reduce CO_2 to form trioses and more complex compounds (such as glucose) derived from trioses.

NADPH are used to reduce CO_2 to form triose phosphates, starch, and sucrose, and other products derived from them. In this chapter we are concerned only with the light-dependent reactions that lead to the synthesis of ATP and NADPH. The reduction of CO_2 is described in Chapter 20.

Photosynthesis in Plants Takes Place in Chloroplasts

In photosynthetic eukaryotic cells, both the light-dependent and the carbon-assimilation reactions take place in the chloroplasts **(Fig. 19–45)**, intracellular organelles that are variable in shape and generally a few micrometers in diameter. Like mitochondria, they are surrounded by two membranes, an outer membrane that is permeable to small molecules and ions, and an inner membrane that encloses the internal compartment. This compartment contains many flattened, membrane-surrounded vesicles or sacs, the **thylakoids**, usually arranged in stacks called **grana** (Fig. 19–45b). Embedded in the thylakoid membranes (commonly called **lamellae**) are the photosynthetic pigments and the enzyme complexes that carry out the light reactions and ATP synthesis. The **stroma** (the aqueous phase enclosed by the inner membrane) contains most of the enzymes required for the carbon-assimilation reactions.

Light Drives Electron Flow in Chloroplasts

In 1937 Robert Hill found that when leaf extracts containing chloroplasts were illuminated, they (1) evolved O_2 and (2) reduced a nonbiological electron acceptor added to the medium, according to the **Hill reaction**:

$$2H_2O + 2A \xrightarrow{\text{light}} 2AH_2 + O_2$$

where A is the artificial electron acceptor, or **Hill reagent**. One Hill reagent, the dye 2,6-dichlorophenolindophenol, is blue when oxidized (A) and colorless when reduced (AH_2), making the reaction easy to follow.

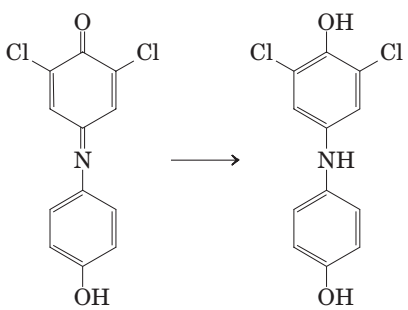

Oxidized form (blue) → Reduced form (colorless)

Dichlorophenolindophenol

When a leaf extract supplemented with the dye was illuminated, the blue dye became colorless and O_2 was evolved. In the dark, neither O_2 evolution nor dye reduction took place. This was the first evidence that absorbed

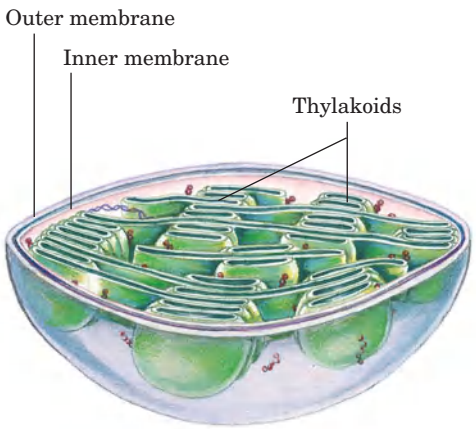

(a)

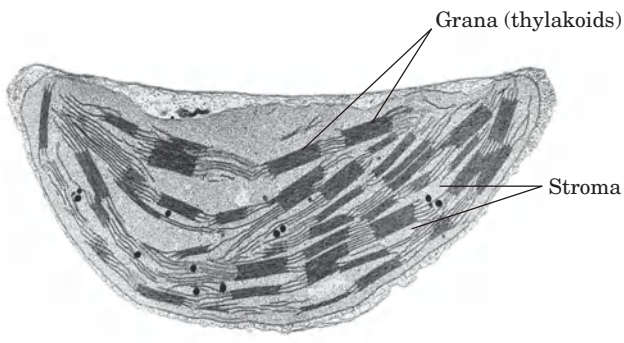

(b)

FIGURE 19–45 Chloroplast. (a) Schematic diagram. **(b)** Electron micrograph at high magnification showing grana, stacks of thylakoid membranes.

light energy causes electrons to flow from H_2O to an electron acceptor. Moreover, Hill found that CO_2 was neither required nor reduced to a stable form under these conditions; O_2 evolution could be dissociated from CO_2 reduction. Several years later Severo Ochoa showed that $NADP^+$ is the biological electron acceptor in chloroplasts, according to the equation

$$2H_2O + 2NADP^+ \xrightarrow{\text{light}} 2NADPH + 2H^+ + O_2$$

To understand this photochemical process, we must first consider the more general topic of the effects of light absorption on molecular structure.

SUMMARY 19.6 General Features of Photophosphorylation

- The light reactions of photosynthesis are those directly dependent on the absorption of light; the resulting photochemistry takes electrons from H_2O and drives them through a series of membrane-bound carriers, producing NADPH and ATP.
- The carbon-assimilation reactions of photosynthesis reduce CO_2 with electrons from NADPH and energy from ATP.

19.7 Light Absorption

Visible light is electromagnetic radiation of wavelengths 400 to 700 nm, a small part of the electromagnetic spectrum **(Fig. 19–46)**, ranging from violet to red. The energy of a single **photon** (a quantum of light) is greater at the violet end of the spectrum than at the red end; shorter wavelength (and higher frequency) corresponds to higher energy. The energy, E, in a single photon of visible light is given by the Planck equation:

$$E = h\nu = hc/\lambda$$

where h is Planck's constant (6.626×10^{-34} J · s), ν is the frequency of the light in cycles/s, c is the speed of light (3.00×10^8 m/s), and λ is the wavelength in meters.

The energy of a photon of visible light ranges from 150 kJ/einstein for red light to ~300 kJ/einstein for violet light.

WORKED EXAMPLE 19–2 Energy of a Photon

The light used by vascular plants for photosynthesis has a wavelength of about 700 nm. Calculate the energy in a "mole" of photons (an einstein) of light of this wavelength, and compare this with the energy needed to synthesize a mole of ATP.

Solution: The energy in a single photon is given by the Planck equation. At a wavelength of 700×10^{-9} m, the energy of a photon is

$$\begin{aligned} E &= hc/\lambda \\ &= [(6.626 \times 10^{-34}\ \text{J} \cdot \text{s})(3.00 \times 10^8\ \text{m/s})]/(7.00 \times 10^{-7}\ \text{m}) \\ &= 2.84 \times 10^{-19}\ \text{J} \end{aligned}$$

An einstein of light is Avogadro's number (6.022×10^{23}) of photons, thus the energy of one einstein of photons at 700 nm is given by

$$\begin{aligned} &(2.84 \times 10^{-19}\ \text{J/photon})(6.022 \times 10^{23}\ \text{photons/einstein}) \\ &\qquad = 17.1 \times 10^4\ \text{J/einstein} \\ &\qquad = 171\ \text{kJ/einstein.} \end{aligned}$$

So, a "mole" of photons of red light has about five times the energy needed to produce a mole of ATP from ADP and P_i (30.5 kJ/mol).

When a photon is absorbed, an electron in the absorbing molecule (chromophore) is lifted to a higher energy level. This is an all-or-nothing event; to be absorbed, the photon must contain a quantity of energy (a **quantum**) that exactly matches the energy of the electronic transition. A molecule that has absorbed a photon is in an **excited state**, which is generally unstable. An electron lifted into a higher-energy orbital usually returns rapidly to its lower-energy orbital; the excited molecule decays to the stable **ground state**, giving up the absorbed quantum as light or heat or using

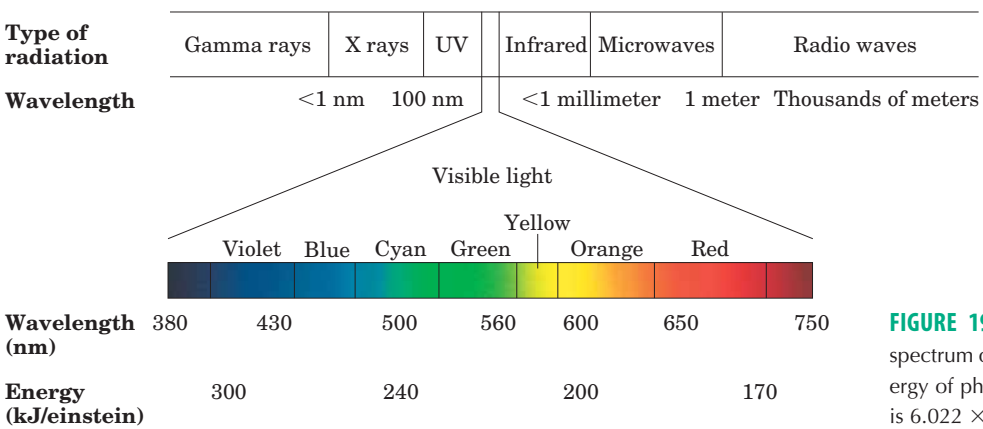

FIGURE 19–46 Electromagnetic radiation. The spectrum of electromagnetic radiation, and the energy of photons in the visible range. One einstein is 6.022×10^{23} photons.

it to do chemical work. Light emission accompanying decay of excited molecules (called **fluorescence**) is always at a longer wavelength (lower energy) than that of the absorbed light (see Box 12–3). An alternative mode of decay important in photosynthesis involves direct transfer of excitation energy from an excited molecule to a neighboring molecule. Just as the photon is a quantum of light energy, so the **exciton** is a quantum of energy passed from an excited molecule to another molecule in a process called **exciton transfer**.

Chlorophylls Absorb Light Energy for Photosynthesis

The most important light-absorbing pigments in the thylakoid membranes are the **chlorophylls**, green pigments with polycyclic, planar structures resembling the protoporphyrin of hemoglobin (see Fig. 5–1), except that Mg^{2+}, not Fe^{2+}, occupies the central position **(Fig. 19–47)**. The four inward-oriented nitrogen atoms of chlorophyll are coordinated with the Mg^{2+}. All chlorophylls have a long **phytol** side chain, esterified to

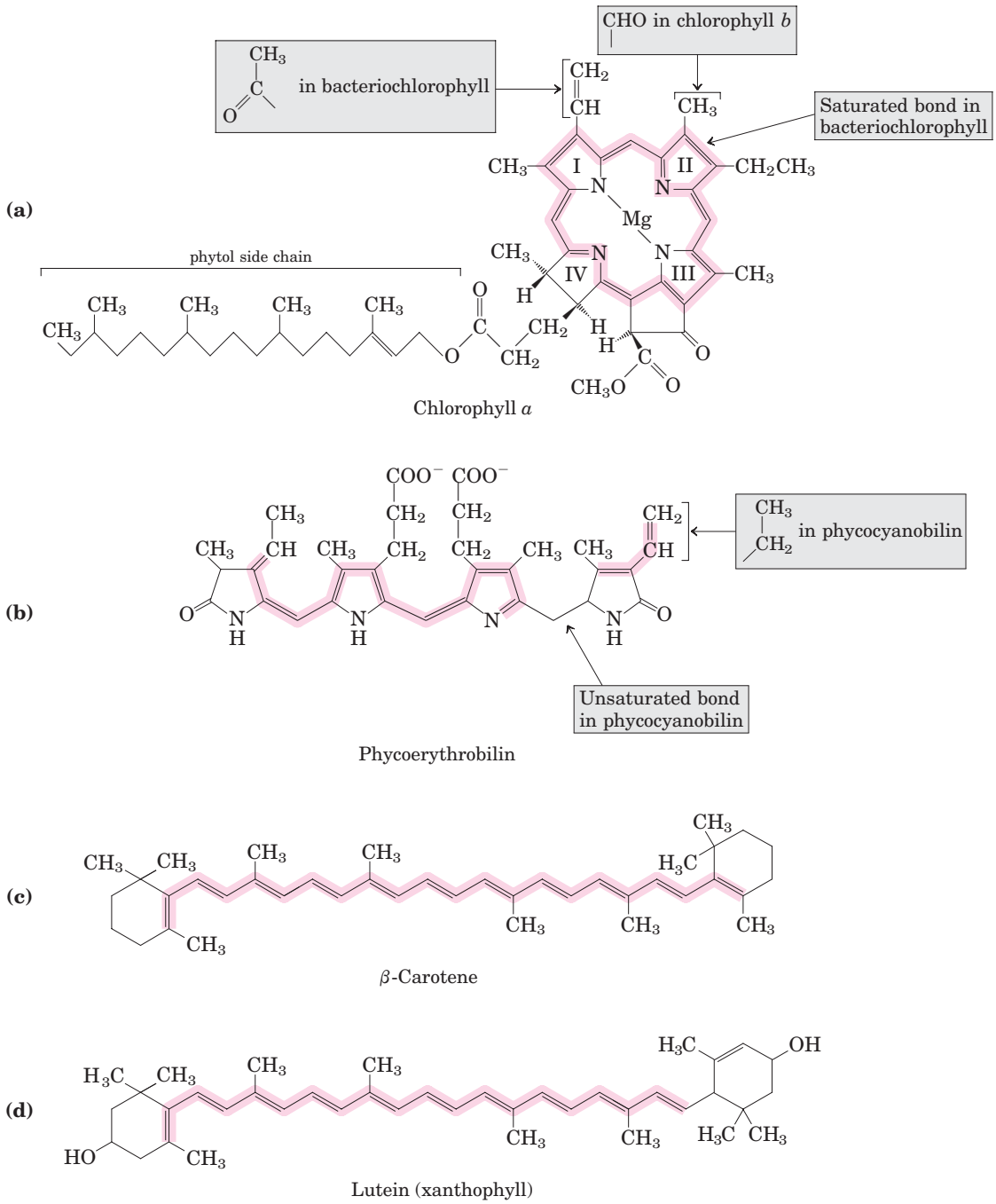

FIGURE 19–47 Primary and secondary photopigments. (a) Chlorophylls *a* and *b* and bacteriochlorophyll are the primary gatherers of light energy. **(b)** Phycoerythrobilin and phycocyanobilin (phycobilins) are the antenna pigments in cyanobacteria and red algae. **(c)** β-Carotene (a carotenoid) and **(d)** lutein (a xanthophyll) are accessory pigments in plants. The areas shaded pink are the conjugated systems (alternating single and double bonds) that largely account for the absorption of visible light.

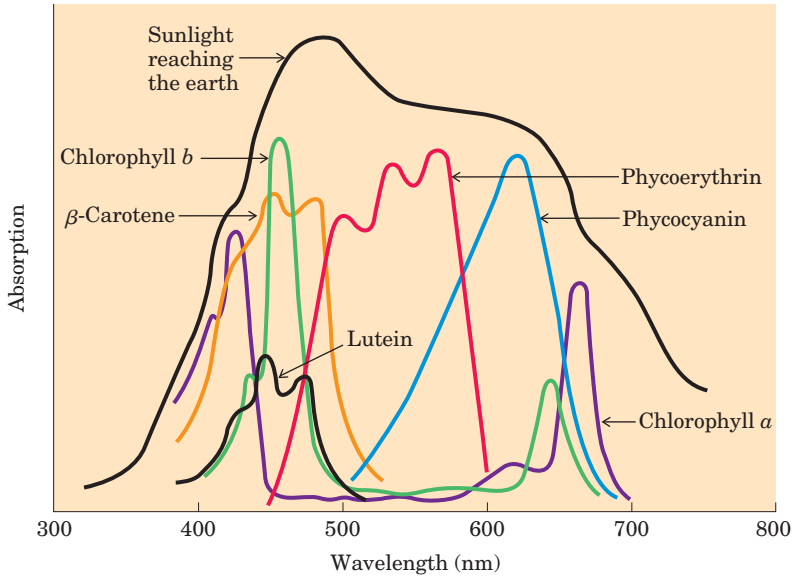

FIGURE 19–48 Absorption of visible light by photopigments. Plants are green because their pigments absorb light from the red and blue regions of the spectrum, leaving primarily green light to be reflected or transmitted. Compare the absorption spectra of the pigments with the spectrum of sunlight reaching the earth's surface; the combination of chlorophylls (*a* and *b*) and accessory pigments enables plants to harvest most of the energy available in sunlight.

The relative amounts of chlorophylls and accessory pigments are characteristic of a particular plant species. Variation in the proportions of these pigments is responsible for the range of colors of photosynthetic organisms, from the deep blue-green of spruce needles, to the greener green of maple leaves, to the red, brown, or purple color of some species of multicellular algae and the leaves of some foliage plants favored by gardeners.

a carboxyl-group substituent in ring IV, and chlorophylls also have a fifth five-membered ring not present in heme.

The heterocyclic five-ring system that surrounds the Mg^{2+} has an extended polyene structure, with alternating single and double bonds. Such polyenes characteristically show strong absorption in the visible region of the spectrum **(Fig. 19–48)**; the chlorophylls have unusually high molar extinction coefficients (see Box 3–1) and are therefore particularly well-suited for absorbing visible light during photosynthesis.

Chloroplasts always contain both chlorophyll *a* and chlorophyll *b* (Fig. 19–47a). Although both are green, their absorption spectra are sufficiently different (Fig. 19–48) that they complement each other's range of light absorption in the visible region. Most plants contain about twice as much chlorophyll *a* as chlorophyll *b*. The pigments in algae and photosynthetic bacteria include chlorophylls that differ only slightly from the plant pigments.

Chlorophyll is always associated with specific binding proteins, forming **light-harvesting complexes (LHCs)** in which chlorophyll molecules are fixed in relation to each other, to other protein complexes, and to the membrane. One light-harvesting complex (LHCII; **Fig. 19–49**) contains seven molecules of chlorophyll *a*, five of chlorophyll *b*, and two of the accessory pigment lutein (see below).

Cyanobacteria and red algae employ **phycobilins** such as phycoerythrobilin and phycocyanobilin (Fig. 19–47b) as their light-harvesting pigments. These open-chain tetrapyrroles have the extended polyene system found in chlorophylls, but not their cyclic structure or central Mg^{2+}. Phycobilins are covalently linked to specific binding proteins, forming **phycobiliproteins**, which associate in highly ordered complexes called

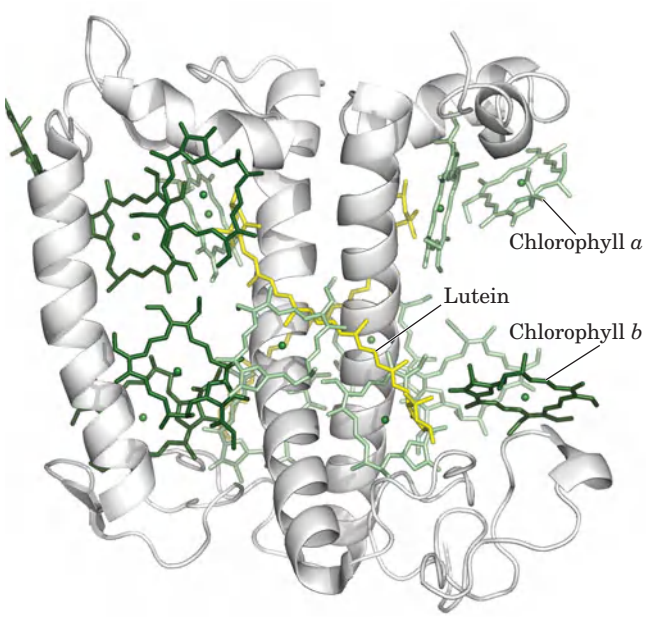

FIGURE 19–49 A light-harvesting complex, LHCII. (PDB ID 2BHW) The functional unit is an LHC trimer, with 36 chlorophyll and 6 lutein molecules. Shown here is a monomer, viewed in the plane of the membrane, with its three transmembrane α-helical segments, seven chlorophyll *a* molecules (light green), five chlorophyll *b* molecules (dark green), and two molecules of the accessory pigment lutein (yellow), which form an internal cross-brace.

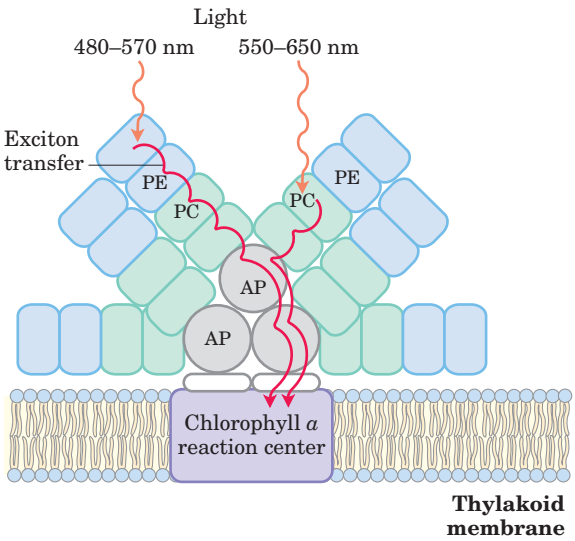

FIGURE 19–50 A phycobilisome. In these highly structured assemblies found in cyanobacteria and red algae, phycobilin pigments bound to specific proteins form complexes called phycoerythrin (PE), phycocyanin (PC), and allophycocyanin (AP). The energy of photons absorbed by PE or PC is conveyed through AP (a phycocyanobilin-binding protein) to chlorophyll *a* of the reaction center by exciton transfer, a process discussed in the text.

phycobilisomes **(Fig. 19–50)** that constitute the primary light-harvesting structures in these microorganisms.

Accessory Pigments Extend the Range of Light Absorption

In addition to chlorophylls, thylakoid membranes contain secondary light-absorbing pigments, or **accessory pigments**, called carotenoids. **Carotenoids** may be yellow, red, or purple. The most important are ***β*-carotene**, which is a red-orange isoprenoid, and the yellow carotenoid **lutein** (Fig. 19–47c, d). The carotenoid pigments absorb light at wavelengths not absorbed by the chlorophylls (Fig. 19–48) and thus are supplementary light receptors.

Experimental determination of the effectiveness of light of different colors in promoting photosynthesis yields an **action spectrum (Fig. 19–51)**, often useful in identifying the pigment primarily responsible for a biological effect of light. By capturing light in a region of the spectrum not used by other organisms, a photosynthetic organism can claim a unique ecological niche. For example, the phycobilins in red algae and cyanobacteria absorb light in the range 520 to 630 nm (Fig. 19–48), allowing them to occupy niches where light of lower or higher wavelength has been filtered out by the pigments of other organisms living in the water above them, or by the water itself.

Chlorophyll Funnels the Absorbed Energy to Reaction Centers by Exciton Transfer

The light-absorbing pigments of thylakoid or bacterial membranes are arranged in functional arrays called

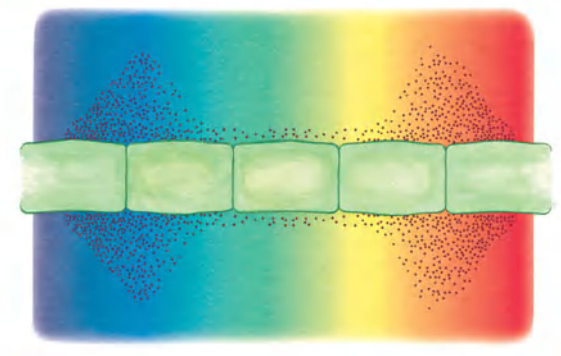

(a)

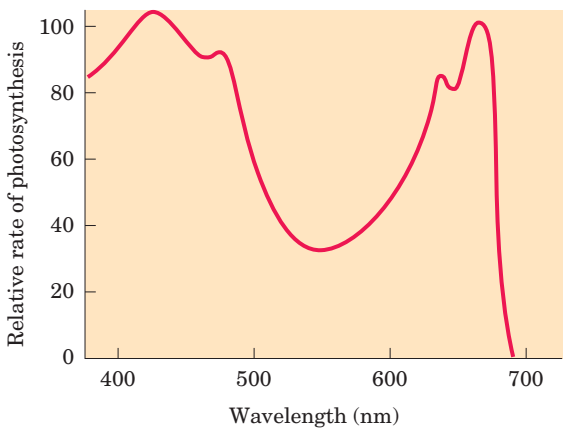

(b)

FIGURE 19–51 Two ways to determine the action spectrum for photosynthesis. (a) Results of a classic experiment performed by T. W. Englemann in 1882 to determine the wavelength of light that is most effective in supporting photosynthesis. Englemann placed cells of a filamentous photosynthetic alga on a microscope slide and illuminated them with light from a prism, so that one part of the filament received mainly blue light, another part yellow, another red. To determine which algal cells carried out photosynthesis most actively, Englemann also placed on the microscope slide bacteria known to migrate toward regions of high O_2 concentration. After a period of illumination, the distribution of bacteria showed highest O_2 levels (produced by photosynthesis) in the regions illuminated with violet and red light.

(b) Results of a similar experiment that used modern techniques (an oxygen electrode) for the measurement of O_2 production. An action spectrum (as shown here) describes the relative rate of photosynthesis for illumination with a constant number of photons of different wavelengths. An action spectrum is useful because, by comparison with absorption spectra (such as those in Fig. 19–48), it suggests which pigments can channel energy into photosynthesis.

photosystems. In spinach chloroplasts, for example, each photosystem contains about 200 chlorophyll and 50 carotenoid molecules. All the pigment molecules in a photosystem can absorb photons, but only a few chlorophyll molecules associated with the **photochemical reaction center** are specialized to transduce light into chemical energy. The other pigment molecules in a photosystem are called **light-harvesting** or **antenna molecules**. They absorb light energy

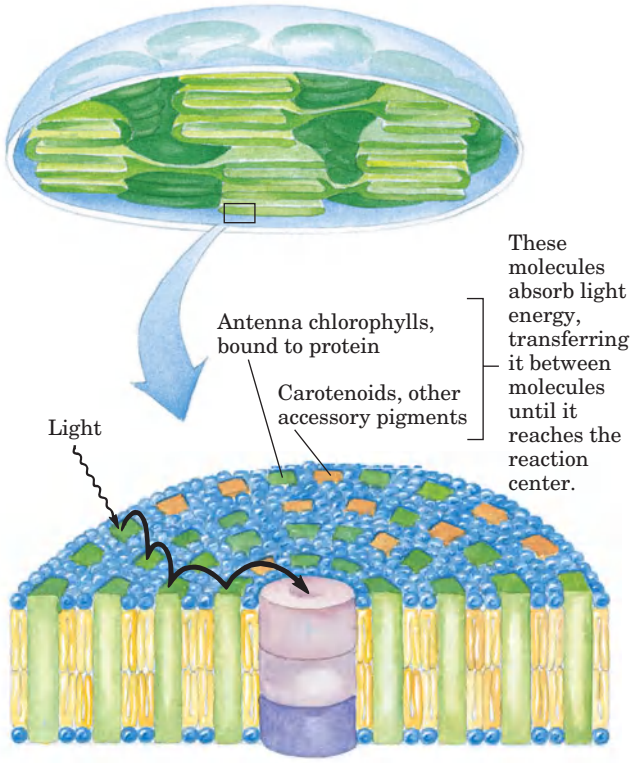

FIGURE 19–52 Organization of photosystems in the thylakoid membrane. Photosystems are tightly packed in the thylakoid membrane, with several hundred antenna chlorophylls and accessory pigments surrounding a photoreaction center. Absorption of a photon by any of the antenna chlorophylls leads to excitation of the reaction center by exciton transfer (black arrow). Also embedded in the thylakoid membrane are the cytochrome b_6f complex and ATP synthase (see Fig. 19–60).

and transmit it rapidly and efficiently to the reaction center **(Fig. 19–52)**.

The chlorophyll molecules in light-harvesting complexes have light-absorption properties that are subtly different from those of free chlorophyll. When isolated chlorophyll molecules in vitro are excited by light, the absorbed energy is quickly released as fluorescence and heat, but when chlorophyll in intact leaves is excited by visible light (**Fig. 19–53**, step ①), very little fluorescence is observed. Instead, the excited antenna chlorophyll transfers energy directly to a neighboring chlorophyll molecule, which becomes excited as the first

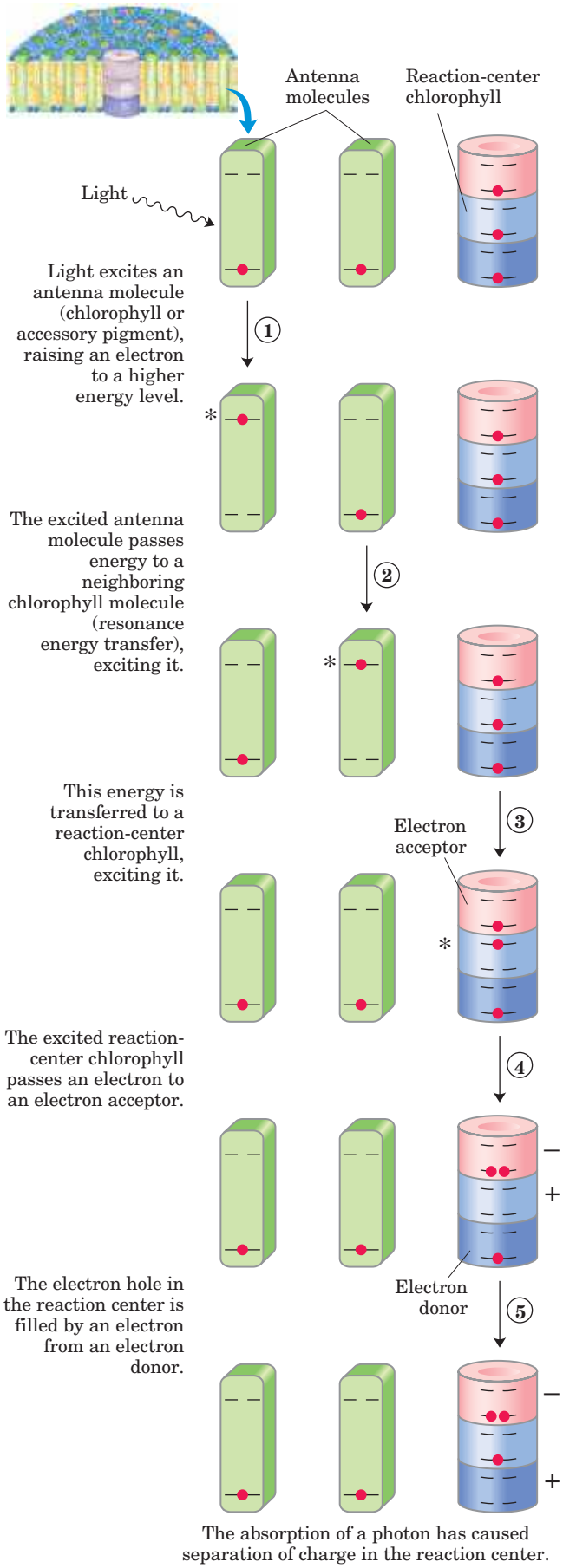

FIGURE 19–53 Exciton and electron transfer. This generalized scheme shows conversion of the energy of an absorbed photon into separation of charges at the reaction center. The steps are further described in the text. Note that step ① may repeat between successive antenna molecules until the exciton reaches a reaction-center chlorophyll. The asterisk (*) represents the excited state of an antenna molecule.

molecule returns to its ground state (step ②). This transfer of energy, exciton transfer, extends to a third, fourth, or subsequent neighbor, until one of a special pair of chlorophyll *a* molecules at the photochemical reaction center is excited (step ③). In this excited chlorophyll molecule, an electron is promoted to a higher-energy orbital. This electron then passes to a nearby electron acceptor that is part of the electron-transfer chain, leaving the reaction-center chlorophyll with a missing electron (an "electron hole," denoted by + in Fig. 19–53) (step ④). The electron acceptor acquires a negative charge in this transaction. The electron lost by the reaction-center chlorophyll is replaced by an electron from a neighboring electron-donor molecule (step⑤), which thereby becomes positively charged. In this way, *excitation by light causes electric charge separation and initiates an oxidation-reduction chain.*

SUMMARY 19.7 Light Absorption

- Photophosphorylation in the chloroplasts of green plants and in cyanobacteria involves electron flow through a series of membrane-bound carriers.
- In the light reactions of plants, absorption of a photon excites chlorophyll molecules and other (accessory) pigments, which funnel the energy into reaction centers in the thylakoid membranes. In the reaction centers, photoexcitation results in a charge separation that produces a strong electron donor (reducing agent) and a strong electron acceptor.

19.8 The Central Photochemical Event: Light-Driven Electron Flow

Light-driven electron transfer in plant chloroplasts during photosynthesis is accomplished by multienzyme systems in the thylakoid membrane. Our current picture of photosynthetic mechanisms is a composite, drawn from studies of plant chloroplasts and a variety of bacteria and algae. Determination of the molecular structures of bacterial photosynthetic complexes (by x-ray crystallography) has given us a much improved understanding of the molecular events in photosynthesis in general.

Bacteria Have One of Two Types of Single Photochemical Reaction Center

One major insight from studies of photosynthetic bacteria came in 1952 when Louis Duysens found that illumination of the photosynthetic membranes of the purple bacterium *Rhodospirillum rubrum* with a pulse of light of a specific wavelength (870 nm) caused a temporary decrease in the absorption of light at that wavelength; a pigment was "bleached" by 870 nm light. Later studies by Bessel Kok and Horst Witt showed similar bleaching of plant chloroplast pigments by light of 680 and 700 nm. Furthermore, addition of the (nonbiological) electron acceptor $[Fe(CN)_6]^{3-}$ (ferricyanide) caused bleaching at these wavelengths *without illumination.* These findings indicated that bleaching of the pigments was due to the loss of an electron from a photochemical reaction center. The pigments were named for the wavelength of maximum bleaching: P870, P680, and P700.

Photosynthetic bacteria have relatively simple phototransduction machinery, with one of two general types of reaction center. One type (found in purple bacteria) passes electrons through **pheophytin** (chlorophyll lacking the central Mg^{2+} ion) to a quinone. The other (in green sulfur bacteria) passes electrons through a quinone to an iron-sulfur center. Cyanobacteria and plants have two photosystems (PSI, PSII), one of each type, acting in tandem. Biochemical and biophysical studies have revealed many of the molecular details of reaction centers of bacteria, which therefore serve as prototypes for the more complex phototransduction systems of plants.

The Pheophytin-Quinone Reaction Center (Type II Reaction Center) The photosynthetic machinery in purple bacteria consists of three basic modules **(Fig. 19–54a)**: a single reaction center (P870), a cytochrome bc_1 electron-transfer complex similar to Complex III of the mitochondrial electron-transfer chain, and an ATP synthase, also similar to that of mitochondria. Illumination drives electrons through pheophytin and a quinone to the cytochrome bc_1 complex; after passing through the complex, electrons flow through cytochrome c_2 back to the reaction center, restoring its preillumination state. This light-driven cyclic flow of electrons provides the energy for proton pumping by the cytochrome bc_1 complex. Powered by the resulting proton gradient, ATP synthase produces ATP, exactly as in mitochondria.

The three-dimensional structures of the reaction centers of purple bacteria (*Rhodopseudomonas viridis* and *Rhodobacter sphaeroides*), deduced from x-ray crystallography, shed light on how phototransduction takes place in a pheophytin-quinone reaction center. The *R. viridis* reaction center **(Fig. 19–55a)** is a large protein complex containing four polypeptide subunits and 13 cofactors: two pairs of bacterial chlorophylls, a pair of pheophytins, two quinones, a nonheme iron, and four hemes in the associated *c*-type cytochrome.

The extremely rapid sequence of electron transfers shown in Figure 19–55b has been deduced from physical studies of the bacterial pheophytin-quinone centers, using brief flashes of light to trigger phototransduction and a variety of spectroscopic techniques to follow the flow of electrons through several carriers. A pair of bacteriochlorophylls—the "special pair," designated $(Chl)_2$—is the site of the initial photochemistry in the bacterial reaction center. Energy from a photon absorbed by one of the

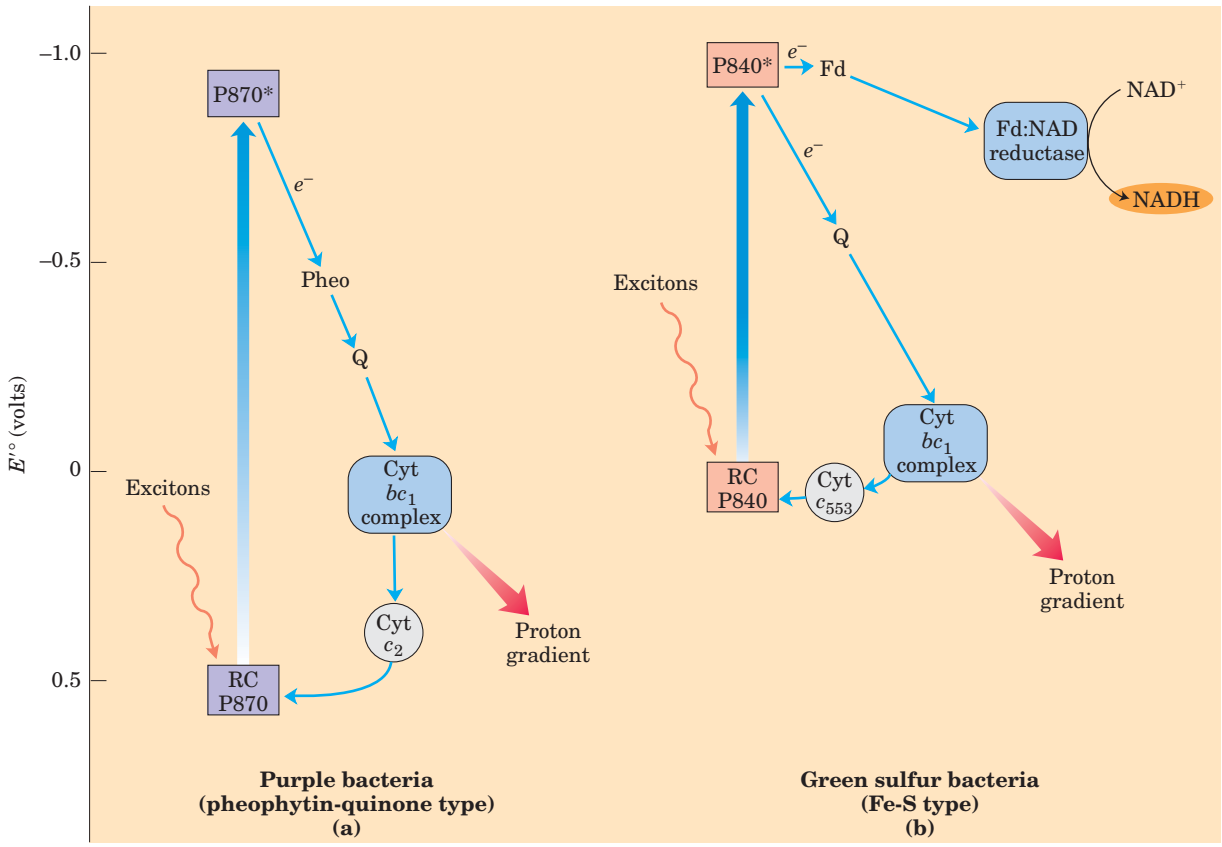

FIGURE 19–54 Functional modules of photosynthetic machinery in purple bacteria and green sulfur bacteria. (a) In purple bacteria, light energy drives electrons from the reaction-center P870 through pheophytin (Pheo), a quinone (Q), and the cytochrome bc_1 complex, then through cytochrome c_2 and thus back to the reaction center. Electron flow through the cytochrome bc_1 complex causes proton pumping, creating an electrochemical potential that powers ATP synthesis. **(b)** Green sulfur bacteria have two routes for electrons driven by excitation of P840: a cyclic route through a quinone to the cytochrome bc_1 complex and back to the reaction center via cytochrome *c*, and a noncyclic route from the reaction center through the iron-sulfur protein ferredoxin (Fd), then to NAD^+ in a reaction catalyzed by ferredoxin:NAD reductase.

many antenna chlorophyll molecules surrounding the reaction center reaches $(Chl)_2$ by exciton transfer. When these two chlorophyll molecules—so close that their bonding orbitals overlap—absorb an exciton, the redox potential of $(Chl)_2$ is shifted, by an amount equivalent to the energy of the photon, converting the special pair to a very strong electron donor. The $(Chl)_2$ donates an electron that passes through a neighboring chlorophyll monomer to pheophytin (Pheo). This produces two radicals, one positively charged (the special pair of chlorophylls) and one negatively charged (the pheophytin):

$$(Chl)_2 + 1 \text{ exciton} \longrightarrow (Chl)_2^* \qquad \text{(excitation)}$$

$$(Chl)_2^* + Pheo \longrightarrow {}^{\bullet}(Chl)_2^+ + {}^{\bullet}Pheo^- \qquad \text{(charge separation)}$$

The pheophytin radical now passes its electron to a tightly bound molecule of quinone (Q_A), converting it to a semiquinone radical, which immediately donates its extra electron to a second, loosely bound quinone (Q_B). Two such electron transfers convert Q_B to its fully reduced form, Q_BH_2, which is free to diffuse in the membrane bilayer, away from the reaction center:

$$2\,{}^{\bullet}Pheo^- + 2H^+ + Q_B \longrightarrow 2\,Pheo + Q_BH_2 \qquad \text{(quinone reduction)}$$

The hydroquinone (Q_BH_2), carrying in its chemical bonds some of the energy of the photons that originally excited P870, enters the pool of reduced quinone (QH_2) dissolved in the membrane and moves through the lipid phase of the bilayer to the cytochrome bc_1 complex.

Like the homologous Complex III in mitochondria, the cytochrome bc_1 complex of purple bacteria carries electrons from a quinol donor (QH_2) to an electron acceptor, using the energy of electron transfer to pump protons across the membrane, producing a proton-motive force. The path of electron flow through this complex is believed to be very similar to that through mitochondrial Complex III, involving a Q cycle (Fig. 19–12) in which protons are consumed on one side of the membrane and released on the other. The ultimate electron acceptor in purple bacteria is the electron-depleted form of P870, ${}^{\bullet}(Chl)_2^+$ (Fig. 19–54a). Electrons move from the cytochrome bc_1 complex to P870 via a soluble *c*-type cytochrome, cytochrome c_2. The electron-transfer process completes the cycle, returning the reaction center to its unbleached state, ready to absorb another exciton from antenna chlorophyll.

A remarkable feature of this system is that all the chemistry occurs in the *solid state*, with reacting species

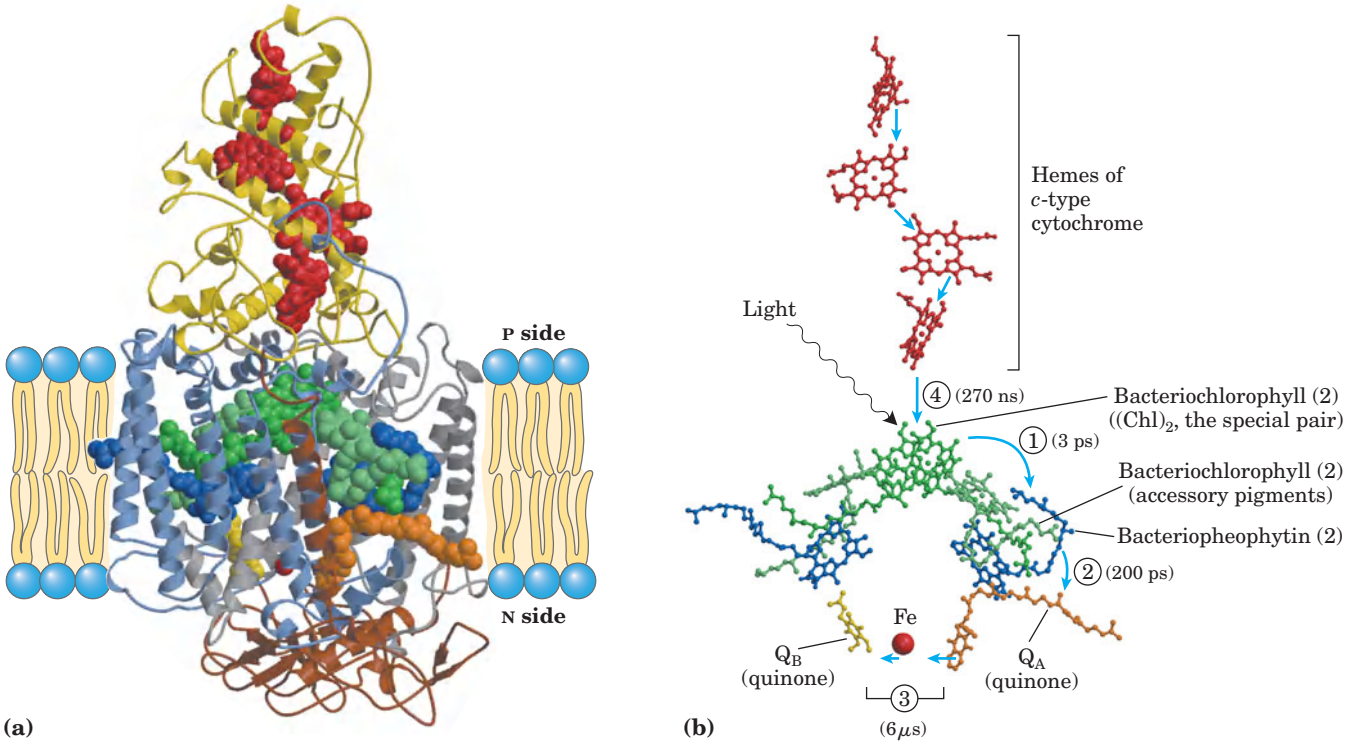

FIGURE 19–55 Photoreaction center of the purple bacterium *Rhodopseudomonas viridis*. (PDB ID 1PRC) **(a)** The system has four components: three subunits, H, M, and L (brown, blue, and gray, respectively), with a total of 11 transmembrane helical segments, and a fourth protein, cytochrome *c* (yellow), associated with the complex at the membrane surface. Subunits L and M are paired transmembrane proteins that together form a cylindrical structure with roughly bilateral symmetry about its long axis. Shown as space-filling models (and in **(b)** as ball-and-stick structures) are the prosthetic groups that participate in the photochemical events. Bound to the L and M chains are two pairs of bacteriochlorophyll molecules (green); one of the pairs—the "special pair," $(Chl)_2$—is the site of the first photochemical changes after light absorption. Also incorporated in the system are a pair of pheophytin *a* (Pheo *a*) molecules (blue); two quinones, menaquinone (Q_A) and ubiquinone (Q_B) (orange and yellow), also arranged with bilateral symmetry; and a single nonheme Fe (red) located approximately on the axis of symmetry between the quinones. Shown at the top of the figure are four heme groups (red) associated with the *c*-type cytochrome of the reaction center. The reaction center of another purple bacterium, *Rhodobacter sphaeroides*, is very similar, except that cytochrome *c* is not part of the crystalline complex.

(b) Sequence of events following excitation of the special pair of bacteriochlorophylls (all components colored as in **(a)**), with the time scale of the electron transfers in parentheses. ① The excited special pair passes an electron to pheophytin, ② from which the electron moves rapidly to the tightly bound menaquinone, Q_A. ③ This quinone passes electrons much more slowly to the diffusible ubiquinone, Q_B, through the nonheme Fe. Meanwhile, ④ the "electron hole" in the special pair is filled by an electron from a heme of cytochrome *c*.

held close together in the right orientation for reaction. The result is a very fast and efficient series of reactions.

The Fe-S Reaction Center (Type I Reaction Center)
Photosynthesis in green sulfur bacteria involves the same three modules as in purple bacteria, but the process differs in several respects and involves additional enzymatic reactions (Fig. 19–54b). Excitation causes an electron to move from the reaction center to the cytochrome bc_1 complex via a quinone carrier. Electron transfer through this complex powers proton transport and creates the proton-motive force used for ATP synthesis, just as in purple bacteria and in mitochondria. However, in contrast to the cyclic flow of electrons in purple bacteria, some electrons flow from the reaction center to an iron-sulfur protein, **ferredoxin**, which then passes electrons via ferredoxin:NAD reductase to NAD^+, producing NADH. The electrons taken from the reaction center to reduce NAD^+ are replaced by the oxidation of H_2S to elemental S, then to SO_4^{2-}, in the reaction that defines the green sulfur bacteria. This oxidation of H_2S by bacteria is chemically analogous to the oxidation of H_2O by oxygenic plants.

Kinetic and Thermodynamic Factors Prevent the Dissipation of Energy by Internal Conversion

The complex construction of reaction centers is the product of evolutionary selection for efficiency in the photosynthetic process. The excited state $(Chl)_2^*$ could in principle decay to its ground state by internal conversion, a very rapid process (10 picoseconds; 1 ps = 10^{-12} s) in which the energy of the absorbed photon is converted to heat (molecular motion). Reaction centers are constructed to prevent the inefficiency that would result from internal conversion. The proteins of the reaction center hold the bacteriochlorophylls, bacteriopheophytins, and quinones in a fixed orientation relative to each other, allowing the photochemical reactions to take place in a virtually solid state. This accounts for the high efficiency and rapidity of the reactions; nothing is left to chance collision

or random diffusion. Exciton transfer from antenna chlorophyll to the special pair of the reaction center is accomplished in less than 100 ps with >90% efficiency. Within 3 ps of the excitation of P870, pheophytin has received an electron and become a negatively charged radical; less than 200 ps later, the electron has reached the quinone Q_B (Fig. 19–55b). The electron-transfer reactions not only are fast but are thermodynamically "downhill"; the excited special pair $(Chl)_2^*$ is a very good electron donor ($E'^\circ = -1$ V), and each successive electron transfer is to an acceptor of substantially less negative E'°. The standard free-energy change for the process is therefore negative and large; recall from Chapter 13 that $\Delta G'^\circ = -n\mathcal{F}\Delta E'^\circ$; here, $\Delta E'^\circ$ is the difference between the standard reduction potentials of the two half-reactions

$$(1)\ (Chl)_2^* \longrightarrow {}^{\cdot}(Chl)_2^+ + e^- \qquad E'^\circ = -1.0\ \text{V}$$

$$(2)\ Q + 2H^+ + 2e^- \longrightarrow QH_2 \qquad E'^\circ = -0.045\ \text{V}$$

Thus

$$\Delta E'^\circ = -0.045\ \text{V} - (-1.0\ \text{V}) \approx 0.95\ \text{V}$$

and

$$\Delta G'^\circ = -2(96.5\ \text{kJ/V} \cdot \text{mol})(0.95\ \text{V}) = -180\ \text{kJ/mol}$$

The combination of fast kinetics and favorable thermodynamics makes the process virtually irreversible and highly efficient. The overall energy yield (the percentage of the photon's energy conserved in QH_2) is >30%, with the remainder of the energy dissipated as heat and entropy.

In Plants, Two Reaction Centers Act in Tandem

The photosynthetic apparatus of modern cyanobacteria, algae, and vascular plants is more complex than the one-center bacterial systems, and it seems to have evolved through the combination of two simpler bacterial photocenters. The thylakoid membranes of chloroplasts have two different kinds of photosystems, each with its own type of photochemical reaction center and set of antenna molecules. The two systems have distinct and complementary functions **(Fig. 19–56)**. **Photosystem II (PSII)** is a pheophytin-quinone type of

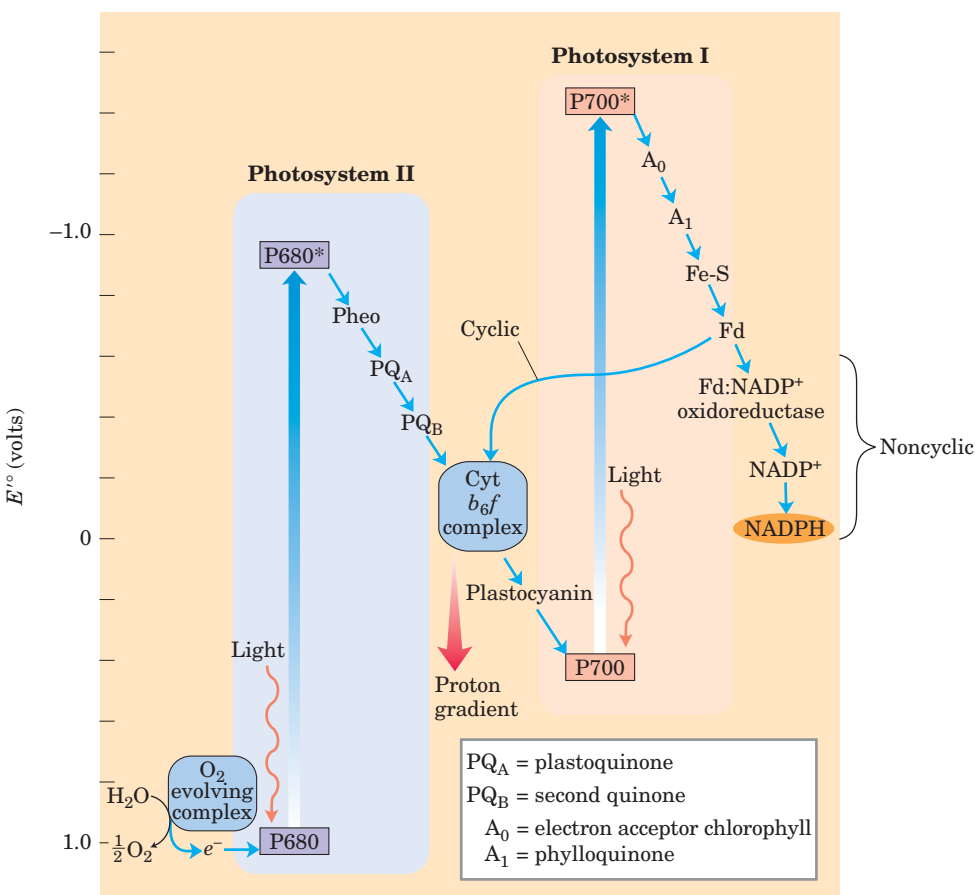

FIGURE 19–56 Integration of photosystems I and II in chloroplasts. This "Z scheme" shows the pathway of electron transfer from H_2O (lower left) to $NADP^+$ (far right) in noncyclic photosynthesis. The position on the vertical scale of each electron carrier reflects its standard reduction potential. To raise the energy of electrons derived from H_2O to the energy level required to reduce $NADP^+$ to NADPH, each electron must be "lifted" twice (heavy arrows) by photons absorbed in PSII and PSI. One photon is required per electron in each photosystem. After excitation, the high-energy electrons flow "downhill" through the carrier chains shown. Protons move across the thylakoid membrane during the water-splitting reaction and during electron transfer through the cytochrome b_6f complex, producing the proton gradient that is essential to ATP formation. An alternative path of electrons is cyclic electron transfer, in which electrons move from ferredoxin back to the cytochrome b_6f complex, instead of reducing $NADP^+$ to NADPH. The cyclic pathway produces more ATP and less NADPH than the noncyclic.

system (like the single photosystem of purple bacteria) containing roughly equal amounts of chlorophylls *a* and *b*. Excitation of its reaction-center P680 drives electrons through the cytochrome b_6f complex with concomitant movement of protons across the thylakoid membrane. **Photosystem I (PSI)** is structurally and functionally related to the type I reaction center of green sulfur bacteria. It has a reaction center designated P700 and a high ratio of chlorophyll *a* to chlorophyll *b*. Excited P700 passes electrons to the Fe-S protein ferredoxin, then to $NADP^+$, producing NADPH. The thylakoid membranes of a single spinach chloroplast have many hundreds of each kind of photosystem.

These two reaction centers in plants act in tandem to catalyze the light-driven movement of electrons from H_2O to $NADP^+$ (Fig. 19–56). Electrons are carried between the two photosystems by the soluble protein **plastocyanin**, a one-electron carrier functionally similar to cytochrome *c* of mitochondria. To replace the electrons that move from PSII through PSI to $NADP^+$, cyanobacteria and plants oxidize H_2O (as green sulfur bacteria oxidize H_2S), producing O_2 (Fig. 19–56, bottom left). This process is called **oxygenic photosynthesis** to distinguish it from the anoxygenic photosynthesis of purple and green sulfur bacteria. All O_2-evolving photosynthetic cells—those of plants, algae, and cyanobacteria—contain both PSI and PSII; organisms with only one photosystem do not evolve O_2. The diagram in Figure 19–56, often called the **Z scheme** because of its overall form, outlines the pathway of electron flow between the two photosystems and the energy relationships in the light reactions. The Z scheme thus describes the complete route by which electrons flow from H_2O to $NADP^+$, according to the equation

$$2H_2O + 2NADP^+ + 8\ \text{photons} \longrightarrow O_2 + 2NADPH + 2H^+$$

For every two photons absorbed (one by each photosystem), one electron is transferred from H_2O to $NADP^+$. To form one molecule of O_2, which requires transfer of four electrons from two H_2O to two $NADP^+$, a total of eight photons must be absorbed, four by each photosystem.

The mechanistic details of the photochemical reactions in PSII and PSI are essentially similar to those of the two bacterial photosystems, with several important additions. In PSII, two very similar proteins, D1 and D2, form an almost symmetric dimer, to which all the electron-carrying cofactors are bound **(Fig. 19–57)**. Excitation of P680 in PSII produces P680*, an excellent electron donor that, within picoseconds, transfers an electron to pheophytin, giving it a negative charge ($^{\cdot}Pheo^-$). With the loss of its electron, P680* is transformed into a radical cation, $P680^+$. $^{\cdot}Pheo^-$ very rapidly passes its extra electron to a protein-bound **plastoquinone**, **PQ_A** (or Q_A), which in turn passes its electron to another, more loosely bound plastoquinone, PQ_B (or Q_B). When PQ_B has acquired two electrons in two such transfers from PQ_A and two protons from the solvent

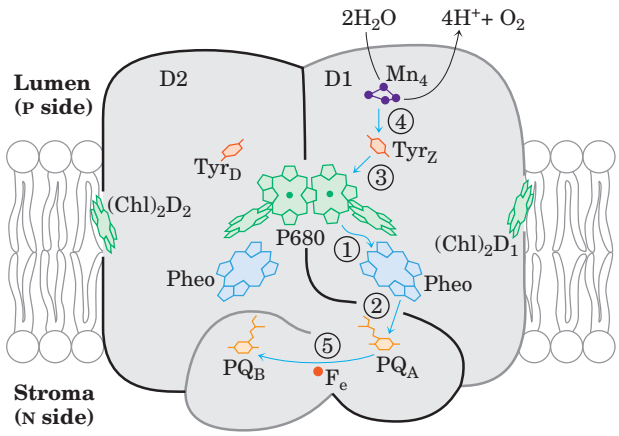

FIGURE 19–57 Photosystem II of the cyanobacterium *Synechococcus elongates*. The monomeric form of the complex shown here has two major transmembrane proteins, D1 and D2, each with its set of cofactors. Although the two subunits are nearly symmetric, electron flow occurs through only one of the two branches of cofactors, that on the right (on D1). The arrows show the path of electron flow from the Mn ion cluster (Mn_4) of the water-splitting enzyme to the quinone PQ_B. The photochemical events occur in the sequence indicated by the step numbers. Notice the close similarity between the positions of cofactors here and the positions in the bacterial photoreaction center shown in Figure 19–55. The role of the Tyr residues is discussed later in the text.

water, it is in its fully reduced quinol form, PQ_BH_2. The overall reaction initiated by light in PSII is

$$4\ P680 + 4H^+ + 2\ PQ_B + 4\ \text{photons} \longrightarrow 4\ P680^+ + 2\ PQ_BH_2 \quad (19\text{–}12)$$

Eventually, the electrons in PQ_BH_2 pass through the cytochrome b_6f complex (Fig. 19–56). The electron initially removed from P680 is replaced with an electron obtained from the oxidation of water, as described below. The binding site for plastoquinone is the point of action of many commercial herbicides that kill plants by blocking electron transfer through the cytochrome b_6f complex and preventing photosynthetic ATP production.

The photochemical events that follow excitation of PSI at the reaction-center P700 are formally similar to those in PSII. The excited reaction-center P700* loses an electron to an acceptor, A_0 (believed to be a special form of chlorophyll, functionally homologous to the pheophytin of PSII), creating A_0^- and $P700^+$ (Fig. 19–56, right side); again, excitation results in charge separation at the photochemical reaction center. $P700^+$ is a strong oxidizing agent, which quickly acquires an electron from plastocyanin, a soluble Cu-containing electron-transfer protein. A_0^- is an exceptionally strong reducing agent that passes its electron through a chain of carriers that leads to $NADP^+$. First, **phylloquinone** (A_1) accepts an electron and passes it to an iron-sulfur protein (through three Fe-S centers in PSI). From here, the electron moves to **ferredoxin** (Fd), another iron-sulfur protein loosely associated with the thylakoid membrane. Spinach ferredoxin (M_r 10,700) contains a 2Fe-2S center (Fig. 19–5) that undergoes one-electron oxidation and reduction reactions. The fourth electron carrier in

the chain is the flavoprotein **ferredoxin:NADP$^+$ oxidoreductase**, which transfers electrons from reduced ferredoxin (Fd_{red}) to $NADP^+$:

$$2Fd_{red} + 2H^+ + NADP^+ \longrightarrow 2Fd_{ox} + NADPH + H^+$$

This enzyme is homologous to the ferredoxin:NAD reductase of green sulfur bacteria (Fig. 19–54b).

Antenna Chlorophylls Are Tightly Integrated with Electron Carriers

The electron-carrying cofactors of PSI and the light-harvesting complexes are part of a supramolecular complex **(Fig. 19–58a)**, the structure of which has been solved crystallographically. The protein consists of three

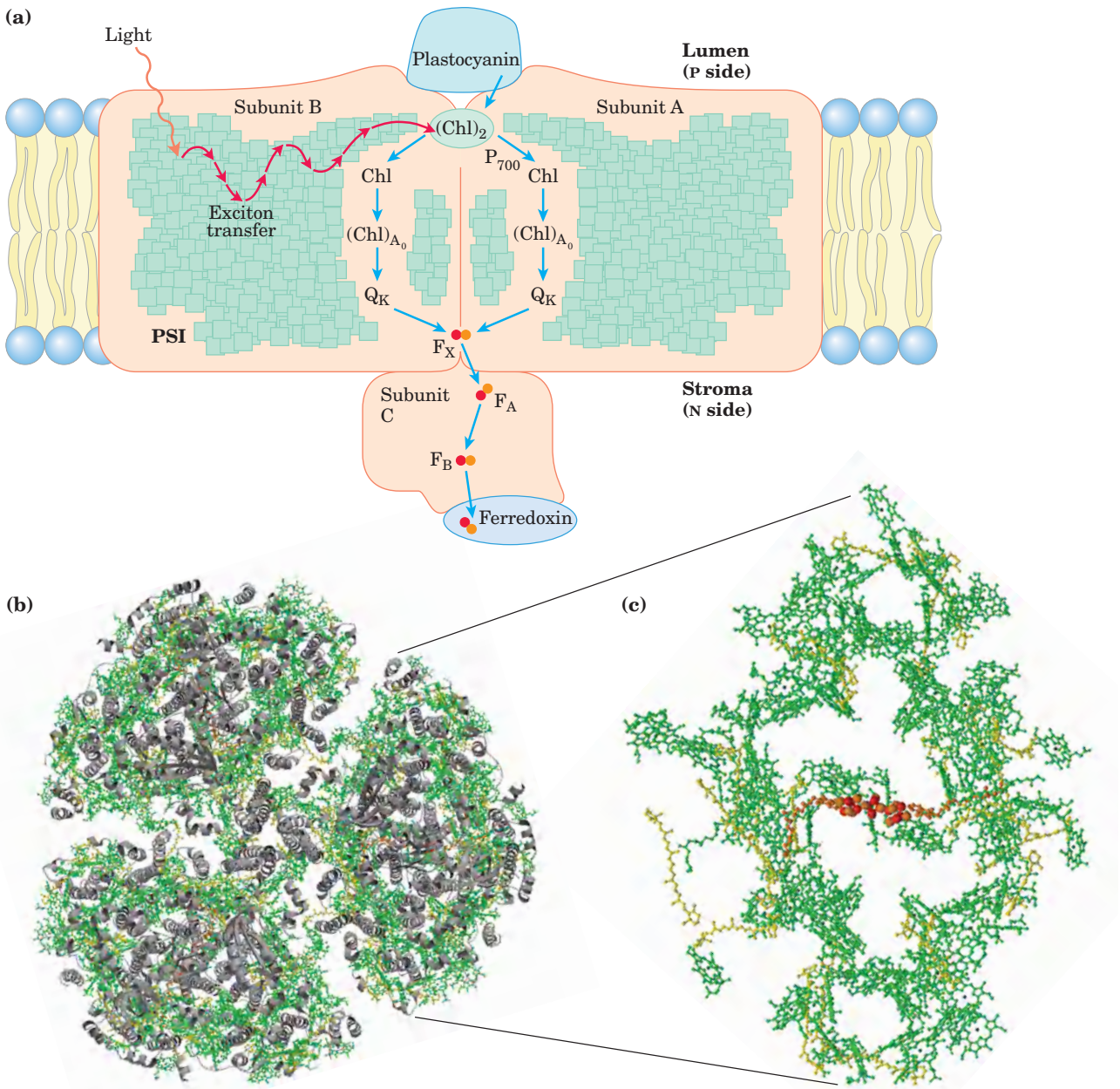

FIGURE 19–58 The supramolecular complex of PSI and its associated antenna chlorophylls. (a) Schematic drawing of the essential proteins and cofactors in a single unit of PSI. A large number of antenna chlorophylls surround the reaction center and convey to it (red arrows) the energy of absorbed photons. The result is excitation of the pair of chlorophyll molecules that constitute P700, greatly decreasing its reduction potential; P700 then passes an electron through two nearby chlorophylls to phylloquinone (Q_K; also called A_1). Reduced phylloquinone is reoxidized as it passes two electrons, one at a time (blue arrows), to an Fe-S protein (F_X) near the N side of the membrane. From F_X, electrons move through two more Fe-S centers (F_A and F_B) to the Fe-S protein ferredoxin in the stroma. Ferredoxin then donates electrons to $NADP^+$ (not shown), reducing it to NADPH, one of the forms in which the energy of photons is trapped in chloroplasts.

(b) The trimeric structure (derived from PDB ID 1JBO), viewed from the thylakoid lumen perpendicular to the membrane, showing all protein subunits (gray) and cofactors. **(c)** A monomer of PSI with all the proteins omitted, revealing the antenna and reaction-center chlorophylls (green with dark green Mg^{2+} ions in the center), carotenoids (yellow), and Fe-S centers of the reaction center (space-filling red and orange structures). The proteins in the complex hold the components rigidly in orientations that maximize efficient exciton transfers between excited antenna molecules and the reaction center.

identical complexes, each composed of 11 different proteins (Fig. 19–58b). In this remarkable structure the many antenna chlorophyll and carotenoid molecules are precisely arrayed around the reaction center (Fig. 19–58c). The reaction center's electron-carrying cofactors are therefore tightly integrated with antenna chlorophylls. This arrangement allows very rapid and efficient exciton transfer from antenna chlorophylls to the reaction center. In contrast to the single path of electrons in PSII, the electron flow initiated by absorption of a photon is believed to occur through both branches of carriers in PSI.

The Cytochrome b_6f Complex Links Photosystems II and I

Electrons temporarily stored in plastoquinol as a result of the excitation of P680 in PSII are carried to P700 of PSI via the cytochrome b_6f complex and the soluble protein plastocyanin (Fig. 19–56, center). Like Complex III of mitochondria, the cytochrome b_6f complex **(Fig. 19–59)** contains a *b*-type cytochrome with two heme groups (designated b_H and b_L), a Rieske iron-sulfur protein (M_r 20,000), and cytochrome *f* (named for the Latin *frons*, "leaf"). Electrons flow through the cytochrome b_6f

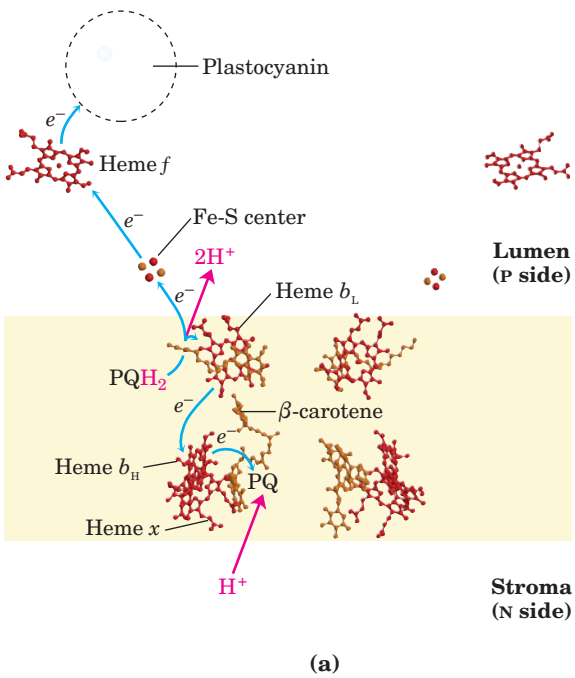

(a)

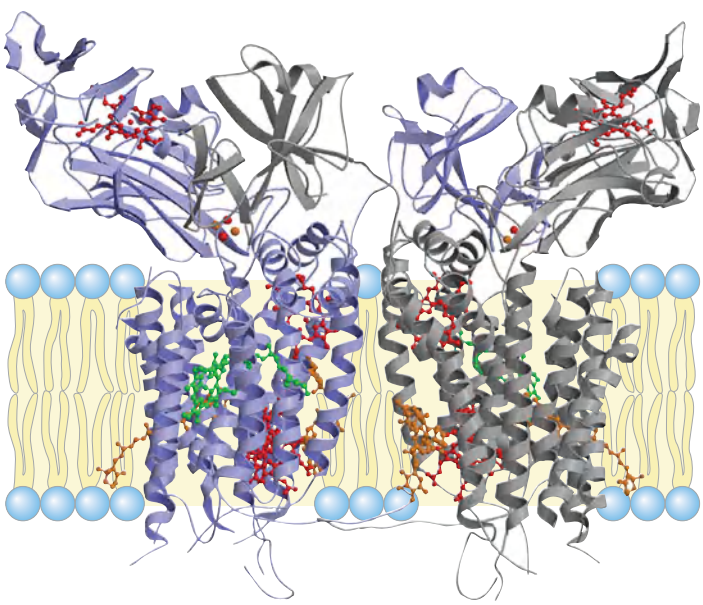

(b)

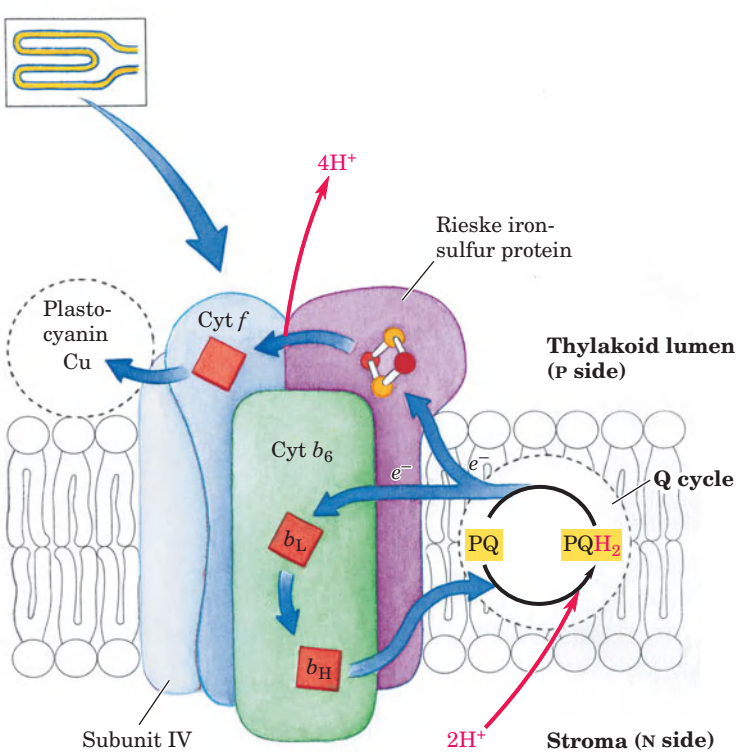

(c)

FIGURE 19–59 Electron and proton flow through the cytochrome b_6f complex. (a) The crystal structure of the complex (PDB ID 1UM3) reveals the positions of the cofactors involved in electron transfers. In addition to the hemes of cytochrome *b* (heme b_H and b_L; also called heme b_N and b_P, respectively, because of their proximity to the N and P sides of the bilayer) and cytochrome *f* (heme *f*), there is a fourth (heme *x*) near heme b_H; there is also a β-carotene of unknown function. Two sites bind plastoquinone: the PQH_2 site near the P side of the bilayer, and the PQ site near the N side. The Fe-S center of the Rieske protein lies just outside the bilayer on the P side, and the heme *f* site is on a protein domain that extends well into the thylakoid lumen. **(b)** The complex is a homodimer arranged to create a cavern connecting the PQH_2 and PQ sites (compare this with the structure of mitochondrial Complex III in Fig. 19–11). This cavern allows plastoquinone to move between the sites of its oxidation and reduction.

(c) Plastoquinol (PQH_2) formed in PSII is oxidized by the cytochrome b_6f complex in a series of steps like those of the Q cycle in the cytochrome bc_1 complex (Complex III) of mitochondria (see Fig. 19–12). One electron from PQH_2 passes to the Fe-S center of the Rieske protein, the other to heme b_L of cytochrome b_6. The net effect is passage of electrons from PQH_2 to the soluble protein plastocyanin, which carries them to PSI.

complex from PQ_BH_2 to cytochrome *f*, then to plastocyanin, and finally to P700, thereby reducing it.

Like Complex III of mitochondria, cytochrome b_6f conveys electrons from a reduced quinone—a mobile, lipid-soluble carrier of two electrons (Q in mitochondria, PQ_B in chloroplasts)—to a water-soluble protein that carries one electron (cytochrome *c* in mitochondria, plastocyanin in chloroplasts). As in mitochondria, the function of this complex involves a Q cycle (Fig. 19–12) in which electrons pass, one at a time, from PQ_BH_2 to cytochrome b_6. This cycle results in the pumping of protons across the membrane; in chloroplasts, the direction of proton movement is from the stromal compartment to the thylakoid lumen, up to four protons moving for each pair of electrons. The result is production of a proton gradient across the thylakoid membrane as electrons pass from PSII to PSI. Because the volume of the flattened thylakoid lumen is small, the influx of a small number of protons has a relatively large effect on lumenal pH. The measured difference in pH between the stroma (pH 8) and the thylakoid lumen (pH 5) represents a 1,000-fold difference in proton concentration—a powerful driving force for ATP synthesis.

Cyclic Electron Flow between PSI and the Cytochrome b_6f Complex Increases the Production of ATP Relative to NADPH

Electron flow from PSII through the cytochrome b_6f complex, then through PSI to $NADP^+$, is sometimes called **noncyclic electron flow**, to distinguish it from **cyclic electron flow**, which occurs to varying degrees depending primarily on the light conditions. The noncyclic path produces a proton gradient, which is used to drive ATP synthesis, and NADPH, which is used in reductive biosynthetic processes. Cyclic electron flow involves only PSI, not PSII (Fig. 19–56). Electrons passing from P700 to ferredoxin do not continue to $NADP^+$, but move back through the cytochrome b_6f complex to plastocyanin. (This electron path parallels that in green sulfur bacteria, shown in Fig. 19–54b.) Plastocyanin then donates electrons to P700, which transfers them to ferredoxin. In this way, electrons are repeatedly recycled through the cytochrome b_6f complex and the reaction center of PSI, each electron propelled around the cycle by the energy of one photon. Cyclic electron flow is not accompanied by net formation of NADPH or evolution of O_2. However, it *is* accompanied by proton pumping by the cytochrome b_6f complex and by phosphorylation of ADP to ATP, referred to as **cyclic photophosphorylation**. The overall equation for cyclic electron flow and photophosphorylation is simply

$$ADP + P_i \xrightarrow{\text{light}} ATP + H_2O$$

By regulating the partitioning of electrons between $NADP^+$ reduction and cyclic photophosphorylation, a plant adjusts the ratio of ATP to NADPH produced in the light-dependent reactions to match its needs for these products in the carbon-assimilation reactions and other biosynthetic processes. As we shall see in Chapter 20, the carbon-assimilation reactions require ATP and NADPH in the ratio 3:2.

This regulation of electron-transfer pathways is part of a short-term adaptation to changes in light color (wavelength) and quantity (intensity), as further described below.

State Transitions Change the Distribution of LHCII between the Two Photosystems

The energy required to excite PSI (P700) is less (light of longer wavelength, lower energy) than that needed to excite PSII (P680). If PSI and PSII were physically contiguous, excitons originating in the antenna system of PSII would migrate to the reaction center of PSI, leaving PSII chronically underexcited and interfering with the operation of the two-center system. This imbalance in the supply of excitons is prevented by separation of the two photosystems in the thylakoid membrane **(Fig. 19–60)**. PSII is located almost exclusively in the tightly appressed membrane stacks of thylakoid grana; its associated light-harvesting complex (LHCII) mediates the tight association of adjacent membranes in the grana. PSI and the ATP synthase complex are located almost exclusively in the nonappressed thylakoid membranes (the stromal lamellae), where they have access to the contents of the stroma, including ADP and $NADP^+$. The cytochrome b_6f complex is present primarily in the grana.

The association of LHCII with PSI and PSII depends on light intensity and wavelength, which can change in the short term, leading to **state transitions** in the chloroplast. In state 1, a critical Ser residue in LCHII is not phosphorylated, and LHCII associates with PSII. Under conditions of intense or blue light, which favor absorption by PSII, that photosystem reduces plastoquinone to plastoquinol (PQH_2) faster than PSI can oxidize it. The resulting accumulation of PQH_2 activates a protein kinase that triggers the transition to state 2 by phosphorylating a Thr residue on LHCII **(Fig. 19–61)**. Phosphorylation weakens the interaction of LHCII with PSII, and some LHCII dissociates and moves to the stromal lamellae; here it captures photons (excitons) for PSI, speeding the oxidation of PQH_2 and reversing the imbalance between electron flow in PSI and PSII. In less intense light (in the shade, with more red light), PSI oxidizes PQH_2 faster than PSII can make it, and the resulting increase in [PQ] triggers dephosphorylation of LHCII, reversing the effect of phosphorylation.

The state transition in LCHII localization is mutually regulated with the transition from cyclic to noncyclic photophosphorylation, described above; the path of electrons is primarily noncyclic in state 1 and primarily cyclic in state 2.

Water Is Split by the Oxygen-Evolving Complex

The ultimate source of the electrons passed to NADPH in plant (oxygenic) photosynthesis is water. Having given up an electron to pheophytin, $P680^+$ (of PSII) must acquire

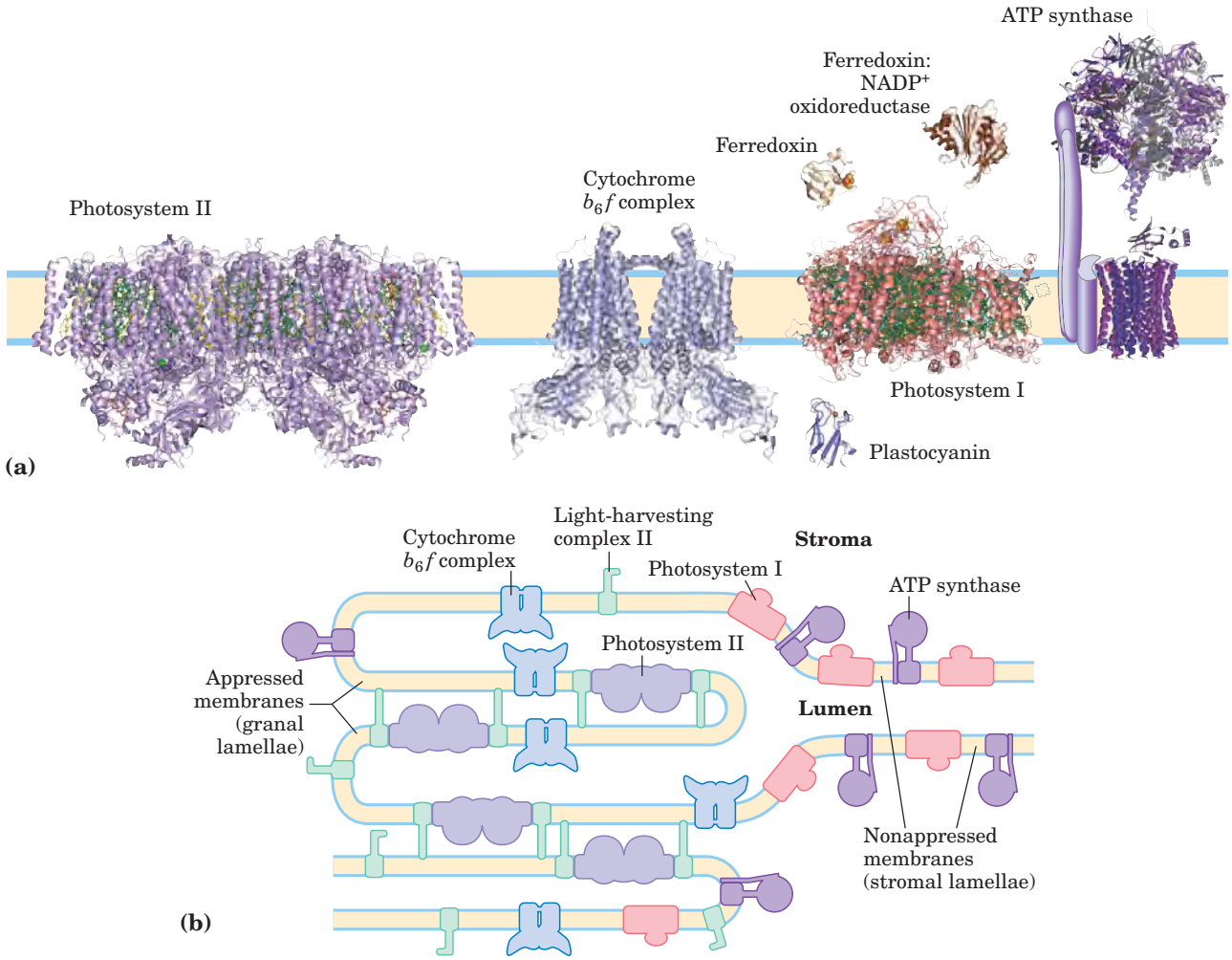

FIGURE 19–60 Localization of PSI and PSII in thylakoid membranes. **(a)** The structures of the complexes and soluble proteins of the photosynthetic apparatus of a vascular plant or alga, drawn to the same scale. The PDB ID for the structure of PSII is 2AXT; for PSI, 1QZV; for cytochrome b_6f, 2E74; for plastocyanin, 1AG6; for ferredoxin, 1A70; for ferredoxin:$NADP^+$ reductase, 1QG0. The ATP synthase structure shown is a composite of that from yeast mitochondria (PDB ID 1QO1) and bovine mitochondria (PDB ID 1BMF). **(b)** Light-harvesting complex LHCII and ATP synthase are located both in appressed regions of the thylakoid membrane (granal lamellae, in which several membranes are in contact) and in nonappressed regions (stromal lamellae), and have ready access to ADP and $NADP^+$ in the stroma. PSII is present almost exclusively in the appressed regions, and PSI almost exclusively in nonappressed regions, exposed to the stroma. LHCII is the "adhesive" that holds appressed lamellae together (see Fig. 19–61).

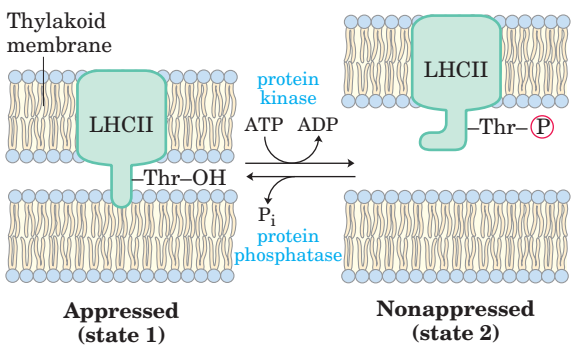

FIGURE 19–61 Balancing of electron flow in PSI and PSII by state transition. A hydrophobic domain of LHCII in one thylakoid lamella inserts into the neighboring lamella and closely appresses the two membranes (state 1). Accumulation of plastoquinol (not shown) stimulates a protein kinase that phosphorylates a Thr residue in the hydrophobic domain of LHCII, which reduces its affinity for the neighboring thylakoid membrane and converts appressed regions to nonappressed regions (state 2). A specific protein phosphatase reverses this regulatory phosphorylation when the [PQ]/[PQH_2] ratio increases.

an electron to return to its ground state in preparation for capture of another photon. In principle, the required electron might come from any number of organic or inorganic compounds. Photosynthetic bacteria use a variety of electron donors for this purpose—acetate, succinate, malate, or sulfide—depending on what is available in a particular ecological niche. About 3 billion years ago, evolution of primitive photosynthetic bacteria (the progenitors of the modern cyanobacteria) produced a photosystem capable of taking electrons from a donor that is always available—

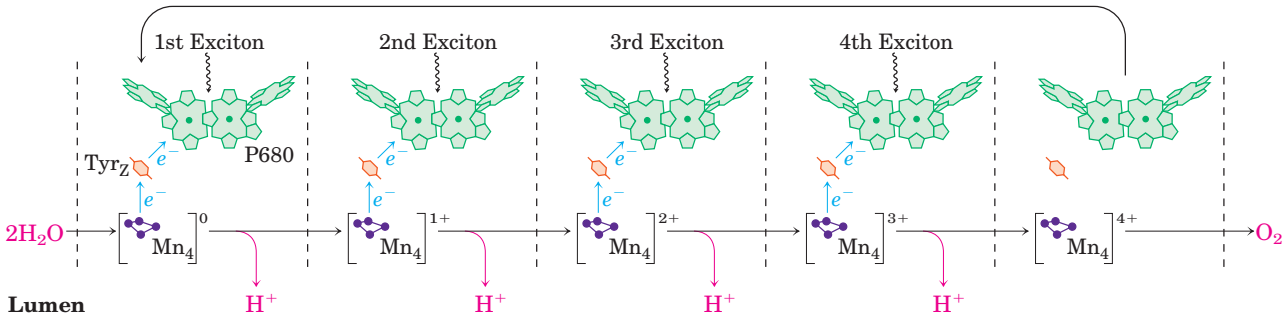

FIGURE 19–62 Water-splitting activity of the oxygen-evolving complex. Shown here is the process that produces a four-electron oxidizing agent—a multinuclear center with several Mn ions—in the water-splitting complex of PSII. The sequential absorption of four photons (excitons), each absorption causing the loss of one electron from the Mn center, produces an oxidizing agent that can remove four electrons from two molecules of water, producing O_2. The electrons lost from the Mn center pass one at a time to an oxidized Tyr residue in a PSII protein, then to $P680^+$.

water. Two water molecules are split, yielding four electrons, four protons, and molecular oxygen:

$$2H_2O \longrightarrow 4H^+ + 4e^- + O_2$$

A single photon of visible light does not have enough energy to break the bonds in water; four photons are required in this photolytic cleavage reaction.

The four electrons abstracted from water do not pass directly to $P680^+$, which can accept only one electron at a time. Instead, a remarkable molecular device, the **oxygen-evolving complex** (also called the **water-splitting complex**), passes four electrons *one at a time* to $P680^+$ **(Fig. 19–62)**. The immediate electron donor to $P680^+$ is a Tyr residue (often designated Z or Tyr_Z) in subunit D1 of the PSII reaction center. The Tyr residue loses both a proton and an electron, generating the electrically neutral Tyr free radical, $^{\bullet}$Tyr:

$$4P680^+ + 4\,Tyr \longrightarrow 4P680 + 4\,{}^{\bullet}Tyr \qquad (19–13)$$

The Tyr radical regains its missing electron and proton by oxidizing a cluster of four manganese ions in the water-splitting complex. With each single-electron transfer, the Mn cluster becomes more oxidized; four single-electron transfers, each corresponding to the absorption of one photon, produce a charge of 4+ on the Mn complex (Fig. 19–62):

$$4\,{}^{\bullet}Tyr + [Mn\ complex]^0 \longrightarrow 4\,Tyr + [Mn\ complex]^{4+} \qquad (19–14)$$

In this state, the Mn complex can take four electrons from a pair of water molecules, releasing 4 H^+ and O_2:

$$[Mn\ complex]^{4+} + 2H_2O \longrightarrow [Mn\ complex]^0 + 4H^+ + O_2 \qquad (19–15)$$

Because the four protons produced in this reaction are released into the thylakoid lumen, the oxygen-evolving complex acts as a proton pump, driven by electron transfer. The sum of Equations 19–12 through 19–15 is

$$2H_2O + 2PQ_B + 4\ photons \longrightarrow O_2 + 2PQ_BH_2 \qquad (19–16)$$

The oxygen-evolving complex is associated with a peripheral membrane protein (M_r 33,000) on the lumenal side of the thylakoid membrane that stabilizes the cluster of four Mn ions (in various oxidation states), one Ca^{2+} ion, five O atoms, and a Cl^- ion, with precise geometry. The chemical changes that take place in this cluster are not fully understood, but this chemistry is essential to life on Earth and of great interest both for its biological significance and as a challenge in bioinorganic chemistry. Manganese can exist in stable oxidation states from 2+ to 7+, so a cluster of Mn ions can certainly donate or accept four electrons. Determination of the structure of the polymetallic center has inspired several reasonable and testable hypotheses. Stay tuned.

SUMMARY 19.8 The Central Photochemical Event: Light-Driven Electron Flow

- Bacteria have a single reaction center; in purple bacteria, it is of the pheophytin-quinone type, and in green sulfur bacteria, the Fe-S type.
- Structural studies of the reaction center of a purple bacterium have provided information about light-driven electron flow from an excited special pair of chlorophyll molecules, through pheophytin, to quinones. Electrons then pass from quinones through the cytochrome bc_1 complex, and back to the photoreaction center.
- An alternative path, in green sulfur bacteria, sends electrons from reduced quinones to NAD^+.
- Cyanobacteria and plants have two different photoreaction centers, arranged in tandem.
- Plant photosystem I passes electrons from its excited reaction center, P700, through a series of carriers to ferredoxin, which then reduces $NADP^+$ to NADPH.
- The reaction center of plant photosystem II, P680, passes electrons to plastoquinone, and the electrons lost from P680 are replaced by electrons from H_2O (electron donors other than H_2O are used in other organisms).
- Flow of electrons through the photosystems produces NADPH and ATP, in the ratio of about 2:3. A second type of electron flow (cyclic flow) produces ATP only and allows variability in the proportions of NADPH and ATP formed.

- The localization of PSI and PSII between the granal and stromal lamellae can change and is indirectly controlled by light intensity, optimizing the distribution of excitons between PSI and PSII for efficient energy capture.
- The light-driven splitting of H_2O is catalyzed by a Mn-containing protein complex; O_2 is produced. The reduced plastoquinone carries electrons to the cytochrome b_6f complex; from here they pass to plastocyanin, and then to P700 to replace those lost during its photoexcitation.
- Electron flow through the cytochrome b_6f complex drives protons across the plasma membrane, creating a proton-motive force that provides the energy for ATP synthesis by an ATP synthase.

19.9 ATP Synthesis by Photophosphorylation

The combined activities of the two plant photosystems move electrons from water to $NADP^+$, conserving some of the energy of absorbed light as NADPH (Fig. 19–56). Simultaneously, protons are pumped across the thylakoid membrane and energy is conserved as an electrochemical potential. We turn now to the process by which this proton gradient drives the synthesis of ATP, the other energy-conserving product of the light-dependent reactions.

In 1954 Daniel Arnon and his colleagues discovered that ATP is generated from ADP and P_i during photosynthetic electron transfer in illuminated spinach chloroplasts. Support for these findings came from the work of Albert Frenkel, who detected light-dependent ATP production in pigment-containing membranous structures called **chromatophores**, derived from photosynthetic bacteria. Investigators concluded that some of the light energy captured by the photosynthetic systems of these organisms is transformed into the phosphate bond energy of ATP. This process is called **photophosphorylation**, to distinguish it from oxidative phosphorylation in respiring mitochondria.

Daniel Arnon, 1910–1994

A Proton Gradient Couples Electron Flow and Phosphorylation

Several properties of photosynthetic electron transfer and photophosphorylation in chloroplasts indicate that a proton gradient plays the same role as in mitochondrial oxidative phosphorylation. (1) The reaction centers, electron carriers, and ATP-forming enzymes are located in a proton-impermeable membrane—the thylakoid membrane—which must be intact to support photophosphorylation. (2) Photophosphorylation can be uncoupled from electron flow by reagents that promote the passage of protons through the thylakoid membrane. (3) Photophosphorylation can be blocked by venturicidin and similar agents that inhibit the formation of ATP from ADP and P_i by the mitochondrial ATP synthase (Table 19–4). (4) ATP synthesis is catalyzed by F_oF_1 complexes, located on the outer surface of the thylakoid membranes, that are very similar in structure and function to the F_oF_1 complexes of mitochondria.

Electron-transferring molecules in the chain of carriers connecting PSII and PSI are oriented asymmetrically in the thylakoid membrane, so photoinduced electron flow results in the net movement of protons across the membrane, from the stromal side to the thylakoid lumen **(Fig. 19–63)**. In 1966 André Jagendorf showed that a pH gradient across the thylakoid membrane (alkaline outside) could furnish the driving force to generate ATP. His early observations provided some of the most important experimental evidence in support of Mitchell's chemiosmotic hypothesis.

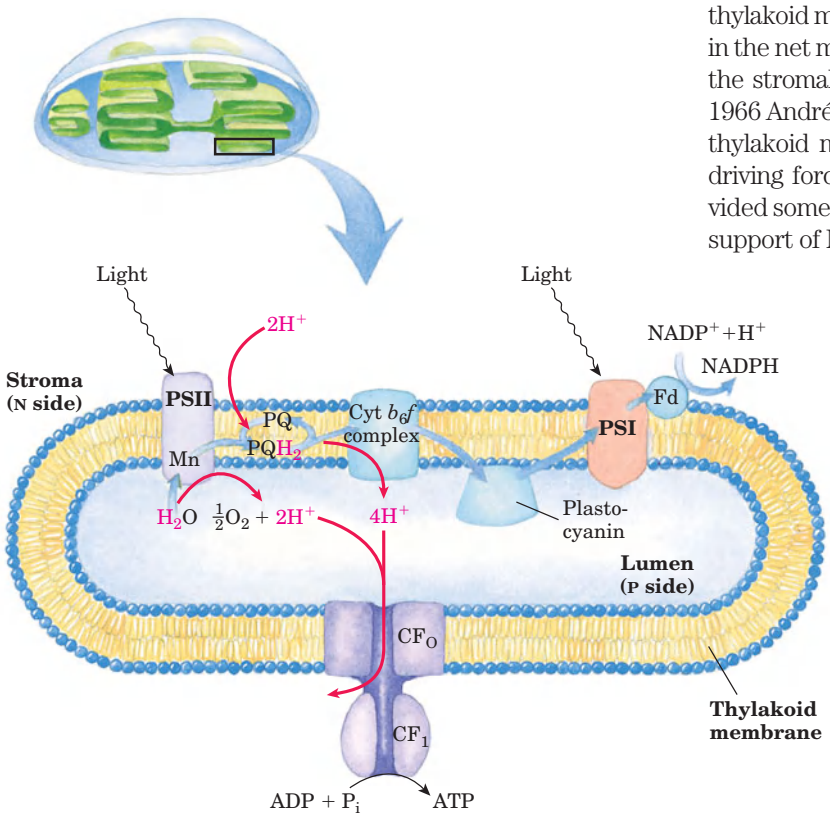

FIGURE 19–63 Proton and electron circuits in thylakoids. Electrons (blue arrows) move from H_2O through PSII, through the intermediate chain of carriers, through PSI, and finally to $NADP^+$. Protons (red arrows) are pumped into the thylakoid lumen by the flow of electrons through the carriers linking PSII and PSI, and reenter the stroma through proton channels formed by the F_o (designated CF_o) of ATP synthase. The F_1 subunit (CF_1) catalyzes synthesis of ATP.


André Jagendorf

Jagendorf incubated chloroplasts, in the dark, in a pH 4 buffer; the buffer slowly penetrated into the inner compartment of the thylakoids, lowering their internal pH. He added ADP and P_i to the dark suspension of chloroplasts and then suddenly raised the pH of the outer medium to 8, momentarily creating a large pH gradient across the membrane. As protons moved out of the thylakoids into the medium, ATP was generated from ADP and P_i. Because the formation of ATP occurred in the dark (with no input of energy from light), this experiment showed that a pH gradient across the membrane is a high-energy state that, as in mitochondrial oxidative phosphorylation, can mediate the transduction of energy from electron transfer into the chemical energy of ATP.

The Approximate Stoichiometry of Photophosphorylation Has Been Established

As electrons move from water to $NADP^+$ in plant chloroplasts, about 12 H^+ move from the stroma to the thylakoid lumen per four electrons passed (that is, per O_2 formed). Four of these protons are moved by the oxygen-evolving complex, and up to eight by the cytochrome b_6f complex. The measurable result is a 1,000-fold difference in proton concentration across the thylakoid membrane ($\Delta pH = 3$). Recall that the energy stored in a proton gradient (the electrochemical potential) has two components: a proton concentration difference (ΔpH) and an electrical potential ($\Delta\psi$) due to charge separation. In chloroplasts, ΔpH is the dominant component; counterion movement apparently dissipates most of the electrical potential. In illuminated chloroplasts, the energy stored in the proton gradient per mole of protons is

$$\Delta G = 2.3RT\Delta pH + Z\mathcal{F}\Delta\psi = -17 \text{ kJ/mol}$$

so the movement of 12 mol of protons across the thylakoid membrane represents conservation of about 200 kJ of energy—enough energy to drive the synthesis of several moles of ATP ($\Delta G'^\circ$ = 30.5 kJ/mol). Experimental measurements yield values of about 3 ATP per O_2 produced.

At least eight photons must be absorbed to drive four electrons from H_2O to NADPH (one photon per electron at each reaction center). The energy in eight photons of visible light is more than enough for the synthesis of three molecules of ATP.

ATP synthesis is not the only energy-conserving reaction of photosynthesis in plants; the NADPH formed in the final electron transfer is also energetically rich. The overall equation for noncyclic photophosphorylation (a term explained below) is

$$2H_2O + 8 \text{ photons} + 2NADP^+ + \sim 3ADP + \sim 3P_i \longrightarrow O_2 + \sim 3ATP + 2NADPH \quad (19\text{–}17)$$

The ATP Synthase of Chloroplasts Is Like That of Mitochondria

The enzyme responsible for ATP synthesis in chloroplasts is a large complex with two functional components, CF_o and CF_1 (*C* denoting its location in chloroplasts). CF_o is a transmembrane proton pore composed of several integral membrane proteins and is homologous to mitochondrial F_o. CF_1 is a peripheral membrane protein complex very similar in subunit composition, structure, and function to mitochondrial F_1.

Electron microscopy of sectioned chloroplasts shows ATP synthase complexes as knoblike projections on the *outside* (stromal, or N) surface of thylakoid membranes; these complexes correspond to the ATP synthase complexes seen to project on the *inside* (matrix, or N) surface of the inner mitochondrial membrane. Thus the relationship between the orientation of the ATP synthase and the direction of proton pumping is the same in chloroplasts and mitochondria. In both cases, the F_1 portion of ATP synthase is located on the more alkaline (N) side of the membrane through which protons flow down their concentration gradient; the direction of proton flow relative to F_1 is the same in both cases: P to N **(Fig. 19–64)**.

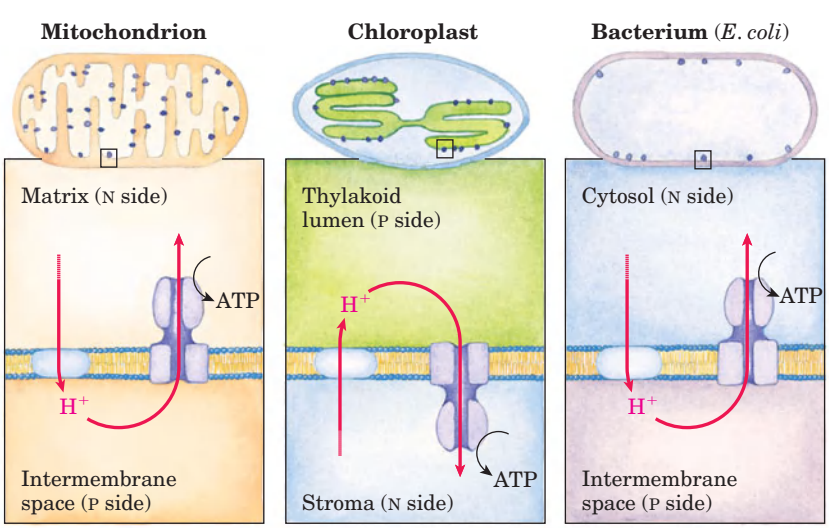

FIGURE 19–64 Comparison of the topology of proton movement and ATP synthase orientation in the membranes of mitochondria, chloroplasts, and the bacterium *E. coli*. In each case, orientation of the proton gradient relative to ATP synthase activity is the same.

The mechanism of chloroplast ATP synthase is also believed to be essentially identical to that of its mitochondrial analog; ADP and P_i readily condense to form ATP on the enzyme surface, and the release of this enzyme-bound ATP requires a proton-motive force. Rotational catalysis sequentially engages each of the three β subunits of the ATP synthase in ATP synthesis, ATP release, and ADP + P_i binding (Figs 19–26, 19–27).

SUMMARY 19.9 ATP Synthesis by Photophosphorylation

- In plants, both the water-splitting reaction and electron flow through the cytochrome b_6f complex are accompanied by proton pumping across the thylakoid membrane. The proton-motive force thus created drives ATP synthesis by a CF_oCF_1 complex similar to the mitochondrial F_oF_1 complex.
- The ATP synthase of chloroplasts (CF_oCF_1) is very similar in both structure and catalytic mechanism to the ATP synthases of mitochondria and bacteria. Physical rotation driven by the proton gradient is accompanied by ATP synthesis at sites that cycle through three conformations, one with high affinity for ATP, one with high affinity for ADP + P_i, and one with low affinity for both nucleotides.

19.10 The Evolution of Oxygenic Photosynthesis

The appearance of oxygenic photosynthesis on Earth about 2.5 billion years ago was a crucial event in the evolution of the biosphere. Until then, the earth had been essentially devoid of molecular oxygen and lacked the ozone layer that protects living organisms from solar UV radiation. Oxygenic photosynthesis made available a nearly limitless supply of reducing agent to drive the production of organic compounds by reductive biosynthetic reactions. And mechanisms evolved that allowed organisms to use O_2 as a terminal electron acceptor in highly energetic electron transfers from organic substrates, employing the energy of oxidation to support their metabolism. The complex photosynthetic apparatus of a modern vascular plant is the culmination of a series of evolutionary events, the most recent of which was the acquisition by eukaryotic cells of a cyanobacterial endosymbiont.

Chloroplasts Evolved from Ancient Photosynthetic Bacteria

Chloroplasts in modern organisms resemble mitochondria in several properties, and are believed to have originated by the same mechanism that gave rise to mitochondria: endosymbiosis. Like mitochondria, chloroplasts contain their own DNA and protein-synthesizing machinery. Some of the polypeptides of chloroplast proteins are encoded by chloroplast genes and synthesized in the chloroplast; others are encoded by nuclear genes, synthesized outside the chloroplast, and imported (Chapter 27). When plant cells grow and divide, chloroplasts give rise to new chloroplasts by division, during which their DNA is replicated and divided between daughter chloroplasts. The machinery and mechanism for light capture, electron flow, and ATP synthesis in modern cyanobacteria are similar in many respects to those in plant chloroplasts. These observations led to the now widely accepted hypothesis that the evolutionary progenitors of modern plant cells were primitive eukaryotes that engulfed photosynthetic cyanobacteria and established stable endosymbiotic relationships with them (see Fig. 1–36).

At least half of the photosynthetic activity on Earth now occurs in microorganisms—algae, other photosynthetic eukaryotes, and photosynthetic bacteria. Cyanobacteria have PSII and PSI in tandem, and the PSII has an associated water-splitting activity resembling that of plants. However, the other groups of photosynthetic bacteria have single reaction centers and do not split H_2O or produce O_2. Many are obligate anaerobes and cannot tolerate O_2; they must use some compound other than H_2O as electron donor. Some photosynthetic bacteria use inorganic compounds as electron (and hydrogen) donors. For example, green sulfur bacteria use hydrogen sulfide:

$$2H_2S + CO_2 \xrightarrow{\text{light}} (CH_2O) + H_2O + 2S$$

These bacteria, instead of producing molecular O_2, form elemental sulfur as the oxidation product of H_2S. (They further oxidize the S to SO_4^{2-}.) Other photosynthetic bacteria use organic compounds such as lactate as electron donors:

$$2\ \text{Lactate} + CO_2 \xrightarrow{\text{light}} (CH_2O) + H_2O + 2\ \text{pyruvate}$$

The fundamental similarity of photosynthesis in plants and bacteria, despite the differences in the electron donors they employ, becomes more obvious when the equation of photosynthesis is written in the more general form

$$2H_2D + CO_2 \xrightarrow{\text{light}} (CH_2O) + H_2O + 2D$$

in which H_2D is an electron (and hydrogen) donor and D is its oxidized form. H_2D may be water, hydrogen sulfide, lactate, or some other organic compound, depending on the species. Most likely, the bacteria that first developed photosynthetic ability used H_2S as their electron source.

The ancient relatives of modern cyanobacteria probably arose by the combination of genetic material from two types of photosynthetic bacteria, with systems of the type seen in modern purple bacteria (with a PSII-like electron path) and green sulfur bacteria (with an electron path resembling that in PSI). The bacterium with two independent photosystems may have used one in one set of conditions, the other in different conditions. Over time, a mechanism to connect the two photosystems for simultaneous use evolved, and the PSII-like system acquired the water-splitting capacity found in modern cyanobacteria.

Modern cyanobacteria can synthesize ATP by oxidative phosphorylation or by photophosphorylation, although they have neither mitochondria nor chloroplasts. The enzymatic machinery for both processes is in a highly convoluted plasma membrane (see Fig. 1–6). Three protein components function in both processes, giving evidence that the processes have a common evolutionary origin **(Fig. 19–65)**. First, the proton-pumping cytochrome b_6f complex carries electrons from plastoquinone to cytochrome c_6 in photosynthesis, and also carries electrons from ubiquinone to cytochrome c_6 in oxidative phosphorylation—the role played by cytochrome bc_1 in mitochondria. Second, cytochrome c_6, homologous to mitochondrial cytochrome c, carries electrons from Complex III to Complex IV in cyanobacteria; it can also carry electrons from the cytochrome b_6f complex to PSI—a role performed in plants by plastocyanin. We therefore see the functional homology between the cyanobacterial cytochrome b_6f complex and the mitochondrial cytochrome bc_1 complex, and between cyanobacterial cytochrome c_6 and plant plastocyanin. The third conserved component is the ATP synthase, which functions in oxidative phosphorylation and photophosphorylation in cyanobacteria, and in the mitochondria and chloroplasts of photosynthetic eukaryotes. The structure and remarkable mechanism of this enzyme have been strongly conserved throughout evolution.

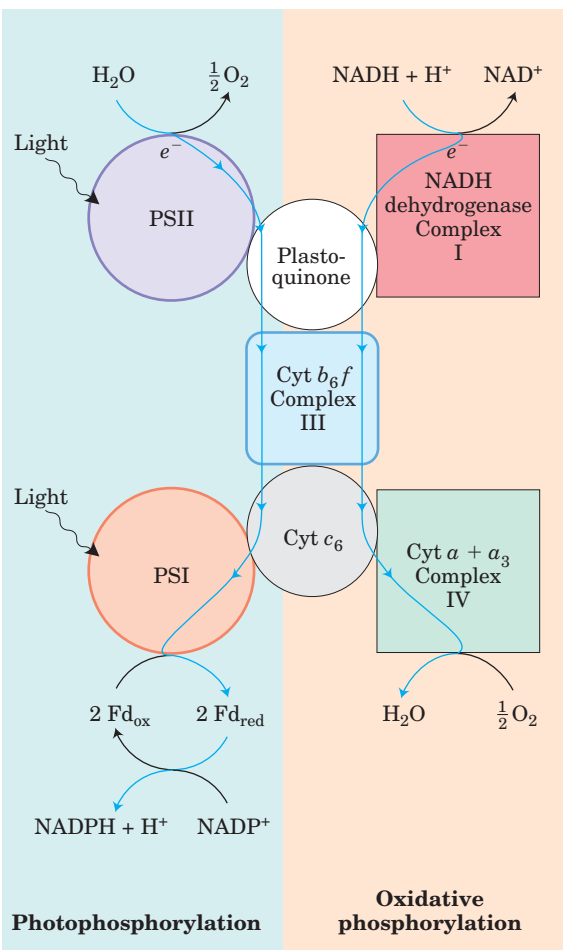

FIGURE 19–65 Dual roles of cytochrome b_6f and cytochrome c_6 in cyanobacteria reflect evolutionary origins. Cyanobacteria use cytochrome b_6f, cytochrome c_6, and plastoquinone for both oxidative phosphorylation and photophosphorylation. **(a)** In photophosphorylation, electrons flow (top to bottom) from water to $NADP^+$. **(b)** In oxidative phosphorylation, electrons flow from NADH to O_2. Both processes are accompanied by proton movement across the membrane, accomplished by a Q cycle.

In *Halobacterium*, a Single Protein Absorbs Light and Pumps Protons to Drive ATP Synthesis

In some modern archaea, a quite different mechanism for converting the energy of light into an electrochemical gradient has evolved. The halophilic ("salt-loving") archaean *Halobacterium salinarum* is descended from ancient evolutionary progenitors. This archaean (commonly referred to as a halobacterium) lives only in brine ponds and salt lakes (Great Salt Lake and the Dead Sea, for example), where the high salt concentration—which can exceed 4 M—results from water loss by evaporation; indeed, halobacteria cannot live in NaCl concentrations lower than 3 M. These organisms are aerobes and normally use O_2 to oxidize organic fuel molecules. However, the solubility of O_2 is so low in brine ponds that sometimes oxidative metabolism must be supplemented by sunlight as an alternative source of energy.

The plasma membrane of *H. salinarum* contains patches of the light-absorbing pigment **bacteriorhodopsin**, which contains retinal (the aldehyde derivative of vitamin A; see Fig. 10–21) as a light-harvesting prosthetic group. When the cells are illuminated, all-*trans*-retinal bound to the bacteriorhodopsin absorbs a photon and undergoes photoisomerization to 13-*cis*-retinal, forcing a conformational change in the protein. The restoration of all-*trans*-retinal is accompanied by the outward movement of protons through the plasma membrane. Bacteriorhodopsin, with only 247 amino acid residues, is the simplest light-driven proton pump known. The difference in the three-dimensional structure of bacteriorhodopsin in the dark and after illumination **(Fig. 19–66a)** suggests a pathway by which a concerted series of proton "hops" could effectively move a proton across the membrane. The chromophore retinal is bound through a Schiff-base linkage to the ε-amino group of a Lys residue. In the dark, the nitrogen of this Schiff base is protonated; in the light, photoisomerization of retinal lowers the pK_a of this group and it releases its proton to a nearby Asp residue, triggering a series of proton hops that ultimately result in the release of a proton at the outer surface of the membrane (Fig. 19–66b).

The electrochemical potential across the membrane drives protons back into the cell through a membrane ATP synthase complex very similar to that of mitochon-

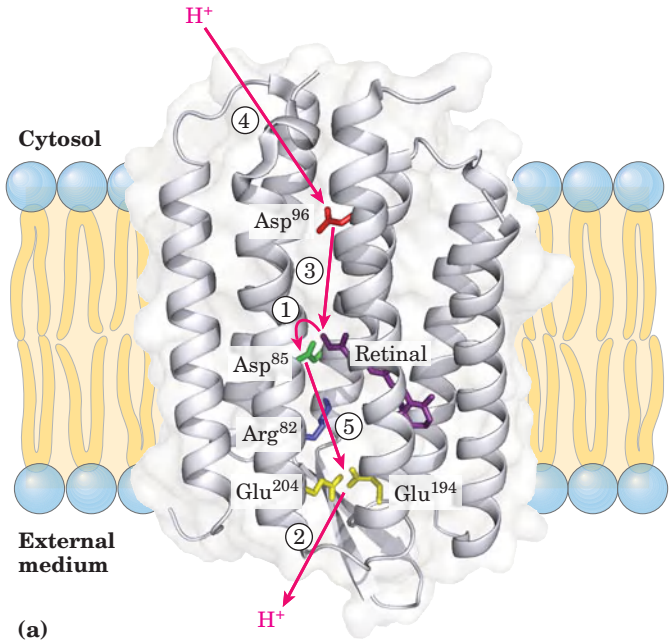

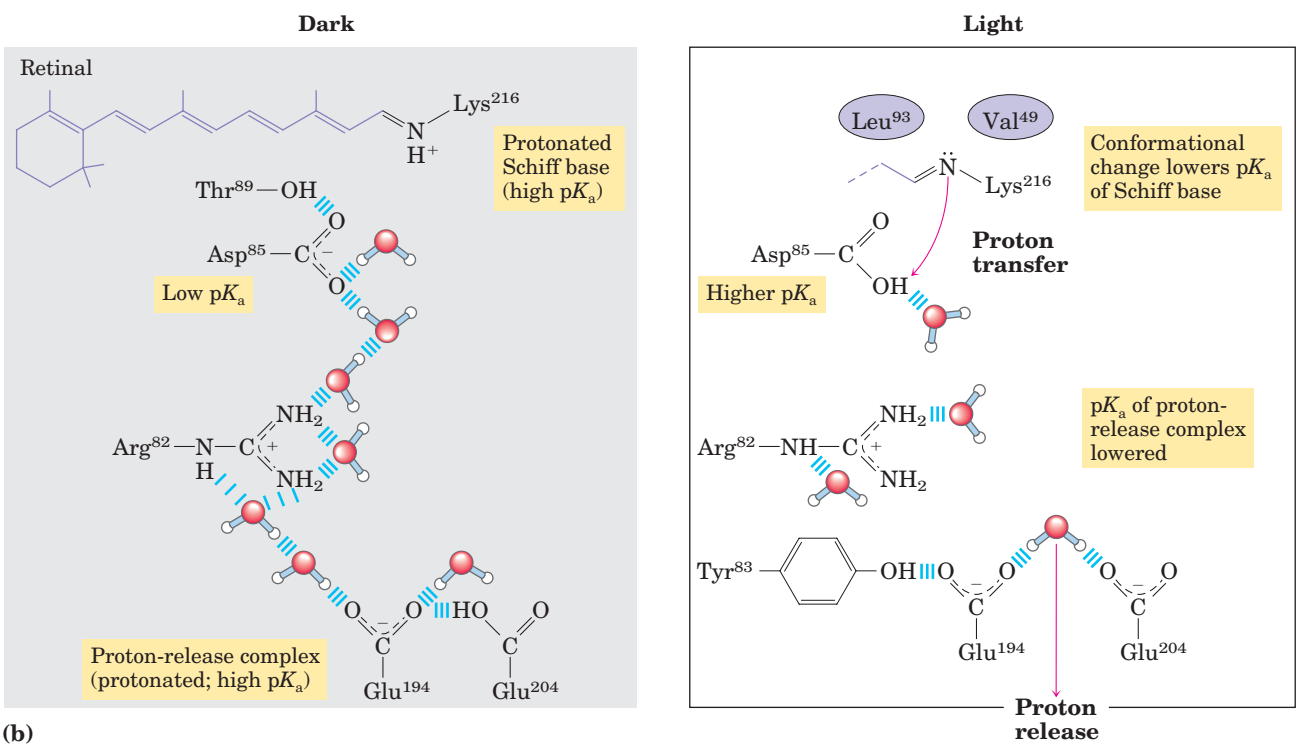

FIGURE 19–66 Evolution of a second mechanism for light-driven proton pumping in a halophilic archaean. (a) Bacteriorhodopsin (M_r 26,000) of *Halobacterium halobium* has seven membrane-spanning α helices (PDB ID 1C8R). The chromophore all-*trans*-retinal (purple) is covalently attached via a Schiff base to the ε-amino group of a Lys residue deep in the membrane interior. Running through the protein are a series of Asp and Glu residues and a series of closely associated water molecules that together provide the transmembrane path for protons (red arrows). Steps ① through ⑤ indicate proton movements, described below.

(b) In the dark (left panel), the Schiff base is protonated. Illumination (right panel) photoisomerizes the retinal, forcing subtle conformational changes in the protein that alter the distance between the Schiff base and its neighboring amino acid residues. Interaction with these neighbors lowers the pK_a of the protonated Schiff base, and the base gives up its proton to a nearby carboxyl group on Asp^{85} (step ① in **(a)**). This initiates a series of concerted proton hops between water molecules (see Fig. 2–13) in the interior of the protein, which ends with ② the release of a proton that was shared by Glu^{194} and Glu^{204} near the extracellular surface. ③ The Schiff base reacquires a proton from Asp^{96}, which ④ takes up a proton from the cytosol. ⑤ Finally, Asp^{85} gives up its proton, leading to reprotonation of the Glu^{204}-Glu^{194} pair. The system is now ready for another round of proton pumping.

dria and chloroplasts. Thus, when O_2 is limited, halobacteria can use light to supplement the ATP synthesized by oxidative phosphorylation. Halobacteria do not evolve O_2, nor do they carry out photoreduction of $NADP^+$; their phototransducing machinery is therefore much simpler than that of cyanobacteria or plants. Never-theless, its proton-pumping mechanism may prove to be prototypical for the many other, more complex, ion pumps. **Bacteriorhodopsin**

SUMMARY 19.10 The Evolution of Oxygenic Photosynthesis

- Modern cyanobacteria are derived from an ancient organism that acquired two photosystems, one of the type now found in purple bacteria, the other of the type found in green sulfur bacteria.
- Many photosynthetic microorganisms obtain electrons for photosynthesis not from water but from donors such as H_2S.
- Cyanobacteria with the tandem photosystems and a water-splitting activity that released oxygen into the atmosphere appeared on Earth about 2.5 billion years ago.
- Chloroplasts, like mitochondria, evolved from bacteria living endosymbiotically in early eukaryotic cells. The ATP synthases of bacteria, cyanobacteria, mitochondria, and chloroplasts share a common evolutionary precursor and a common enzymatic mechanism.
- An entirely different mechanism for converting light energy to a proton gradient has evolved in the modern archaea, in which the light-harvesting pigment is retinal.

Key Terms

Terms in bold are defined in the glossary.

chemiosmotic theory 707
nicotinamide nucleotide–linked dehydrogenases 709
flavoproteins 709
reducing equivalent 710
ubiquinone (coenzyme Q, Q) 710
cytochromes 710
iron-sulfur proteins 711
Rieske iron-sulfur proteins 711
Complex I 712
vectorial 713
Complex II 715
succinate dehydrogenase 715
reactive oxygen species (ROS) 715
superoxide radical ($^{\bullet}O_2^-$) 715
Complex III 715
cytochrome bc_1 complex 715
Q cycle 716
Complex IV 716
cytochrome oxidase 716
respirasomes 718
proton-motive force 720
ATP synthase 723
F_1ATPase 725
rotational catalysis 728
P/O ratio 729
P/2e^- ratio 729
malate-aspartate shuttle 731
glycerol 3-phosphate shuttle 732
acceptor control 733
mass-action ratio 733
brown adipose tissue (BAT) 736
thermogenin 736
cytochrome P-450 736
xenobiotics 736
apoptosis 737
apoptosome 738
caspase 738
heteroplasmy 740
homoplasmy 740
light-dependent reactions 742
light reactions 742
carbon-assimilation reactions 742
carbon-fixation reaction 742
thylakoid 743
grana 743
stroma 743
Hill reaction 743
photon 744
quantum 744
excited state 744
ground state 744
fluorescence 745
exciton 745
exciton transfer 745
chlorophylls 745
light-harvesting complexes (LHCs) 746
accessory pigments 747
carotenoids 747
action spectrum 747
photosystem 747
photochemical reaction center 747
light-harvesting (antenna) molecules 747
photosystem II (PSII) 752
photosystem I (PSI) 753
plastocyanin 753
oxygenic photosynthesis 753
plastoquinone (PQ_A) 753
ferredoxin 753
cyclic electron flow 756
noncyclic electron flow 756
cyclic photophosphorylation 756
oxygen-evolving complex 758
water-splitting complex 758
photophosphorylation 759

Further Reading

History and General Background

Arnon, D.I. (1984) The discovery of photosynthetic phosphorylation. *Trends Biochem. Sci.* **9**, 258–262.

Beinert, H. (1995) These are the moments when we live! From Thunberg tubes and manometry to phone, fax and FedEx. In *Selected Topics in the History of Biochemistry: Personal Recollections*, Comprehensive Biochemistry, Vol. 38, Elsevier Science Publishing Co., Inc., New York.

An engaging personal account of the exciting period when the biochemistry of respiratory electron transfer was worked out.

Blankenship, R.E. (2002) *Molecular Mechanisms of Photosynthesis*, Blackwell Science Inc., London.

An intermediate-level discussion of all aspects of photosynthesis.

Govindjee, Beatty, J.T., Gest, H., & Allen, J.F. (eds). (2006) *Discoveries in Photosynthesis*, Advances in Photosynthesis and Respiration, Vol. 20, Springer Verlag, Dordrecht, The Netherlands.

A wonderful description of the historical background to discoveries in photosynthesis, told by the people who made that history.

Harold, F.M. (1986) *The Vital Force: A Study in Bioenergetics*, W. H. Freeman and Company, New York.

A very readable synthesis of the principles of bioenergetics and their application to energy transductions.

Heldt, H.-W. (1997) *Plant Biochemistry and Molecular Biology*, Oxford University Press, Oxford.

A textbook of plant biochemistry with excellent discussions of photophosphorylation.

Keilin, D. (1966) *The History of Cell Respiration and Cytochrome*, Cambridge University Press, London.

An authoritative and absorbing account of the discovery of cytochromes and their roles in respiration, written by the man who discovered cytochromes.

Kresge, N., Simoni, R.D., & Hill, R.L. (2004) Britton Chance: Olympian and developer of stop-flow methods. *J. Biol. Chem.* **279**, e10, www.jbc.org.

A JBC Classic (on the website under "Classic Articles") describing the technology used to determine the sequence of electron carriers.

Kresge, N., Simoni, R.D., & Hill, R.L. (2006) Forty years of superoxide dismutase research: the work of Irwin Fridovich. *J. Biol. Chem.* **281**, e17, www.jbc.org.

A JBC Classic Article.

Lane, N. (2005) *Power, Sex, Suicide: Mitochondria and the Meaning of Life*, Oxford University Press, Oxford.

An entry-level description of the roles of mitochondria in energy conservation and in apoptosis.

Mitchell, P. (1979) Keilin's respiratory chain concept and its chemiosmotic consequences. *Science* **206**, 1148–1159.

Mitchell's Nobel lecture, outlining the evolution of the chemiosmotic hypothesis.

Nicholls, D.G. & Ferguson, S.J. (2002) *Bioenergetics 3*, Academic Press, Amsterdam.

Up-to-date, comprehensive, well-illustrated treatment of all aspects of mitochondrial and chloroplast energy transductions.

Scheffler, I.E. (1999) *Mitochondria*, Wiley-Liss, New York.

An excellent survey of mitochondrial structure and function.

Slater, E.C. (1987) The mechanism of the conservation of energy of biological oxidations. *Eur. J. Biochem.* **166**, 489–504.

A clear and critical account of the evolution of the chemiosmotic model.

OXIDATIVE PHOSPHORYLATION

Electron-Transfer Reactions in Mitochondria

Adam-Vizi, V. & Chinopoulos, C. (2006) Bioenergetics and the formation of mitochondrial reactive oxygen species. *Trends Pharmacol.* **27**, 639–645.

Babcock, G.T. & Wikström, M. (1992) Oxygen activation and the conservation of energy in cell respiration. *Nature* **356**, 301–309.

Advanced discussion of the reduction of water and pumping of protons by cytochrome oxidase.

Boekema, E.J. & Braun, H.-P. (2007) Supramolecular structure of the mitochondrial oxidative phosphorylation system. *J. Biol. Chem.* **282**, 1–4.

Brandt, U. (1997) Proton-translocation by membrane-bound NADH:ubiquinone-oxidoreductase (complex I) through redox-gated ligand conduction. *Biochim. Biophys. Acta* **1318**, 79–91.

Advanced discussion of models for electron movement through Complex I.

Brandt, U. (2006) Energy converting NADH:quinone oxidoreductase (complex I) *Annu. Rev. Biochem.* **75**, 69–92.

Advanced discussion of the structure of Complex I and the implications for function.

Brandt, U. & Trumpower, B. (1994) The protonmotive Q cycle in mitochondria and bacteria. *Crit. Rev. Biochem. Mol. Biol.* **29**, 165–197.

Advanced description of the possible mechanisms of the Q cycle.

Crofts, A.R. & Berry, E.A. (1998) Structure and function of the cytochrome bc_1 complex of mitochondria and photosynthetic bacteria. *Curr. Opin. Struct. Biol.* **8**, 501–509.

Heinemeyer, J., Braun, H.-P., Boekema, E.J., & Kouril, R. (2007) A structural model of the cytochrome *c* reductase/oxidase supercomplex from yeast mitochondria. *J. Biol. Chem.* **282**, 12,240–12,248.

Primary research supporting the existence of supercomplexes in mitochondria.

Hosler, J.P., Ferguson-Miller, S., & Mills, D.A. (2006) Energy transduction: proton transfer through the respiratory complexes. *Annu. Rev. Biochem.* **75**, 165–187.

Advanced description of electron transfer.

Lenaz, G., Fato, R., Genova, M.L., Bergamini, C., Bianchi, C., & Biondi, A. (2006) Mitochondrial Complex I: structural and functional aspects. *Biochim. Biophys. Acta* **1757**, 1406–1420.

Intermediate-level review of Complex I structure and function.

Lenaz, G. & Genova, M.L. (2007) Kinetics of integrated electron transfer in the mitochondrial respiratory chain: random collisions vs. solid state electron channeling. *Am. J. Physiol. Cell Physiol.* **292**, 1221–1239.

Test of the hypothesis that supercomplexes exist in mitochondria.

Michel, H., Behr, J., Harrenga, A., & Kannt, A. (1998) Cytochrome *c* oxidase: structure and spectroscopy. *Annu. Rev. Biophys. Biomol. Struct.* **27**, 329–356.

Advanced review of Complex IV structure and function.

Osyczka, A., Moser, C.C., & Dutton, P.L. (2005) Fixing the Q cycle. *Trends Biochem. Sci.* **30**, 176–182.

Intermediate-level review of the Q cycle.

Rottenberg, H. (1998) The generation of proton electrochemical potential gradient by cytochrome *c* oxidase. *Biochim. Biophys. Acta* **1364**, 1–16.

Sazanov, L.A. (2007) Respiratory complex I: mechanistic and structural insights provided by the crystal structure of the hydrophilic domain. *Biochemistry* **46**, 2275–2286.

Primary research paper on structure of Complex I.

Smith, J.L. (1998) Secret life of cytochrome bc_1. *Science* **281**, 58–59.

Sun, F., Huo, X., Zhai, Y., Wang, A., Xu, J., Su, D., Bartlam, M., & Rao, Z. (2005) Crystal structure of mitochondrial respiratory protein complex II. *Cell* **121**, 1043–1057.

Tielens, A.G.M., Rotte, C., van Hellemond, J.J., & Martin, W. (2002) Mitochondria as we don't know them. *Trends Biochem. Sci.* **27**, 564–572.

Intermediate-level discussion of the many organisms in which mitochondria do not depend on oxygen as the final electron donor.

Tsukihara, T., Aoyama, H., Yamashita, E., Tomizaki, T., Yamaguchi, H., Shinzawa-Itoh, K., Nakashima, R., Yaono, R., & Yoshikawa, S. (1996) The whole structure of the 13-subunit oxidized cytochrome *c* oxidase at 2.8 Å. *Science* **272**, 1136–1144.

The solution by x-ray crystallography of the structure of this huge membrane protein.

Wikström, M. & Verkhovsky, M.I. (2007) Mechanism and energetics of proton translocation by the respiratory heme-copper oxidases. *Biochim. Biophys. Acta* **1767**, 1200–1214.

Xia, D., Yu, C.-A., Kim, H., Xia, J.-Z., Kachurin, A.M., Zhang, L., Yu, L., & Deisenhofer, J. (1997) Crystal structure of the cytochrome bc_1 complex from bovine heart mitochondria. *Science* **277**, 60–66.

Report revealing the crystallographic structure of Complex III.

Yankovskaya, V., Horsefield, R., Törnroth, S., Luna-Chavez, C., Myoshi, H., Léger, C., Byrne, B., Cecchini, G., & Iwata, S. (2003) Architecture of succinate dehydrogenase and reactive oxygen species generation. *Science* **299**, 700–704.

Advanced review of this class of electron-transfer processes.

Zhang, M., Mileykovskaya, E., & Dowhan, W. (2005) Cardiolipin is essential for organization of complexes III and IV into a supercomplex in intact yeast mitochondria. *J. Biol. Chem.* **280**, 29,403–29,408.
Primary research paper.

ATP Synthesis

Abrahams, J.P., Leslie, A.G.W., Lutter, R., & Walker, J.E. (1994) The structure of F_1-ATPase from bovine heart mitochondria determined at 2.8 Å resolution. *Nature* **370**, 621–628.

Bianchet, M.A., Hullihen, J., Pedersen, P.L., & Amzel, L.M. (1998) The 2.80 Å structure of rat liver F_1-ATPase: configuration of a critical intermediate in ATP synthesis-hydrolysis. *Proc. Natl. Acad. Sci. USA* **95**, 11,065–11,070.
Research paper that provided important structural detail in support of the catalytic mechanism.

Boyer, P.D. (1997) The ATP synthase—a splendid molecular machine. *Annu. Rev. Biochem.* **66**, 717–749.
An account of the historical development and current state of the binding-change model, written by its principal architect.

Cabezón, E., Montgomery, M.G., Leslie, A.G.W., & Walker, J.E. (2003) The structure of bovine F_1-ATPase in complex with its regulatory protein IF_1. *Nat. Struct. Biol.* **10**, 744–750.

Hinkle, P.C., Kumar, M.A., Resetar, A., & Harris, D.L. (1991) Mechanistic stoichiometry of mitochondrial oxidative phosphorylation. *Biochemistry* **30**, 3576–3582.
A careful analysis of experimental results and theoretical considerations on the question of nonintegral P/O ratios.

Khan, S. (1997) Rotary chemiosmotic machines. *Biochim. Biophys. Acta* **1322**, 86–105.
Detailed review of the structures that underlie proton-driven rotary motion of ATP synthase and bacterial flagella.

Kresge, N., Simoni, R.D., & Hill, R.L. (2006) ATP synthesis and the binding change mechanism: the work of Paul D. Boyer. *J. Biol. Chem.* **281**, e18, www.jbc.org.
A JBC Classic Article.

Kresge, N., Simoni, R.D., & Hill, R.L. (2006) Unraveling the enzymology of oxidative phosphorylation: the work of Efraim Racker. *J. Biol. Chem.* **281**, e4, www.jbc.org.
A JBC Classic Article.

Nishizaka, T., Oiwa, K., Noji, H., Kimura, S., Muneyuki, E., Yoshida, M., & Kinosita, K., Jr. (2004) Chemomechanical coupling in F_1-ATPase revealed by simultaneous observation of nucleotide kinetics and rotation. *Nat. Struct. Mol. Biol.* **11**, 142–148.
Beautiful demonstration of the rotary motion of ATP synthase.

Sambongi, Y., Iko, Y., Tanabe, M., Omote, H., Iwamoto-Kihara, A., Ueda, I., Yanagida, T., Wada, Y., & Futai, M. (1999) Mechanical rotation of the c subunit oligomer in ATP synthase (F_oF_1): direct observation. *Science* **286**, 1722–1724.
The experimental evidence for rotation of the entire cylinder of c subunits in F_oF_1.

Stock, D., Leslie, A.G.W., & Walker, J.E. (1999) Molecular architecture of the rotary motor in ATP synthase. *Science* **286**, 1700–1705.
The first crystallographic view of the F_o subunit, in the yeast F_oF_1. See also R. H. Fillingame's editorial comment in the same issue of *Science*.

Weber, J. & Senior, A.E. (1997) Catalytic mechanism of F_1-ATPase. *Biochim. Biophys. Acta* **1319**, 19–58.
An advanced review of kinetic, structural, and biochemical evidence for the ATP synthase mechanism.

Regulation of Oxidative Phosphorylation

Brand, M.D. & Murphy, M.P. (1987) Control of electron flux through the respiratory chain in mitochondria and cells. *Biol. Rev. Camb. Philos. Soc.* **62**, 141–193.
An advanced description of respiratory control.

Harris, D.A. & Das, A.M. (1991) Control of mitochondrial ATP synthesis in the heart. *Biochem. J.* **280**, 561–573.
Advanced discussion of the regulation of ATP synthase by Ca^{2+} and other factors.

Klingenberg, M. & Huang, S.-G. (1999) Structure and function of the uncoupling protein from brown adipose tissue. *Biochim. Biophys. Acta* **1415**, 271–296.

Nury, H., Dahout-Gonzalez, C., Trezeguet, V., Lauquin, G.J.M., Brandolin, G., & Pebay-Peyroula, E. (2006) Relations between structure and function of the mitochondrial ADP/ATP carrier. *Annu. Rev. Biochem.* **75**, 713–741.
Advanced review.

Semenza, G.L. (2007) Oxygen-dependent regulation of mitochondrial respiration by hypoxia-inducible factor 1. *Biochem. J.* **405**, 1–9.
Intermediate-level review.

Simon, M.C. (2006) Coming up for air: HIF-1 and mitochondrial oxygen consumption. *Cell Metab.* **3**, 150–151.
Short, intermediate-level review of the hypoxia-inducible factor.

Mitochondria in Thermogenesis, Steroid Synthesis, and Apoptosis

Kroemer, G., Galluzzi, L., & Brenner, C. (2007) Mitochondrial membrane permeabilization in cell death. *Physiol. Rev.* **87**, 99–163.
Advanced, comprehensive review of role of cytochrome *c* in apoptosis.

McCord, J.M. (2002) Superoxide dismutase in aging and disease: an overview. *Methods Enzymol.* **349**, 331–341.

Riedl, S.J. & Salvesen, G.S. (2007) The apoptosome: signaling platform of cell death. *Nat. Rev. Mol. Cell Biol.* **8**, 405–413.
Intermediate-level review.

Mitochondrial Genes: Their Origin and Effects of Mutations

Abou-Sleiman, P.M., Muqit, M.M.K., & Wood, N.W. (2006) Expanding insights of mitochondrial dysfunction in Parkinson's disease. *Nat. Rev. Neurosci.* **7**, 207–219.

Boudina, S. & Abel, E.D. (2006) Mitochondrial uncoupling: a key contributer to reduced cardiac efficiency in diabetes. *Physiology* **21**, 250–258.

Brandon, M., Baldi, P., & Wallace, D.C. (2006) Mitochondrial mutations in cancer. *Oncogene* **25**, 4647–4662.

Chatterjee, A., Mambo, E., & Sidransky, D. (2006) Mitochondrial DNA mutations in human cancer. *Oncogene* **25**, 4663–4674.

Chen, Z.J. & Butow, R.A. (2005) The organization and inheritance of the mitochondrial genome. *Nat. Rev. Genet.* **6**, 815–825.
Intermediate-level review.

de Duve, C. (2007) The origin of eukaryotes: a reappraisal. *Nat. Rev. Genet.* **8**, 395–403.
Intermediate-level discussion of the evidence for the endosymbiotic origins of mitochondria and chloroplasts.

Freeman, H., Shimomura, K., Horner, E., Cox, R.D., & Ashcroft, F.M. (2006) Nicotinamide nucleotide transhydrogenase: a key role in insulin secretion. *Cell Metab.* **3**, 35–45.

Houstek, J., Pickova, A., Vojtiskova, A., Mracek, T., Pecina, P., & Jesina, P. (2006) Mitochondrial diseases and genetic defects of ATP synthase. *Biochim. Biophys. Acta* **1757**, 1400–1405.

Neubauer, S. (2007) The failing heart—an engine out of fuel. *New Engl. J. Med.* **356**, 1140–1151.
Intermediate-level review of defects in oxidative phosphorylation and heart disease.

Remedi, M.S., Nichols, C.G., & Koster, J.C. (2006) The mitochondria and insulin release: *Nnt* just a passing relationship. *Cell Metab.* **3**, 5–7.

Smeitink, J.A., Zeviani, M., Turnbull, D.M., & Jacobs, H.T. (2006) Mitochondrial medicine: a metabolic perspective on the pathology of oxidative phosphorylation disorders. *Cell Metab.* **3**, 9–13.

Taylor, R.W. & Turnbull, D.M. (2005) Mitochondrial DNA mutations in human disease. *Nat. Rev. Genet.* **6**, 389–402.
Intermediate-level review.

Wallace, D.C. (1999) Mitochondrial disease in man and mouse. *Science* **283**, 1482–1487.

Wiederkehr, A. & Wollheim, C.B. (2006) Minireview: implication of mitochondria in insulin secretion and action. *Endocrinology* **147**, 2643–2649.
Intermediate-level discussion of mitochondrial function in β cells.

PHOTOSYNTHESIS

Light Absorption

Cogdell, R.J., Isaacs, N.W., Howard, T.D., McLuskey, K., Fraser, N.J., & Prince, S.M. (1999) How photosynthetic bacteria harvest solar energy. *J. Bacteriol.* **181**, 3869–3879.
A short, intermediate-level review of the structure and function of the light-harvesting complex of the purple bacteria and exciton flow to the reaction center.

Green, B.R., Pichersky, E., & Kloppstech, K. (1991) Chlorophyll *a*/*b*-binding proteins: an extended family. *Trends Biochem. Sci.* **16**, 181–186.
An intermediate-level description of the proteins that orient chlorophyll molecules in chloroplasts.

Kargul, J., Nield, J., & Barber, J. (2003) Three-dimensional reconstruction of a light-harvesting Complex I–Photosystem I (LHCI-PSI) supercomplex from the green alga *Chlamydomonas reinhardtii*. *J. Biol. Chem.* **278**, 16,135–16,141.

Zuber, H. (1986) Structure of light-harvesting antenna complexes of photosynthetic bacteria, cyanobacteria and red algae. *Trends Biochem. Sci.* **11**, 414–419.

Light-Driven Electron Flow

Amunts, A., Drory, O., & Nelson, N. (2007) The structure of a plant photosystem I supercomplex at 3.4 Å resolution. *Nature* **447**, 58–63.
Determination of PSI structure by crystallography.

Barber, J. (2002) Photosystem II: a multisubunit membrane protein that oxidizes water. *Curr. Opin. Struct. Biol.* **12**, 523–530.
A short, intermediate-level summary of the structure of PSII.

Barber, J. & Anderson, J.M. (eds). (2002) Photosystem II: Molecular Structure and Function. Proceedings of a Meeting, 13–14 March 2002. *Philos. Trans. R. Soc. (Biol. Sci.)* **357** (1426).
A collection of 16 papers on photosystem II.

Biochim. Biophys. Acta Bioenerg. (2007) **1767** (6).
This journal issue contains 10 reviews on the structure and function of photosystems.

Chitnis, P.R. (2001) Photosystem I: function and physiology. *Annu. Rev. Plant Physiol. Plant Mol. Biol.* **52**, 593–626.
An advanced and lengthy review.

Dau, H. & Haumann, M. (2007) Eight steps preceding O–O bond formation in oxygenic photosynthesis—a basic reaction cycle of the photosystem II manganese complex. *Biochim. Biophys. Acta* **1767**, 472–483.
One of several papers in this issue dealing with models for the water-splitting mechanism.

Deisenhofer, J. & Michel, H. (1991) Structures of bacterial photosynthetic reaction centers. *Annu. Rev. Cell Biol.* **7**, 1–23.
Description of the structure of the reaction center of purple bacteria and implications for the function of bacterial and plant reaction centers.

Ferreira, K.N., Iverson, T.M., Maghlaoul, K., Barber, J., & Iwata, S. (2004) Architecture of the photosynthetic oxygen-evolving center. *Science* **303**, 1831–1838.

Fromme, P., Jordan, P., & Krauss, N. (2001) Structure of photosystem I. *Biochim. Biophys. Acta* **1507**, 5–31.

Hankamer, B., Barber, J., & Boekema, E.J. (1997) Structure and membrane organization of photosystem II in green plants. *Annu. Rev. Plant Physiol. Plant Mol. Biol.* **48**, 541–571.
Advanced review.

Heathcote, P., Fyfe, P.K., & Jones, M.R. (2002) Reaction centres: the structure and evolution of biological solar power. *Trends. Biochem Sci.* **27**, 79–87.
Intermediate-level review of photosystems I and II.

Huber, R. (1990) A structural basis of light energy and electron transfer in biology. *Eur. J. Biochem.* **187**, 283–305.
Huber's Nobel lecture, describing the physics and chemistry of phototransductions; an exceptionally clear and well-illustrated discussion, based on crystallographic studies of reaction centers.

Jensen, P.E., Bassi, R., Boekema, E.J., Dekker, J.P., Jansson, S., Leister, D., Robinson, C., & Scheller, H.V. (2007) Structure, function and regulation of plant photosystem I. *Biochim. Biophys. Acta* **1767**, 335–352.

Jordan, P., Fromme, P., Witt, H.T., Klukas, O., Saenger, W., & Krauss, N. (2001) Three-dimensional structure of cyanobacterial photosystem I at 2.5 Å. *Nature* **411**, 909–917.

Kamiya, N. & Shen, J.-R. (2003) Crystal structure of oxygen-evolving photosystem II from *Thermosynechococcus vulcanus* at 3.7 Å resolution. *Proc. Natl. Acad. Sci. USA* **100**, 98–103.

Kargul, J., Nield, J., & Barber, J. (2003) Three-dimensional reconstruction of a light-harvesting complex I–photosystem I (LHCI-PSI) supercomplex from the green alga *Chlamydomonas reinhardtii:* insights into light harvesting for PSI. *J. Biol. Chem.* **278**, 16,135–16,141.

Kok, B., Forbush, B., & McGloin, M. (1970) Cooperation of charges in photosynthetic O_2 evolution: 1. A linear 4-step mechanism. *Photochem. Photobiol.* **11**, 457–475.
Classic experiment showing the need for four photons to split water.

Kramer, D.M., Avenson, T.J., & Edwards, G.E. (2007) Dynamic flexibility in the light reactions of photosynthesis governed by both electron and proton transfer reactions. *Trends Plant Sci.* **9**, 349–357.
Intermediate-level review of regulation of state transitions.

Vink, M., Zer, H., Alumot, N., Gaathon, A., Niyogi, K., Herrmann, R.G., Andersson, B., & Ohad, I. (2004) Light-modulated exposure of the light-harvesting complex II (LHCII) to protein kinase(s) and state transition in *Chlamydomonas reinhardtii* xanthophyll mutants. *Biochemistry* **43**, 7824–7833.

Yano, J., Kern, J., Sauer, K., Latimer, M.J., Pushkar, Y., Biesiadka, J., Loll, B., Saenger, W., Messinger, J., Zouni, A., & Yachandra, V.K. (2006) Where water is oxidized to dioxygen: structure of the photosynthetic Mn_4Ca cluster. *Science* **314**, 821–825.

ATP Synthesis by Photophosphorylation

Jagendorf, A.T. (1967) Acid-base transitions and phosphorylation by chloroplasts. *Fed. Proc.* **26**, 1361–1369.
Classic experiment establishing the ability of a proton gradient to drive ATP synthesis in the dark.

The Evolution of Oxygenic Photosynthesis

Allen, J.F. & Martin, W. (2007) Out of thin air. *Nature* **445**, 610–612.
Short, intermediate-level discussion of how the modern Z scheme evolved.

Luecke, H. (2000) Atomic resolution structures of bacteriorhodopsin photocycle intermediates: the role of discrete water molecules in the function of this light-driven ion pump. *Biochim. Biophys. Acta* **1460**, 133–156.

Advanced review of a proton pump that employs an internal chain of water molecules.

Luecke, H., Schobert, B., Richter, H.-T., Cartailler, J.-P., & Lanyi, J.K. (1999) Structural changes in bacteriorhodopsin during ion transport at 2 angstrom resolution. *Science* **286**, 255–264.

This article, accompanied by an editorial comment in the same *Science* issue, describes the model for H^+ translocation by proton hopping.

Poole, A.M. & Penny, D. (2007) Evaluating hypotheses for the origin of eukaryotes. *BioEssays* **29**, 74–84.

Intermediate-level discussion of the endosymbiont-origin theory.

Stiller, J.W. (2007) Plastid endosymbiosis, genome evolution and the origin of green plants. *Trends Plant Sci.* **12**, 391–396.

Problems

1. Oxidation-Reduction Reactions The NADH dehydrogenase complex of the mitochondrial respiratory chain promotes the following series of oxidation-reduction reactions, in which Fe^{3+} and Fe^{2+} represent the iron in iron-sulfur centers, Q is ubiquinone, QH_2 is ubiquinol, and E is the enzyme:

(1) $NADH + H^+ + E\text{-}FMN \longrightarrow NAD^+ + E\text{-}FMNH_2$

(2) $E\text{-}FMNH_2 + 2Fe^{3+} \longrightarrow E\text{-}FMN + 2Fe^{2+} + 2H^+$

(3) $2Fe^{2+} + 2H^+ + Q \longrightarrow 2Fe^{3+} + QH_2$

Sum: $NADH + H^+ + Q \longrightarrow NAD^+ + QH_2$

For each of the three reactions catalyzed by the NADH dehydrogenase complex, identify (a) the electron donor, (b) the electron acceptor, (c) the conjugate redox pair, (d) the reducing agent, and (e) the oxidizing agent.

2. All Parts of Ubiquinone Have a Function In electron transfer, only the quinone portion of ubiquinone undergoes oxidation-reduction; the isoprenoid side chain remains unchanged. What is the function of this chain?

3. Use of FAD Rather Than NAD^+ in Succinate Oxidation All the dehydrogenases of glycolysis and the citric acid cycle use NAD^+ ($E'°$ for NAD^+/NADH is -0.32 V) as electron acceptor except succinate dehydrogenase, which uses covalently bound FAD ($E'°$ for FAD/$FADH_2$ in this enzyme is 0.050 V). Suggest why FAD is a more appropriate electron acceptor than NAD^+ in the dehydrogenation of succinate, based on the $E'°$ values of fumarate/succinate ($E'° = 0.031$), NAD^+/NADH, and the succinate dehydrogenase FAD/$FADH_2$.

4. Degree of Reduction of Electron Carriers in the Respiratory Chain The degree of reduction of each carrier in the respiratory chain is determined by conditions in the mitochondrion. For example, when NADH and O_2 are abundant, the steady-state degree of reduction of the carriers decreases as electrons pass from the substrate to O_2. When electron transfer is blocked, the carriers before the block become more reduced and those beyond the block become more oxidized (see Fig. 19–6). For each of the conditions below, predict the state of oxidation of ubiquinone and cytochromes b, c_1, c, and $a + a_3$.

(a) Abundant NADH and O_2, but cyanide added
(b) Abundant NADH, but O_2 exhausted
(c) Abundant O_2, but NADH exhausted
(d) Abundant NADH and O_2

5. Effect of Rotenone and Antimycin A on Electron Transfer Rotenone, a toxic natural product from plants, strongly inhibits NADH dehydrogenase of insect and fish mitochondria. Antimycin A, a toxic antibiotic, strongly inhibits the oxidation of ubiquinol.

(a) Explain why rotenone ingestion is lethal to some insect and fish species.

(b) Explain why antimycin A is a poison.

(c) Given that rotenone and antimycin A are equally effective in blocking their respective sites in the electron-transfer chain, which would be a more potent poison? Explain.

6. Uncouplers of Oxidative Phosphorylation In normal mitochondria the rate of electron transfer is tightly coupled to the demand for ATP. When the rate of use of ATP is relatively low, the rate of electron transfer is low; when demand for ATP increases, electron-transfer rate increases. Under these conditions of tight coupling, the number of ATP molecules produced per atom of oxygen consumed when NADH is the electron donor—the P/O ratio—is about 2.5.

(a) Predict the effect of a relatively low and a relatively high concentration of uncoupling agent on the rate of electron transfer and the P/O ratio.

(b) Ingestion of uncouplers causes profuse sweating and an increase in body temperature. Explain this phenomenon in molecular terms. What happens to the P/O ratio in the presence of uncouplers?

(c) The uncoupler 2,4-dinitrophenol was once prescribed as a weight-reducing drug. How could this agent, in principle, serve as a weight-reducing aid? Uncoupling agents are no longer prescribed, because some deaths occurred following their use. Why might the ingestion of uncouplers lead to death?

7. Effects of Valinomycin on Oxidative Phosphorylation When the antibiotic valinomycin is added to actively respiring mitochondria, several things happen: the yield of ATP decreases, the rate of O_2 consumption increases, heat is released, and the pH gradient across the inner mitochondrial membrane increases. Does valinomycin act as an uncoupler or as an inhibitor of oxidative phosphorylation? Explain the experimental observations in terms of the antibiotic's ability to transfer K^+ ions across the inner mitochondrial membrane.

8. Mode of Action of Dicyclohexylcarbodiimide (DCCD) When DCCD is added to a suspension of tightly coupled, actively respiring mitochondria, the rate of electron transfer (measured by O_2 consumption) and the rate of ATP production dramatically decrease. If a solution of 2,4-dinitrophenol is now added to the preparation, O_2 consumption returns to normal but ATP production remains inhibited.

(a) What process in electron transfer or oxidative phosphorylation is affected by DCCD?

(b) Why does DCCD affect the O_2 consumption of mitochondria? Explain the effect of 2,4-dinitrophenol on the inhibited mitochondrial preparation.

(c) Which of the following inhibitors does DCCD most resemble in its action: antimycin A, rotenone, or oligomycin?

9. Compartmentalization of Citric Acid Cycle Components Isocitrate dehydrogenase is found only in the mitochondrion, but malate dehydrogenase is found in both the cytosol and mitochondrion. What is the role of cytosolic malate dehydrogenase?

10. The Malate–α-Ketoglutarate Transport System The transport system that conveys malate and α-ketoglutarate across the inner mitochondrial membrane (see Fig. 19–29) is inhibited by *n*-butylmalonate. Suppose *n*-butylmalonate is added to an aerobic suspension of kidney cells using glucose exclusively as fuel. Predict the effect of this inhibitor on (a) glycolysis, (b) oxygen consumption, (c) lactate formation, and (d) ATP synthesis.

11. Cellular ADP Concentration Controls ATP Formation Although both ADP and P_i are required for the synthesis of ATP, the rate of synthesis depends mainly on the concentration of ADP, not P_i. Why?

12. Time Scales of Regulatory Events in Mitochondria Compare the likely time scales for the adjustments in respiratory rate caused by (a) increased [ADP] and (b) reduced pO_2. What accounts for the difference?

13. The Pasteur Effect When O_2 is added to an anaerobic suspension of cells consuming glucose at a high rate, the rate of glucose consumption declines greatly as the O_2 is used up, and accumulation of lactate ceases. This effect, first observed by Louis Pasteur in the 1860s, is characteristic of most cells capable of both aerobic and anaerobic glucose catabolism.

(a) Why does the accumulation of lactate cease after O_2 is added?

(b) Why does the presence of O_2 decrease the rate of glucose consumption?

(c) How does the onset of O_2 consumption slow down the rate of glucose consumption? Explain in terms of specific enzymes.

14. Respiration-Deficient Yeast Mutants and Ethanol Production Respiration-deficient yeast mutants (p^-; "petites") can be produced from wild-type parents by treatment with mutagenic agents. The mutants lack cytochrome oxidase, a deficit that markedly affects their metabolic behavior. One striking effect is that fermentation is not suppressed by O_2—that is, the mutants lack the Pasteur effect (see Problem 13). Some companies are very interested in using these mutants to ferment wood chips to ethanol for energy use. Explain the advantages of using these mutants rather than wild-type yeast for large-scale ethanol production. Why does the absence of cytochrome oxidase eliminate the Pasteur effect?

15. Advantages of Supercomplexes for Electron Transfer There is growing evidence that mitochondrial Complexes I, II, III, and IV are part of a larger supercomplex. What might be the advantage of having all four complexes within a supercomplex?

16. How Many Protons in a Mitochondrion? Electron transfer translocates protons from the mitochondrial matrix to the external medium, establishing a pH gradient across the inner membrane (outside more acidic than inside). The tendency of protons to diffuse back into the matrix is the driving force for ATP synthesis by ATP synthase. During oxidative phosphorylation by a suspension of mitochondria in a medium of pH 7.4, the pH of the matrix has been measured as 7.7.

(a) Calculate $[H^+]$ in the external medium and in the matrix under these conditions.

(b) What is the outside-to-inside ratio of $[H^+]$? Comment on the energy inherent in this concentration difference. (Hint: See Eqn 11–4, p. 396.)

(c) Calculate the number of protons in a respiring liver mitochondrion, assuming its inner matrix compartment is a sphere of diameter 1.5 μm.

(d) From these data, is the pH gradient alone sufficient to generate ATP?

(e) If not, suggest how the necessary energy for synthesis of ATP arises.

17. Rate of ATP Turnover in Rat Heart Muscle Rat heart muscle operating aerobically fills more than 90% of its ATP needs by oxidative phosphorylation. Each gram of tissue consumes O_2 at the rate of 10.0 μmol/min, with glucose as the fuel source.

(a) Calculate the rate at which the heart muscle consumes glucose and produces ATP.

(b) For a steady-state concentration of ATP of 5.0 μmol/g of heart muscle tissue, calculate the time required (in seconds) to completely turn over the cellular pool of ATP. What does this result indicate about the need for tight regulation of ATP production? (Note: Concentrations are expressed as micromoles per gram of muscle tissue because the tissue is mostly water.)

18. Rate of ATP Breakdown in Insect Flight Muscle ATP production in the flight muscle of the fly *Lucilia sericata* results almost exclusively from oxidative phosphorylation. During flight, 187 mL of O_2/hr • g of body weight is needed to maintain an ATP concentration of 7.0 μmol/g of flight muscle. Assuming that flight muscle makes up 20% of the weight of the fly, calculate the rate at which the flight-muscle ATP pool turns over. How long would the reservoir of ATP last in the absence of oxidative phosphorylation? Assume that reducing equivalents are transferred by the glycerol 3-phosphate shuttle and that O_2 is at 25 °C and 101.3 kPa (1 atm).

19. Mitochondrial Disease and Cancer Mutations in the genes that encode certain mitochondrial proteins are associated with a high incidence of some types of cancer. How might defective mitochondria lead to cancer?

20. Variable Severity of a Mitochondrial Disease Individuals with a disease caused by a specific defect in the mitochondrial genome may have symptoms ranging from mild to severe. Explain why.

21. Transmembrane Movement of Reducing Equivalents Under aerobic conditions, extramitochondrial NADH

must be oxidized by the mitochondrial electron-transfer chain. Consider a preparation of rat hepatocytes containing mitochondria and all the cytosolic enzymes. If [4-^{3}H]NADH is introduced, radioactivity soon appears in the mitochondrial matrix. However, if [7-^{14}C]NADH is introduced, no radioactivity appears in the matrix. What do these observations reveal about the oxidation of extramitochondrial NADH by the electron-transfer chain?

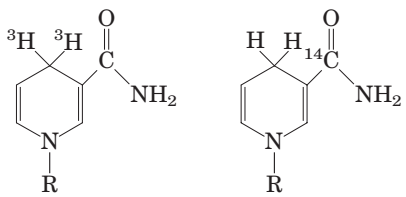

[4-^{3}H]NADH [7-^{14}C]NADH

22. High Blood Alanine Level Associated with Defects in Oxidative Phosphorylation Most individuals with genetic defects in oxidative phosphorylation are found to have relatively high concentrations of alanine in their blood. Explain this in biochemical terms.

23. NAD Pools and Dehydrogenase Activities Although both pyruvate dehydrogenase and glyceraldehyde 3-phosphate dehydrogenase use NAD^+ as their electron acceptor, the two enzymes do not compete for the same cellular NAD pool. Why?

24. Diabetes as a Consequence of Mitochondrial Defects Glucokinase is essential in the metabolism of glucose in pancreatic β cells. Humans with two defective copies of the glucokinase gene exhibit a severe, neonatal diabetes, whereas those with only one defective copy of the gene have a much milder form of the disease (mature onset diabetes of the young, MODY2). Explain this difference in terms of the biology of the β cell.

25. Effects of Mutations in Mitochondrial Complex II Single nucleotide changes in the gene for succinate dehydrogenase (Complex II) are associated with midgut carcinoid tumors. Suggest a mechanism to explain this observation.

26. Photochemical Efficiency of Light at Different Wavelengths The rate of photosynthesis, measured by O_2 production, is higher when a green plant is illuminated with light of wavelength 680 nm than with light of 700 nm. However, illumination by a combination of light of 680 nm and 700 nm gives a higher rate of photosynthesis than light of either wavelength alone. Explain.

27. Balance Sheet for Photosynthesis In 1804 Theodore de Saussure observed that the total weight of oxygen and dry organic matter produced by plants is greater than the weight of carbon dioxide consumed during photosynthesis. Where does the extra weight come from?

28. Role of H_2S in Some Photosynthetic Bacteria Illuminated purple sulfur bacteria carry out photosynthesis in the presence of H_2O and $^{14}CO_2$, but only if H_2S is added and O_2 is absent. During the course of photosynthesis, measured by formation of [^{14}C]carbohydrate, H_2S is converted to elemental sulfur, but no O_2 is evolved. What is the role of the conversion of H_2S to sulfur? Why is no O_2 evolved?

29. Boosting the Reducing Power of Photosystem I by Light Absorption When photosystem I absorbs red light at 700 nm, the standard reduction potential of P700 changes from 0.40 V to about −1.2 V. What fraction of the absorbed light is trapped in the form of reducing power?

30. Electron Flow through Photosystems I and II Predict how an inhibitor of electron passage through pheophytin would affect electron flow through (a) photosystem II and (b) photosystem I. Explain your reasoning.

31. Limited ATP Synthesis in the Dark In a laboratory experiment, spinach chloroplasts are illuminated in the absence of ADP and P_i, then the light is turned off and ADP and P_i are added. ATP is synthesized for a short time in the dark. Explain this finding.

32. Mode of Action of the Herbicide DCMU When chloroplasts are treated with 3-(3,4-dichlorophenyl)-1,1-dimethylurea (DCMU, or diuron), a potent herbicide, O_2 evolution and photophosphorylation cease. Oxygen evolution, but not photophosphorylation, can be restored by addition of an external electron acceptor, or Hill reagent. How does DCMU act as a weed killer? Suggest a location for the inhibitory action of this herbicide in the scheme shown in Figure 19–56. Explain.

33. Effect of Venturicidin on Oxygen Evolution Venturicidin is a powerful inhibitor of the chloroplast ATP synthase, interacting with the CF_o part of the enzyme and blocking proton passage through the CF_oCF_1 complex. How would venturicidin affect oxygen evolution in a suspension of well-illuminated chloroplasts? Would your answer change if the experiment were done in the presence of an uncoupling reagent such as 2,4-dinitrophenol (DNP)? Explain.

34. Bioenergetics of Photophosphorylation The steady-state concentrations of ATP, ADP, and P_i in isolated spinach chloroplasts under full illumination at pH 7.0 are 120.0, 6.0, and 700.0 μM, respectively.

(a) What is the free-energy requirement for the synthesis of 1 mol of ATP under these conditions?

(b) The energy for ATP synthesis is furnished by light-induced electron transfer in the chloroplasts. What is the minimum voltage drop necessary (during transfer of a pair of electrons) to synthesize ATP under these conditions? (You may need to refer to Eqn 13–7, p. 515.)

35. Light Energy for a Redox Reaction Suppose you have isolated a new photosynthetic microorganism that oxidizes H_2S and passes the electrons to NAD^+. What wavelength of light would provide enough energy for H_2S to reduce NAD^+ under standard conditions? Assume 100% efficiency in the photochemical event, and use E'° of −243 mV for H_2S and −320 mV for NAD^+. See Figure 19–46 for the energy equivalents of wavelengths of light.

36. Equilibrium Constant for Water-Splitting Reactions The coenzyme $NADP^+$ is the terminal electron acceptor in chloroplasts, according to the reaction

$$2H_2O + 2NADP^+ \longrightarrow 2NADPH + 2H^+ + O_2$$

Use the information in Table 19–2 to calculate the equilibrium constant for this reaction at 25 °C. (The relationship between K'_{eq} and $\Delta G'^\circ$ is discussed on p. 492.) How can the chloroplast overcome this unfavorable equilibrium?

37. Energetics of Phototransduction During photosynthesis, eight photons must be absorbed (four by each photosystem) for every O_2 molecule produced:

$$2H_2O + 2NADP^+ + 8 \text{ photons} \longrightarrow 2NADPH + 2H^+ + O_2$$

Assuming that these photons have a wavelength of 700 nm (red) and that the light absorption and use of light energy are 100% efficient, calculate the free-energy change for the process.

38. Electron Transfer to a Hill Reagent Isolated spinach chloroplasts evolve O_2 when illuminated in the presence of potassium ferricyanide (a Hill reagent), according to the equation

$$2H_2O + 4Fe^{3+} \longrightarrow O_2 + 4H^+ + 4Fe^{2+}$$

where Fe^{3+} represents ferricyanide and Fe^{2+}, ferrocyanide. Is NADPH produced in this process? Explain.

39. How Often Does a Chlorophyll Molecule Absorb a Photon? The amount of chlorophyll *a* (M_r 892) in a spinach leaf is about 20 $\mu g/cm^2$ of leaf surface. In noonday sunlight (average energy reaching the leaf is 5.4 J/cm^2 • min), the leaf absorbs about 50% of the radiation. How often does a single chlorophyll molecule absorb a photon? Given that the average lifetime of an excited chlorophyll molecule in vivo is 1 ns, what fraction of the chlorophyll molecules are excited at any one time?

40. Effect of Monochromatic Light on Electron Flow The extent to which an electron carrier is oxidized or reduced during photosynthetic electron transfer can sometimes be observed directly with a spectrophotometer. When chloroplasts are illuminated with 700 nm light, cytochrome *f*, plastocyanin, and plastoquinone are oxidized. When chloroplasts are illuminated with 680 nm light, however, these electron carriers are reduced. Explain.

41. Function of Cyclic Photophosphorylation When the [NADPH]/[$NADP^+$] ratio in chloroplasts is high, photophosphorylation is predominantly cyclic (see Fig. 19–56). Is O_2 evolved during cyclic photophosphorylation? Is NADPH produced? Explain. What is the main function of cyclic photophosphorylation?

Data Analysis Problem

42. Photophosphorylation: Discovery, Rejection, and Rediscovery In the 1930s and 1940s, researchers were beginning to make progress toward understanding the mechanism of photosynthesis. At the time, the role of "energy-rich phosphate bonds" (today, "ATP") in glycolysis and cellular respiration was just becoming known. There were many theories about the mechanism of photosynthesis, especially about the role of light. This problem focuses on what was then called the "primary photochemical process"—that is, on what it is, exactly, that the energy from captured light produces in the photosynthetic cell. Interestingly, one important part of the modern model of photosynthesis was proposed early on, only to be rejected, ignored for several years, then finally revived and accepted.

In 1944, Emerson, Stauffer, and Umbreit proposed that "the function of light energy in photosynthesis is the formation of 'energy-rich' phosphate bonds" (p. 107). In their model (hereafter, the "Emerson model"), the free energy necessary to drive both CO_2 fixation *and* reduction came from these "energy-rich phosphate bonds" (i.e., ATP), produced as a result of light absorption by a chlorophyll-containing protein.

This model was explicitly rejected by Rabinowitch (1945). After summarizing Emerson and coauthors' findings, Rabinowitch stated: "Until more positive evidence is provided, we are inclined to consider as more convincing a general argument against this hypothesis, which can be derived from energy considerations. Photosynthesis is eminently a problem of energy *accumulation*. What good can be served, then, by converting light quanta (even those of red light, which amount to about 43 kcal per Einstein) into 'phosphate quanta' of only 10 kcal per mole? This appears to be a start in the wrong direction—toward *dissipation* rather than toward accumulation of energy" (Vol. I, p. 228). This argument, along with other evidence, led to the abandonment of the Emerson model until the 1950s, when it was found to be correct—albeit in a modified form.

For each piece of information from Emerson and coauthors' article presented in (a) through (d) below, answer the following three questions:

1. How does this information support the Emerson model, in which light energy is used directly by chlorophyll *to make ATP*, and the ATP then provides the energy to drive CO_2 fixation and reduction?
2. How would Rabinowitch explain this information, based on his model (and most other models of the day), in which light energy is used directly by chlorophyll *to make reducing compounds*? Rabinowitch wrote: "Theoretically, there is no reason why *all* electronic energy contained in molecules excited by the absorption of light should not be available for oxidation-reduction" (Vol. I, p. 152). In this model, the reducing compounds are then used to fix and reduce CO_2, and the energy for these reactions comes from the large amounts of free energy released by the reduction reactions.
3. How is this information explained by our modern understanding of photosynthesis?

(a) Chlorophyll contains a Mg^{2+} ion, which is known to be an essential cofactor for many enzymes that catalyze phosphorylation and dephosphorylation reactions.

(b) A crude "chlorophyll protein" isolated from photosynthetic cells showed phosphorylating activity.

(c) The phosphorylating activity of the "chlorophyll protein" was inhibited by light.

(d) The levels of several different phosphorylated compounds in photosynthetic cells changed dramatically in response to light exposure. (Emerson and coworkers were not able to identify the specific compounds involved.)

As it turned out, the Emerson and Rabinowitch models were both partly correct and partly incorrect.

(e) Explain how the two models relate to our current model of photosynthesis.

In his rejection of the Emerson model, Rabinowitch went on to say: "The difficulty of the phosphate storage theory appears most clearly when one considers the fact that, in weak light, eight or ten quanta of light are sufficient to reduce one molecule of carbon dioxide. If each quantum should produce one molecule of high-energy phosphate, the accumulated energy would be only 80–100 kcal per Einstein—while photosynthesis requires *at least* 112 kcal per mole, and probably more, because of losses in irreversible partial reactions" (Vol. 1, p. 228).

(f) How does Rabinowitch's value of 8 to 10 photons per molecule of CO_2 reduced compare with the value accepted today? You need to consult Chapter 20 for some of the information required here.

(g) How would you rebut Rabinowitch's argument, based on our current knowledge about photosynthesis?

References

Emerson, R.L., Stauffer, J.F., & Umbreit, W.W. (1944) Relationships between phosphorylation and photosynthesis in *Chlorella*. *Am. J. Botany* **31**, 107–120.

Rabinowitch, E.I. (1945) *Photosynthesis and Related Processes*, Interscience Publishers, New York.

20

. . . the discovery of the long-lived isotope of carbon, carbon-14, by Samuel Ruben and Martin Kamen in 1940 provided the ideal tool for the tracing of the route along which carbon dioxide travels on its way to carbohydrate.

—Melvin Calvin, Nobel Address, 1961

Carbohydrate Biosynthesis in Plants and Bacteria

We have now reached a turning point in our study of cellular metabolism. Thus far in Part II we have described how the major metabolic fuels—carbohydrates, fatty acids, and amino acids—are degraded through converging *catabolic* pathways to enter the citric acid cycle and yield their electrons to the respiratory chain, and how this exergonic flow of electrons to oxygen is coupled to the endergonic synthesis of ATP. We now turn to *anabolic* pathways, which use chemical energy in the form of ATP and NADH or NADPH to synthesize cellular components from simple precursor molecules. Anabolic pathways are generally reductive rather than oxidative. Catabolism and anabolism proceed simultaneously in a dynamic steady state, so the energy-yielding degradation of cellular components is counterbalanced by biosynthetic processes, which create and maintain the intricate orderliness of living cells.

Plants must be especially versatile in their handling of carbohydrates, for several reasons. First, plants are autotrophs, able to convert inorganic carbon (as CO_2) into organic compounds. Second, biosynthesis occurs primarily in plastids, membrane-bounded organelles unique to photosynthetic organisms, and the movement of intermediates between cellular compartments is an important aspect of metabolism. Third, plants are not motile: they cannot move to find better supplies of water, sunlight, or nutrients. They must have sufficient metabolic flexibility to allow them to adapt to changing conditions in the place where they are rooted. Finally, plants have thick cell walls made of carbohydrate polymers, which must be assembled outside the plasma membrane and which constitute a significant proportion of the cell's carbohydrate.

The chapter begins with a description of the process by which CO_2 is assimilated into trioses and hexoses, then considers photorespiration, an important side reaction during CO_2 fixation, and the ways in which certain plants avoid this side reaction. We then look at how the biosynthesis of sucrose (for sugar transport) and starch (for energy storage) is accomplished by mechanisms analogous to those employed by animal cells to make glycogen. The next topic is the synthesis of the cellulose of plant cell walls and the peptidoglycan of bacterial cell walls, illustrating the problems of energy-dependent biosynthesis outside the plasma membrane. Finally, we discuss how the various pathways that share pools of common intermediates are segregated within organelles yet integrated with one another.

20.1 Photosynthetic Carbohydrate Synthesis

The synthesis of carbohydrates in animal cells always employs precursors having at least three carbons, all of which are less oxidized than the carbon in CO_2. Plants and photosynthetic microorganisms, by contrast, can synthesize carbohydrates from CO_2 and water, reducing CO_2 at the expense of the energy and reducing power furnished by the ATP and NADPH that are generated by the light-dependent reactions of photosynthesis **(Fig. 20–1)**. Plants (and other autotrophs) can use CO_2 as the sole source of the carbon atoms required for the biosynthesis of cellulose and starch, lipids and proteins, and the many other organic components of plant cells. By contrast, heterotrophs cannot bring about the net reduction of CO_2 to achieve a net synthesis of glucose.